

Fragile Phases As Affine Monoids: Classification and Material Examples

Zhi-Da Song,^{1,*} Luis Elcoro,^{2,*} Yuan-Feng Xu,³ Nicolas Regnault,^{4,1} and B. Andrei Bernevig^{1,3,5,†}

¹*Department of Physics, Princeton University, Princeton, New Jersey 08544, USA*

²*Department of Condensed Matter Physics, University of the Basque Country UPV/EHU, Apartado 644, 48080 Bilbao, Spain*

³*Max Planck Institute of Microstructure Physics, 06120 Halle, Germany*

⁴*Laboratoire de Physique de l'Ecole normale supérieure PSL University,
CNRS, Sorbonne Université, Université Paris Diderot,
Sorbonne Paris Cité, 24 rue Lhomond, 75005 Paris France*

⁵*Physics Department, Freie Universität Berlin, Arnimallee 14, 14195 Berlin, Germany*

(Dated: May 19, 2020)

Topological phases in electronic structures contain a new type of topology, called fragile, which can arise, for example, when an Elementary Band Representation (Atomic Limit Band) splits into a particular set of bands. We obtain, for the first time, a complete classification of the fragile topological phases which can be diagnosed by symmetry eigenvalues, to find an incredibly rich structure which far surpasses that of stable/strong topological states. We find and enumerate all hundreds of thousands of different fragile topological phases diagnosed by symmetry eigenvalues (available at [this http URL](#)), and link the mathematical structure of these phases to that of Affine Monoids in mathematics. Furthermore, we predict and calculate, for the first time, (hundred of realistic) materials where fragile topological bands appear, and show-case the very best ones.

I. INTRODUCTION

Since the birth of topological insulators (TIs) [1–9], researchers have found topological states of matter to be a theoretically and experimentally versatile field where new phenomena are uncovered every year [10–12]. From topological semimetals [13–22], to topological crystalline insulators with symmorphic and non-symmorphic symmetries [23–29], to higher order topological insulators [30–36], the field of topological electronic phases of matter keeps evolving. As researchers steadily theoretically solve and experimentally find materials for several topological phases, new, further unknown types of topological phases arise.

Recent substantial progress in the field has led to the development of techniques [37–45] which can be used for a high-throughput discovery of topological materials, the beginning of which has been undertaken in [46–49]. Topological Quantum Chemistry (TQC) [37, 40, 41, 50] and the associated [Bilbao Crystallographic Server \(BCS\)](#) [37, 40, 51], have provided for a classification of *all* the atomic limits - whose basis are the so-called Elementary Band Representations (EBRs) - existent in the 230 non-magnetic space groups (SGs). TQC defines topological phases as the phases not adiabatically continuable to a sum of EBRs. This leads to different large series of topological states. The first series are the so-called eigenvalue stable (strong, weak and crystalline) topological states, whose characters at high symmetry points cannot be expressed as linear combination (sum or difference) of characters of EBRs. These have been fully classified and progress towards material high-throughput has been

made [37, 38, 43, 44, 46–48], with several partial catalogues of topological materials already existed. The second series are the so-called fragile states of matter - which here we call eigenvalue fragile phases (EFPs) - they cannot be written purely as a sum of characters (traces of representations) of EBRs but can be written as sums and differences of characters of EBRs. Last, there exist stable/fragile states also not characterizable by characters or irreps - they are characterized by the flow of Berry phases. These fragile phases currently lack classifications - and lack any material examples. A schematic of the classifications is shown in Fig. 1.

Fragile states show up in the examples of TQC [37, 56] although their potential has only been fully identified after [38, 42, 54, 55, 57–62]. Refs. [55–59] have discovered a small number of models of EFP by applying the methods of TQC but neither a general, complete, (or even partial) classification, nor *any* material examples for these phases are known. This leaves us in the un-enviable situation of being far from a theoretical understanding of a so far purely theoretical phase of matter. In this work, we perform —for the first time— three separate tasks. **(1)** We provide an elegant, mathematical framework to *fully* classify and diagnose *all* the EFPs. **(2)** We apply this formalism to the spin-orbit coupling (SOC) doubled groups with time-reversal symmetry (TRS) and classify all the 340,590 EFPs that can exist - a much richer structure than in stable/strong topological phases. **(3)** We provide examples of one hundred fragile bands in different real materials, some of them extremely well isolated in energy from other bands. Our framework is closely related to the mathematical theories of polyhedra and affine monoids, bringing highly esoteric mathematical concepts into real material structures. (See Appendix F for a mathematical definition.) Thus we call our method the polyhedron method. To underscore the importance of fragile topology, the low-lying states of twisted bilayer graphene

* These authors contributed equally to this work

† bernevig@princeton.edu

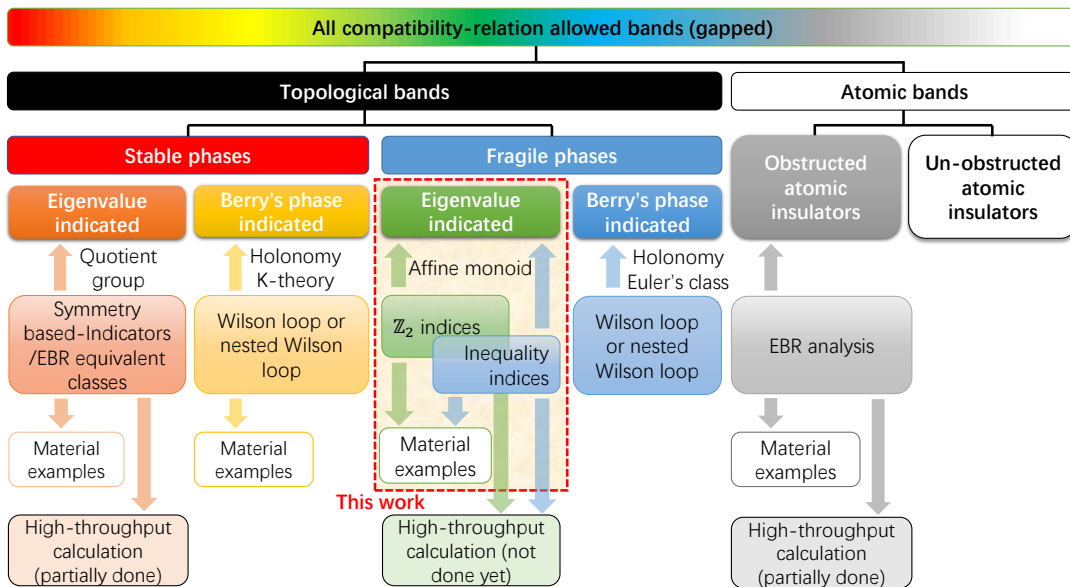


FIG. 1. The classification of topological bands, where the shaded area represent the contents of the present work. All the band structures are classified into three categories: stable topological bands, fragile topological bands, and atomic (trivial) bands. The stable or fragile topological bands are further classified into two sub-categories: those indicated by symmetry eigenvalues and those not indicated by symmetry eigenvalues. The atomic bands are also classified into two subcategories depending on whether the Wannier functions locate at the positions of atoms. The not-eigenvalue-indicated topological states are usually identified by the Wilson loop method [30, 52–55]; but the general framework to calculate their topological invariants is still unknown. The eigenvalue-indicated stable topological states are classified by the TQC [37] and other theories [38, 50]. The present work finishes the classification of eigenvalue-indicated fragile topological states (EFPs).

(TBG), a wonder-material engineered of two twisted layers of graphene [63–68], is predicted to exhibit a fragile topology [55, 58, 59, 69, 70].

II. EFPS IN VIEWPOINT OF TQC

To obtain the mathematical structure of EFPs we first review their definition from the viewpoint of TQC. A band structure is *partially* indexed by its decomposition into irreducible representations (irreps) at the high symmetry momenta [37–39]. Such a decomposition is described by a “symmetry data vector”, where entries give the multiplicities of the irreps in the decomposition. To be specific, we write the symmetry data vector as

$$B = (m_{1K_1}, m_{2K_1}, \dots, m_{1K_2}, m_{2K_2}, \dots)^T. \quad (1)$$

Here K_1, K_2, \dots are a known set of sufficient high symmetry momenta (maximal k-vectors in [40]), and m_{iK} is the multiplicity of the i -th irrep of the little group at K . (Different maximal k-vectors can have different irreps.) For example, for a one-dimensional system with only inversion symmetry, the symmetry data vector is written as $B = (m_{+0}, m_{-0}, m_{+\pi}, m_{-\pi})^T$, where the four entries represent the multiplicities of the inversion even(+)/odd(-) irrep at $k = 0, \pi$, respectively. The symmetry data vector of a gapped band structure necessarily satisfies

a set of rules called “compatibility relations” (available for all SGs on the BCS [37–41, 51]), which dictate if a given band structure can exist in the Brillouin Zone (BZ). In the 1D example, the compatibility relation is trivial and enforces an equal band number at $k = 0, \pi$: $m_{+0} + m_{-0} = m_{+\pi} + m_{-\pi}$. We always assume that the symmetry data vector satisfies the compatibility relations. For the symmetry data to be consistent with a *trivial* insulator, it should be induced by local orbitals forming representations of the SG in real space. Such trivial insulators are labeled as band representations (BRs); their symmetry data vectors are defined as “trivial”. The generators of BRs are the EBRs [71, 72].

In the 1D example, there are four EBRs, induced by the even(+)/odd(-) orbital at $x = 0/\frac{1}{2}$, respectively. They are $\text{ebr}_1 = (1, 0, 1, 0)^T$, $\text{ebr}_2 = (0, 1, 0, 1)^T$, $\text{ebr}_3 = (1, 0, 0, 1)^T$, and $\text{ebr}_4 = (0, 1, 1, 0)^T$, respectively. In general, we can define the EBR matrix as $EBR = (\text{ebr}_1, \text{ebr}_2, \dots)$, where the i -th column of the EBR matrix ebr_i is the i -th EBR of the corresponding SG. A symmetry data vector B is trivial if and only if there exist $p_1, p_2, \dots \in \mathbb{N}$ (\mathbb{N} stands for the non-negative integers) such that $B = p_1 \text{ebr}_1 + p_2 \text{ebr}_2 + \dots$, or, equivalently,

$$\exists p = (p_1, p_2, \dots)^T \in \mathbb{N}^{N_{EBR}} \text{ s.t. } B = EBR \cdot p. \quad (2)$$

Here N_{EBR} is the number of EBRs in the SG. Crucially, the EBRs may not be linearly independent: given B the

corresponding p may not be unique.

Because bands are only partially defined by symmetry data vectors, not all trivial symmetry data vectors imply trivial insulators (topological insulator in space group $P1$ have trivial symmetry data vectors). Hence nontrivial symmetry data is a sufficient but not necessary condition for a band to be topological nontrivial.

For any symmetry data vector B satisfying compatibility relations, there always exists $p \in \mathbb{Q}^{N_{EBR}}$ (rational number) such that $B = EBR \cdot p$ (for a proof, see [38] and also in more detail [73]). Due to this property, *nontrivial* symmetry data vectors can be further classified into two cases, both included in the TQC formalism [37, 42]: (i) B cannot be written as an integer combination of EBRs but can only be written as fractional rational combination of EBRs, (ii) B can be written as an integer combination of EBRs, and at least one of the coefficients is *necessarily* negative. Case-(i) is characterized by topological indices: symmetry-based indicators [38, 44] or EBR equivalence classes [37], and implies robust topology [38, 43, 44]. Case-(ii), on the other hand, implies fragile topology [42, 54–57], and no classification, indices, or material examples are known for it. We provide a full classification and 100 material examples below. A symmetry data vector in case-(ii) can be generally written as $B = \sum_i p_i \text{ebr}_i - \sum_j q_j \text{ebr}_j$, with $p_i, q_j \in \mathbb{N}$ and $p_i q_i = 0$ for all i . (Although not all vectors written in such form represent fragile phases. For example, if $\text{ebr}_1 + \text{ebr}_2 = \text{ebr}_3$, then $\text{ebr}_3 - \text{ebr}_2 = \text{ebr}_1$ is not fragile.) The topologically nontrivial restriction is that B does not decompose to a sum of EBRs. Once coupled to an atomic insulator BR $\sum_j q_j \text{ebr}_j$, the total band structure, i.e., $\sum_i p_i \text{ebr}_i$, represents a trivial symmetry data vector removing the topology imposed by symmetry eigenvalues - thus “fragile”.

We now introduce a convenient parametrization of the symmetry data. We can always write the Smith Decomposition of the EBR matrix as $EBR = L\Lambda R$, with L (correspondingly R) an $N_B \times N_B$ (correspondingly $N_{EBR} \times N_{EBR}$) unimodular integer matrices, N_B the length of symmetry data vector, Λ a $N_B \times N_{EBR}$ matrix with diagonal integer entries $\Lambda_{ij} = \delta_{ij} \lambda_i$ for $i = 1, 2 \dots N_B$, $j = 1, 2 \dots N_{EBR}$, where $\lambda_i > 0$ for $r = 1 \dots r$ and $\lambda_i = 0$ for $i > r$, with r the EBR matrix rank (Appendix A). For $B = EBR \cdot p$, for some $p \in \mathbb{Q}^{N_{EBR}}$, we can equivalently write the symmetry data vector as

$$B_i = \sum_{j=1}^r L_{ij} \lambda_j y_j, \quad (3)$$

where y is defined as $y_j = (Rp)_j$ ($j = 1 \dots r$). While, in general, the map from p to y is many-to-one due to linear dependence of EBRs, the map from y to B is one-to-one: if y and y' map to the same B , $(\sum_j L_{ij} \lambda_j y_j = \sum_j L_{ij} \lambda_j y'_j)$, multiplying L^{-1} on both sides gives $y = y'$. Table S1 in [74] tabulates the parametrizations in all SGs.

As the symmetry data vector B entries represent the

multiplicities of the irreps they should be integer non-negative valued for any physical band structure, conditions which are not automatically guaranteed by the parametrization in Eq. (3). We ask: what conditions should the y -vector satisfy so that B is: (1) non-negative (zero and strictly positive), (2) integer. For (2), since the L matrix is unimodular, B is an integer vector iff $\lambda_i y_i$ ($i = 1 \dots r$) are all integers, or $y_i = c_i / \lambda_i$ where $c_i = (L^{-1}B)_i \in \mathbb{Z}$. For the trivial and for the nontrivial fragile (case-(ii)) symmetry data vectors, both of which can be written as integer combinations of EBRs - $p \in \mathbb{Z}^{N_{EBR}}$, the corresponding $y_i = (Rp)_i$ vector must be an integer. A fractional y , where $c_i \neq 0 \pmod{\lambda_i}$ for some i , corresponds to a symmetry data vector B in the nontrivial case-(i). In fact, $c_i = (L^{-1}B)_i \pmod{\lambda_i}$ are the symmetry-based indicators [38, 43, 44] or equivalently, the distinct EBR equivalence classes of [37]. In this article, we take the y vector always integer to consider trivial and nontrivial fragile (case-(ii)) symmetry data vectors B .

All the EFPs (nontrivial case-(ii)) have trivial symmetry-based indicators. Instead, the EFPs are diagnosed by the *fragile indices*. We prove that all band structures with time-reversal symmetry and SOC have only two kinds of fragile indices: a \mathbb{Z}_2 -type (modulo 2) and an inequality-type (Appendix C). We give examples of both these cases.

III. EXAMPLES OF FRAGILE INDICES

A. Example of \mathbb{Z}_2 -type fragile indices

We consider SG 199 ($I2_13$). SG 199 has three EBRs, as shown in Fig. 2. ebr_1 and ebr_3 split into disconnected branches. According to Ref. [37], in each of the splitted EBRs, at least one branch is topological. For example, the upper branch in ebr_1 is not an EBR and hence must be topological. Since it can be written as $\text{ebr}_3 - \text{ebr}_2$, it at least has a fragile topology.

Now we apply a complete analysis on the EFPs in SG 199. Since there are only three EBRs, the EBR matrix has three columns. Arranging the irreps in order of $\bar{\Gamma}_5$, $\bar{\Gamma}_6\bar{\Gamma}_7$, \bar{H}_5 , $\bar{H}_6\bar{H}_7$, \bar{P}_4 , \bar{P}_5 , \bar{P}_6 , \bar{P}_7 , we can write the EBR matrix as

$$EBR = \begin{pmatrix} 0 & 2 & 2 \\ 2 & 1 & 2 \\ 0 & 2 & 2 \\ 2 & 1 & 2 \\ 2 & 0 & 1 \\ 0 & 1 & 1 \\ 0 & 1 & 1 \\ 2 & 2 & 3 \end{pmatrix}. \quad (4)$$

Here we have omitted the N point because N has only one type of irrep. The Smith Decomposition of the $EBR =$

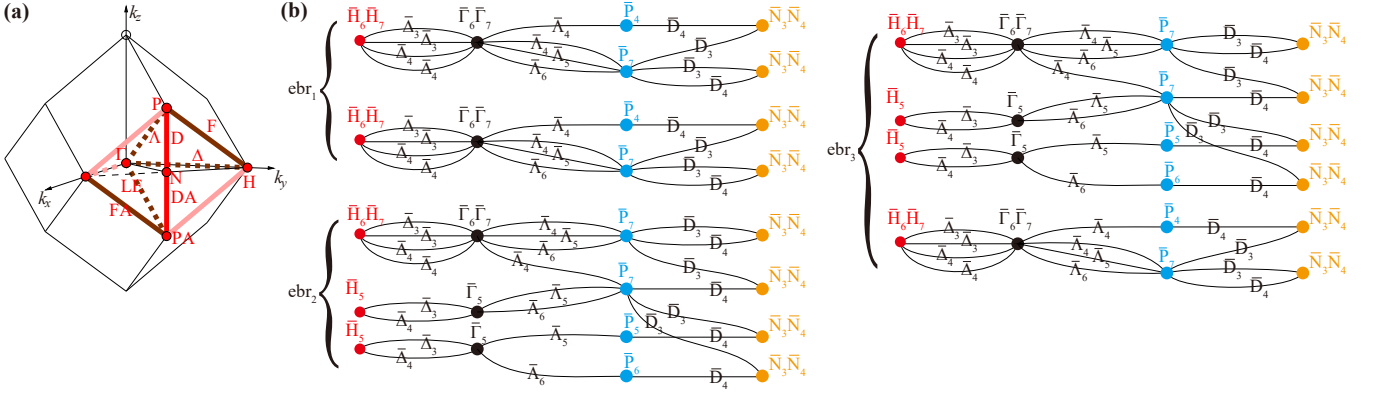


FIG. 2. (a) BZ of SG 199 ($I2_13$). (b) The EBRs of SG 199. The dots and lines represent high symmetry points and the high symmetry lines connecting the high symmetry points, respectively. The symbols of irreps, *e.g.*, $\Gamma_6\Gamma_7$, are defined on the REPRESENTATIONS DSG tool of the BCS [37, 40, 51].

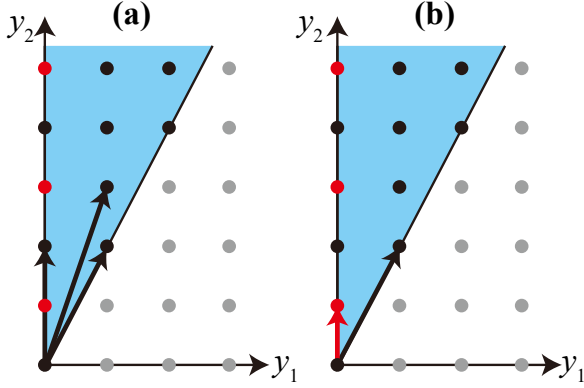


FIG. 3. (a) EFPs in SG 199 ($I2_13$). The shaded area represents the cone Y , the black points represent the trivial points in \bar{Y} , the red points represent the EFPs, and the grey points correspond to un-physical symmetry data. The three bold vectors $(0,2)^T$, $(1,2)^T$, $(1,3)^T$ are the generators of trivial points. (b) The Hilbert bases of \bar{Y} . The two bold vectors, *i.e.*, $(0,1)^T$, $(1,2)^T$, generates all the points in \bar{Y} . $(0,1)^T$ is nontrivial and corresponds to a fragile root, and $(1,2)^T$ is trivial and corresponds to an EBR.

LAR matrix is

$$\begin{pmatrix} 2 & 0 & 1 & 0 & 0 & 0 & 0 & 0 \\ -1 & 1 & 0 & 0 & 0 & 0 & 0 & 0 \\ 2 & 0 & 0 & 1 & 0 & 0 & 0 & 0 \\ -1 & 1 & 0 & 0 & 1 & 0 & 0 & 0 \\ -2 & 1 & 0 & 0 & 0 & 1 & 0 & 0 \\ 1 & 0 & 0 & 0 & 0 & 0 & 1 & 0 \\ 1 & 0 & 0 & 0 & 0 & 0 & 0 & 1 \\ 0 & 1 & 0 & 0 & 0 & 0 & 0 & 0 \end{pmatrix} \begin{pmatrix} 1 & 0 & 0 \\ 0 & 1 & 0 \\ 0 & 0 & 0 \\ 0 & 0 & 0 \\ 0 & 0 & 0 \\ 0 & 0 & 0 \\ 0 & 0 & 0 \\ 0 & 0 & 0 \end{pmatrix} \begin{pmatrix} 0 & 1 & 1 \\ 2 & 2 & 3 \\ -1 & -1 & -1 \end{pmatrix}, \quad (5)$$

The Λ matrix has only two nonzero elements, meaning $r = 2$, so the symmetry data is parameterized by a two-component integer vector $y = (y_1, y_2)^T$. From Eq. (3),

the symmetry data vector is then given by

$$B = (2y_1, -y_1 + y_2, 2y_1, -y_1 + y_2, -2y_1 + y_2, y_1, y_1, y_2)^T. \quad (6)$$

To ensure $B \geq 0$, the y -vector should satisfy $y_2 \geq 2y_1 \geq 0$. Therefore, the physical symmetry data vectors, *i.e.*, B 's, belong to the set of integer points \bar{Y} in the 2D cone (open triangle) $Y = \{y \in \mathbb{R}^2 | y_2 \geq 2y_1 \geq 0\}$ defined as

$$\bar{Y} = \mathbb{Z}^2 \cap Y = \{y \in \mathbb{Z}^2 | y_2 \geq 2y_1 \geq 0\}. \quad (7)$$

and shown in Fig. 3a. The trivial symmetry data vectors can be written as sums of EBRs, *i.e.*, $B = EBR \cdot p$ for $p \in \mathbb{N}^{N_{EBR}}$. They are represented by the y vectors belonging to

$$\bar{X} = \{y \in \mathbb{Z}^T | y_i = (Rp)_i \quad p \in \mathbb{N}^{N_{EBR}}\}. \quad (8)$$

In the case of Eq. (5), we can write the trivial points as

$$\bar{X} = \{p_1(0,2)^T + p_2(1,2)^T + p_3(1,3)^T \mid p_{1,2,3} \in \mathbb{N}\}, \quad (9)$$

i.e., the black points in Fig. 3a, generated by non-negative p combinations of the three vectors $(0,2)^T, (1,2)^T, (1,3)^T$. One can find that $(0,2)^T, (1,2)^T, (1,3)^T$ correspond to the ebr_1, ebr_2 , and ebr_3 shown in Fig. 2, respectively. We deduce that the nontrivial fragile symmetry data vectors, or the EFPs, are represented by the points in $\bar{Y} - \bar{X}$; these are the red points in Fig. 3a.

We provide the explicit index for EFPs in SG 199. Consider the subset $y_1 = 0$ of \bar{Y} . Only one generator, *i.e.*, $(0,2)^T$, satisfies this constraint. All the *trivial* points in the $y_1 = 0$ subset of \bar{Y} are generated by it. The points $(0, 2p+1)^T$ ($p \in \mathbb{N}$) cannot be reached by non-negative combinations p of EBRs and are nontrivial (fragile). Thus one fragile criterion of SG 199 is given by

$$y_1 = 0, \quad \text{and} \quad y_2 = 1 \pmod{2}, \quad (10)$$

where $y_2 \pmod{2}$ is the \mathbb{Z}_2 index, and $y_1 = 0$ is the condition for the EFP to be diagnosable. Are there

any other fragile indices (for other points in \bar{Y})? For y_2 even (remembering $y_2 \geq 2y_1$), we can rewrite y as $y = y_1(1, 2)^T + (\frac{1}{2}y_2 - y_1)(0, 2)^T$ and reach all points in this subspace of \bar{Y} ; for y_2 odd and $y_1 \geq 1$, Eq. (7) implies $y_2 \geq 2y_1 + 1$, and we can rewrite y as $y = (1, 3)^T + (y_1 - 1)(1, 2)^T + (\frac{1}{2}y_2 - \frac{1}{2} - y_1)(0, 2)^T$ and reach all points in this subspace of \bar{Y} . In both cases, we find the points are trivial. Hence only y_2 odd and $y_1 = 0$ are fragile and Eq. (10) is the only fragile index in SG 199. In Fig. 3, we present a diagrammatic illustration of the points in \bar{Y} and points in \bar{X} , from which one immediately concludes Eq. (10). A (Hilbert) basis for all points in \bar{Y} - will be provided later.

B. Example of inequality-type fragile indices

We consider SG 70 (*Fddd*). The Smith Decomposition of the $EBR = LAR$ matrix is

$$\begin{pmatrix} -2 & -1 & -1 & 0 & 1 \\ 2 & 3 & 1 & 0 & 0 \\ 0 & 1 & 0 & 0 & 1 \\ -1 & 2 & 0 & 0 & 0 \\ 1 & 0 & 0 & 1 & 0 \end{pmatrix} \begin{pmatrix} 1 & 0 & 0 & 0 & 0 \\ 0 & 1 & 0 & 0 & 0 \\ 0 & 0 & 4 & 0 & 0 \\ 0 & 0 & 0 & 0 & 0 \\ 0 & 0 & 0 & 0 & 0 \end{pmatrix} \begin{pmatrix} 1 & 1 & 3 & 3 & 1 \\ 1 & 2 & 2 & 2 & 2 \\ -1 & -2 & -2 & -3 & -1 \\ 0 & 0 & 0 & 0 & 1 \\ 0 & 0 & 1 & 0 & 0 \end{pmatrix}, \quad (11)$$

where the corresponding TRS and double-group irreps are $\bar{\Gamma}_5, \bar{\Gamma}_6, \bar{\Gamma}_3\bar{\Gamma}_4, \bar{\Gamma}_2\bar{\Gamma}_2, \bar{\Gamma}_3\bar{\Gamma}_3$, respectively. Irreps at the maximal k -vectors Y and Z (not shown) are determined by the irreps at Γ using TRS and compatibility relations (see [37–41, 51]).

The Λ matrix has only three nonzero elements ($r = 3$), so the symmetry data is parameterized by a three-component integer vector $y = (y_1, y_2, y_3)^T$. By requiring the symmetry data vector $B \geq 0$, we obtain a set of inequalities for y defining a 3D cone

$$Y = \{y \in \mathbb{R}^3 \mid 2y_2 \geq y_1 \geq 0, -2y_1 - y_2 \geq 4y_3 \geq -2y_1 - 3y_2\}. \quad (12)$$

The physical symmetry data vectors B 's are represented by integer points in Y , i.e., $\bar{Y} = \mathbb{Z}^3 \cap Y$. Each inequality in Eq. (12) specifies a plane in \mathbb{R}^3 : the plane separates the points that do or do not satisfy the inequality. The cone Y is cut out by four such planes specified by the four inequalities in Eq. (12). As shown in Eq. 3a, these planes cross each other at four rays contained in this cone. We obtain the directions of the four rays as $\mathbf{r}_1 = (0, 4, -1)^T$, $\mathbf{r}_2 = (0, 4, -3)^T$, $\mathbf{r}_3 = (8, 4, -7)^T$, $\mathbf{r}_4 = (8, 4, -5)^T$. For example, the planes $y_1 = 0$ and $-2y_1 - y_2 = 4y_3$ intersect each other on the line $t \cdot \mathbf{r}_1$, $t \in \mathbb{R}$; the planes $y_1 = 0$ and $2y_2 = y_1$ intersect on the line $t \cdot (0, 0, 1)$, $t \in \mathbb{R}$, which (except for $t = 0$, a point which is already included in the other ray $t \cdot \mathbf{r}_1$) does not satisfy the second inequality in Eq. (12) and hence do not provide a separate ray.

The trivial points in Y (and \bar{Y}) are given by Eq. (8). For simplicity, we first consider points in the cone

$$X = \{y \in \mathbb{R}^r \mid y_i = (Rp)_i \quad p \in \mathbb{R}_+^{N_{EBR}}\}. \quad (13)$$

In the general case $\mathbb{Z}^r \cap X$ is a superset of \bar{X} (their difference being the non-integer $p > 0$, such that $y \in \mathbb{Z}^r$).

Due to the definition of X , and since $r = 3$ in Eq. (13) for SG 70, it seems that (the first 3 rows of) each column of R corresponds to a generator of X . However, in Eq. (11), (the first 3 rows of) the first column of R , i.e., $(1, 1, -1)^T$, can be spanned by the second and third columns as $\frac{1}{4}(1, 2, -2)^T + \frac{1}{4}(3, 2, -2)^T$, thus X is generated by the last four columns of R . (There exists a linear dependence between the 4 vectors defined by the first 3 rows of each of the last 4 columns of R , but it involves negative coefficients, and hence the vectors are linearly independent in X .) As shown in Fig. 4a, each of the four generators corresponds to a ray of X : $\mathbf{r}'_1 = (2, 4, -2)^T$, $\mathbf{r}'_2 = (2, 4, -4)^T$, $\mathbf{r}'_3 = (6, 4, -6)^T$, $\mathbf{r}'_4 = (6, 4, -4)^T$ (the rays are chosen as twice the generators for aesthetical purposes in Fig. 4a). Using elementary vector algebra, as explained in Appendix B, one finds the inequalities defining X ,

$$X = \{y \in \mathbb{R}^3 \mid 3y_2 \geq 2y_1 \geq y_2, -2y_1 - y_2 \geq 4y_3 \geq -2y_1 - 3y_2\}. \quad (14)$$

Illustrated in Fig. 4a, X is, as it should be, a subset of Y . The first/last two defining inequalities of X are tighter than/identical to the first/last two of Y , respectively. For a point in Y to be outside the trivial X , at least one of the first two inequalities of X should be violated, i.e.,

$$2y_1 - 3y_2 > 0 \quad \text{or} \quad y_2 - 2y_1 > 0. \quad (15)$$

Eq. (15) gives two inequality-type fragile indices for SG 70, which can also be obtained in a diagrammatic method. From Fig. 4a, we see that the boundaries separating X and Y , i.e., $\mathbf{O}\mathbf{r}'_1\mathbf{r}'_2$ and $\mathbf{O}\mathbf{r}'_3\mathbf{r}'_4$, are parallel to the y_3 -axis, where \mathbf{O} stands for the origin. (Notice that all $\mathbf{r}_1 - \mathbf{r}_2, \mathbf{r}_3 - \mathbf{r}_4, \mathbf{r}'_1 - \mathbf{r}'_2, \mathbf{r}'_3 - \mathbf{r}'_4$ are parallel to y_3 .) We project the cones to the y_1y_2 plane to obtain Fig. 4b, from which we immediately conclude Eq. (15).

Since in general $\mathbb{Z}^r \cap X$ is a superset of \bar{X} , in principle there can be nontrivial points in $\mathbb{Z}^r \cap X - \bar{X}$. For example, for SG 199, X (defined by Eq. (13)) is spanned by the rays $(0, 1)^T$ and $(1, 2)^T$ and is hence identical to Y (Fig. 4a). Thus Eq. (10) identifies points in $\mathbb{Z}^2 \cap X - \bar{X}$. However, for SG 70, there is no such point in $\mathbb{Z}^3 \cap X - \bar{X}$. We verify this by explicitly listing the integer points in X and by applying a general technique we introduce in Appendix C to calculate $\mathbb{Z}^r \cap X - \bar{X}$.

IV. THE POLYHEDRON METHOD

We have outlined the polyhedron method through the two previous examples. Now we summarize its general principle.

A. Polyhedron description of symmetry data vectors

In Eq. (3) we parameterized the symmetry data as $B = \sum_j (LA)_j y_j$, where $(LA)_j$ represents the j th column of

r	SG	Basis		Index		r	SG	Basis		Index		r	SG	Basis		Index							
		ebr	root	ieq	\mathbb{Z}_2			ebr	root	ieq	\mathbb{Z}_2			ebr	root	ieq	\mathbb{Z}_2						
2	199	1	1	0	1	4	218	2	6	6	0	8	148	8	140	24	0						
	208	1	1	0	1		219	2	6	6	0		71	10	132	28	0	166	8	140	24	0	
	210	1	1	0	1		220	5	5	4	4		85	10	16	24	0	193	9	975	30	24	
	214	1	1	0	1		11	9	8	8	0		125	10	16	24	0	200	8	64	24	0	
3	70	5	10	2	0	5	13	9	8	8	0	6	129	10	16	24	0	9	224	11	90	40	0
	150	2	2	1	3		14	8	8	8	0		132	10	92	24	0		226	11	334	28	0
	157	2	2	1	3		15	9	60	12	0		163	8	68	12	4		227	13	464	26	0
	159	4	2	1	1		49	9	8	8	0		165	6	40	12	12		2	16	1136	240	0
	173	4	2	1	1		51	9	8	8	0		190	9	51	10	0		10	16	1136	240	0
	182	4	2	1	1		53	8	8	8	0		201	10	8	12	0		47	16	1136	240	0
	185	2	2	1	3		55	8	8	8	0		203	10	84	16	0		87	14	1188	56	0
	186	4	2	1	1		58	8	8	8	0		205	8	6	2	0		139	14	1188	56	0
4	63	7	4	4	0	5	66	9	60	12	0	7	206	8	13	4	4	10	147	8	668	56	16
	64	6	4	4	0		67	9	8	8	0		215	5	16	16	0		162	8	668	56	16
	72	7	4	4	0		74	9	60	12	0		216	9	36	14	0		164	8	668	56	16
	121	6	4	4	0		81	8	8	8	0		222	7	22	12	0		176	12	3070	54	0
	126	6	8	4	0		82	8	8	8	0		12	12	224	56	0		192	11	723	30	24
	130	7	8	4	0		86	8	16	8	0		65	12	224	56	0		194	12	3070	54	0
	135	7	8	4	0		88	8	78	12	0		84	12	700	56	0		174	15	615	108	0
	137	6	8	4	0		111	8	8	8	0		128	11	128	12	0		187	15	615	108	0
	138	7	8	4	0		115	8	8	8	0		131	12	700	56	0		225	14	3208	34	0
	143	6	6	3	5		119	8	8	8	0		140	12	220	24	0		229	14	868	88	0
	149	6	6	3	5		134	8	16	8	0		188	12	102	18	28		83	20	58840	240	0
	156	6	6	3	5		136	8	44	12	0		189	10	49	20	0		123	20	58840	240	0
	158	6	6	3	5		141	8	78	12	0		202	8	48	12	0		175	17	72598	228	0
	168	3	3	2	3		167	6	10	4	0		204	8	24	16	0		191	17	72598	228	0
	177	3	3	2	3		217	3	8	8	0		223	4	57	28	16		221	20	51308	116	0
	183	3	3	2	3		228	5	7	8	4		8	124	14	252	24		0				
184	3	3	2	3	230	5	19	4	4	127	12	328		24	0								

TABLE I. Sizes of Hilbert bases and numbers of fragile indices in SGs with time-reversal symmetry and significant SOC. SGs that do not have fragile indices are not tabulated. “rank” represents the rank of the EBR matrix. “ebr” and “root” represent the numbers of EBRs and fragile roots in the Hilbert bases of \bar{Y} , respectively. And, “ieq” and “ \mathbb{Z}_2 ” represent the numbers of inequality-type indices and \mathbb{Z}_2 -type indices, respectively.

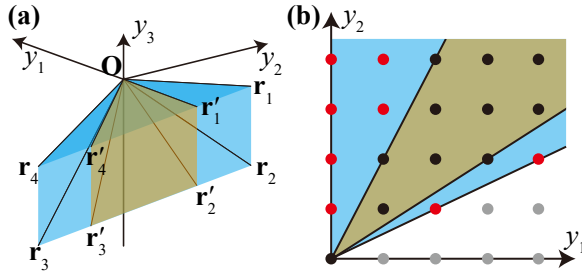


FIG. 4. (a) The cones Y and X for SG 70 ($Fddd$). The blue and yellow regions represent Y and X , respectively. The ray vectors for Y/X are $\mathbf{r}_{1,2,3,4}/\mathbf{r}'_{1,2,3,4}$ respectively, given in the main text. (b) The projections of Y and X in the y_1y_2 plane. The black points correspond to trivial symmetry data vectors B , the red points correspond to EFPs, and the grey points are un-physical.

(LA). Now we define a polyhedral cone as

$$Y = \left\{ y \in \mathbb{R}^r \mid \sum_j (LA)_j y_j \geq 0 \right\}. \quad (16)$$

The physical symmetry data vectors $B \in \mathbb{N}$ are faithfully represented by integer points $\bar{Y} = \mathbb{Z}^r \cap Y$. Due to Theorem 4 in Appendix F, Y can be represented by its rays and lines as

$$Y = \{ Ray \cdot p + Line \cdot q \mid p \in \mathbb{R}_+^m, q \in \mathbb{R}^n \}. \quad (17)$$

where $Ray = (Ray_1, Ray_2, \dots)$ is an $r \times m$ matrix, and $Line = (Line_1, Line_2, \dots)$ is an $r \times n$ matrix. The difference between rays and lines is that rays have directions but lines do not. Correspondingly, the coefficients on rays (p_i 's) are nonnegative but the coefficients on lines (q_j 's) can be either nonnegative or negative. For example, in Fig. 3, Y has two rays $(0, 1)^T$ and $(1, 2)^T$, but no lines. A polyhedral cone is called *pointed* if it does not contain lines. Now we show that for any space group Y is a pointed polyhedral cone. Choosing $p = 0$ and arbitrary q , due to Eq. (16) we have $LA_{:,1:r} Line \cdot q \geq 0$ as well as $LA_{:,1:r} Line \cdot q \leq 0$ since we can replace q with $-q$, and thus $\forall q \in \mathbb{R}^n$, $LA_{:,1:r} Line \cdot q = 0$. As $LA_{:,1:r}$ is a rank- r matrix, there must be $Line = 0$. In this paper, Eq. (16) is called the H-representation of polyhedron and Eq. (17) is called the V-representation. The algorithm to determine the V-representation from the H-representation and vice

versa is available in many mathematics packages such as the *SageMath* package [75].

The trivial B -vectors, which decompose into positive sums of EBRs, are given as \bar{X} (Eq. (8)). \bar{X} is a subset of \bar{Y} , thus fragile symmetry data vectors are generated from points in $\bar{Y} - \bar{X}$. To classify them, we introduce an auxiliary polyhedral cone X (Eq. (13)), which can be thought as an extension of \bar{X} to allow non-negative real (not only integer) combination coefficients p_i . The nontrivial points can then be divided into two parts: $\bar{Y} - \mathbb{Z}^r \cap X$ and $\mathbb{Z}^r \cap X - \bar{X}$. Points in $\bar{Y} - \mathbb{Z}^r \cap X = \mathbb{Z}^r \cap (Y - X)$ correspond to symmetry data vectors B that cannot be written as non-negative combinations of the EBRs, even if the combination coefficients p_i are allowed to be rational numbers. Points in $\mathbb{Z}^r \cap X - \bar{X}$, on the other hand, correspond to symmetry data that can be written as non-negative rational combinations of EBRs but cannot be written as non-negative integer combinations of EBRs.

Readers might refer to Appendix B1 for more examples of X and Y .

Points in $\mathbb{Z}^r \cap (Y - X)$ are outside X and so violate the inequalities of X . Thus, in general, points in $\mathbb{Z}^r \cap (Y - X)$ are diagnosed by the inequality-type indices, as in SG 70. On the other hand, points in $\mathbb{Z}^r \cap X - \bar{X}$ are always near the boundary of X and are diagnosed by the \mathbb{Z}_2 -type indices. In the following we discuss these two types of indices in detail.

B. Inequality-type fragile indices

Now let us work out the inequality-type fragile criteria for $\mathbb{Z}^r \cap (Y - X)$. First, we assume the H-representation of X as $X = \{y \in \mathbb{R}^r | Ay \geq 0, Bx = 0\}$, where $A \in \mathbb{Q}^{n \times r}$, $B \in \mathbb{Q}^{m \times r}$, r is the rank of EBR, and n, m some positive integers. (See Theorem 4 for the general form of H-representation.) Now we show that B must be zero. Since the first r rows of R has the rank r , X is an r -dimensional object. Presence of nonzero B implies constraints on the points in X and hence a lower-dimension of X . Thus B has to be zero and the H-representation of X can always be written as

$$X = \{x \in \mathbb{R}^r | Ax \geq 0\}. \quad (18)$$

For a point y in $\mathbb{Z}^r \cap (Y - X)$, there should be some row in A , denoted as a , such that $ay < 0$, so that $y \notin X$. Therefore, in principle, each row of A gives an inequality-type fragile index $-ay$ and $-ay > 0$ implies fragile phase. One needs to check whether $ay < 0$ is allowed in Y : if not allowed, there is no need to introduce the corresponding fragile index. The method (with an example) to remove such unallowed criteria is given in Appendix C1.

C. \mathbb{Z}_2 -type fragile indices

As proved in Appendix C, points in $\mathbb{Z}^r \cap X - \bar{X}$ are always near the boundary of X - the distances from these points to the boundary are always 0 or 1 - and so belong to some lower-dimensional sub-polyhedron of X . Integer sums (per Eq. (8)) of the generators of \bar{X} belonging to this lower-dimensional subspace may not reach every integer point in this subspace. For example, in SG 199, all the points in $\mathbb{Z}^r \cap X - \bar{X}$ also belong to the sub-cone $\{y \in \mathbb{Z}^2 | y_1 = 0, y_2 \geq 0\}$. The only \bar{X} generator in this sub-cone is $(0, 2)^T$. Thus $(0, y_2)$ cannot be generated if y_2 is odd, and $\mathbb{Z}^r \cap X - \bar{X} = \{y \in \mathbb{Z}^2 | y_1 = 0, y_2 \geq 0, y_2 \bmod 2 = 1\}$. As detailed in C, points in $\mathbb{Z}^r \cap X - \bar{X}$ can always be characterized by the decomposition coefficients of the \bar{X} generators that are restricted in some lower-dimensional subspace. If these coefficients are fractional, the corresponding symmetry data vectors B are nontrivial. Due to these fractional coefficients, in principle such diagnosis involves the modulo operation (see Eq. (10)). We find that only the modulo 2 operation is involved (see Eq. (10)), and we call these indices \mathbb{Z}_2 -type.

D. Fragile indices in all SGs

In Table I we summarize the numbers of inequality-type and \mathbb{Z}_2 -type indices in all SGs; in Table S2 of [74] we explicitly tabulate all the fragile indices.

The mathematics of EFPs is much richer than that of robust topology. The latter usually forms a group. For example in absence of TRS, according to the Chern number, the band insulators form an additive group \mathbb{Z} [76–78]; in the presence of TRS (and without any other symmetries), according to the \mathbb{Z}_2 invariant, the band insulators form a \mathbb{Z}_2 group [1–3]. However, neither \bar{Y} nor \bar{X} form a group. Instead, \bar{Y} and \bar{X} are semigroups: A general element, except the identity, does not have an inverse. To be specific, both \bar{Y} and \bar{X} can be written as $M = \{r_1 p_1 + r_2 p_2 + \dots + r_n p_n | p_1 \dots p_n \in \mathbb{N}\}$, for some n , and $r_1 p_1 + r_2 p_2 + \dots + r_n p_n = 0 \Rightarrow p = 0$, where r_i 's are the generators which are no longer constrained to all be the columns of R . (See Appendix B for the proof that \bar{Y} can be written in this form.) For example in SG 199, \bar{Y} can be written as $\{p_1(0, 1)^T + p_2(1, 2)^T | p_{1,2} \in \mathbb{N}\}$ (see Fig. 3). M is a *positive affine monoid* in mathematics, and we make use of monoid properties to obtain the EFP roots.

V. THE EFP ROOTS

We find that the EFPs and the trivial states are always generated by a finite set of generators. (\bar{Y} in SG 199 is generated by $(0, 1)^T$ and $(1, 2)^T$ (Fig. 3b). We call the nontrivial states in the generators of \bar{Y} the *EFP roots*. (Trivial states in the generators of \bar{Y} are EBRs.) By definition, an EFP can always be written as a sum

	$\bar{\Gamma}_7$	$\bar{\Gamma}_8$	$\bar{\Gamma}_9$	\bar{K}_4	\bar{K}_5	\bar{K}_6	\bar{M}_5		
E	2	2	2	E	1	1	2	E	2
$2C_6$	0	$-\sqrt{3}$	$\sqrt{3}$	$2C_3$	-1	-1	1	C_2	0
$2C_3$	-2	1	1	$3\sigma_v$	$-i$	i	0	σ_d	0
C_2	0	0	0					σ_v	0
$3\sigma_d$	0	0	0						
$3\sigma_v$	0	0	0						

TABLE II. Character tables of irreps at high symmetry momenta in SG $P6mm$ (with TRS). The little co-groups at Γ , K , and M are C_{6v} , C_{3v} , and C_{2v} respectively. C_6 , C_3 , C_2 represent the 6-, 3-, 2-fold rotations, and σ_d and σ_v represent the two classes of mirrors.

of EFP roots plus some EBRs. Thus the EFP roots can be thought as the *non-redundant* representatives of the EFPs. We worked out all the EFP roots in all SGs in presence of the TRS and the SOC, as tabulated in Table S3 of [74]. The numbers of EFP roots in all SGs are summarized in Table I. As discussed in Appendix B, as a positive affine monoid, \bar{Y} is generated by the *Hilbert bases*: all of the elements \bar{Y} can be written as a sum of Hilbert bases with positive coefficients, and none of the Hilbert bases can be written as a sum of other elements with positive coefficients. The Hilbert bases form a *unique* minimal set of generators of \bar{Y} . For a given SG, we first calculate the Hilbert bases and then identify the topological nontrivial ones as the EFP roots. There are two commonly used algorithms to get the Hilbert bases—the Normaliz algorithm [79] and the Hemmecke algorithm [80]. In this work, we mainly use the Hemmecke algorithm. In Table I we tabulate the numbers of EBRs and EFP roots in the Hilbert bases in all SGs.

We now present some examples of the roots for two known fragile phases. First we look at the SG 2 ($P\bar{1}$). Γ , R , T , U , V , X , Y , Z stand for the TRS momenta $(0, 0, 0)$, (π, π, π) , $(0, \pi, \pi)$, $(\pi, 0, \pi)$, $(\pi, \pi, 0)$, $(\pi, 0, 0)$, $(0, \pi, 0)$, $(0, 0, \pi)$, respectively. We find 1136 EFP roots in SG 2 (Table I). (We finally found that, upon coordinate rotation and gauge transformation, only 3 fragile roots are independent. See Table S8 of the SM of [73].) Two of the roots are given by

$$2\bar{\Gamma}_2\bar{\Gamma}_2 + 2\bar{R}_3\bar{R}_3 + 2\bar{T}_3\bar{T}_3 + 2\bar{U}_3\bar{U}_3 + 2\bar{V}_3\bar{V}_3 + 2\bar{X}_3\bar{X}_3 + 2\bar{Y}_3\bar{Y}_3 + 2\bar{Z}_2\bar{Z}_2, \quad (19)$$

and

$$4\bar{\Gamma}_2\bar{\Gamma}_2 + 4\bar{R}_3\bar{R}_3 + 4\bar{T}_3\bar{T}_3 + 4\bar{U}_3\bar{U}_3 + 4\bar{V}_3\bar{V}_3 + 4\bar{X}_3\bar{X}_3 + 4\bar{Y}_3\bar{Y}_3 + 4\bar{Z}_3\bar{Z}_3, \quad (20)$$

The subscript 2 (3) means that corresponding Kramer pair is odd (even) under inversion. Due to the Fu-Kane formula [81], Eq. (19) is the double of a centrosymmetric weak TI with the index $(0; 001)$. In Ref. [82], it has been shown that double of a 2D centro-symmetric TI remains nontrivial since its entanglement spectrum is gapless. Eq. (19) can be thought as a stacking of centrosymmetric double 2D TIs in the 001-direction. Eq. (20), on

the other hand, is four times of a 3D centrosymmetric TI. In Refs. [32, 35, 43, 44] it was shown that double of a 3D centrosymmetric TI is an inversion-protected topological crystalline insulator HOTI. Eq. (20) shows that the double of a HOTI is a fragile phase.

Secondly we look at SG 183 ($P6mm$) - the SG of graphene. As discussed in Refs. [55–58], in presence of C_2T symmetry ($(C_2T)^2 = 1$), a two-band system can host a fragile topology, and the topological invariant is given as the two-band Wilson loop winding. Refs. [55–57] have made use of TQC and similar methods to analyze the fragile phases in graphene. We relate the analysis of Refs. [55, 56] to our classification in which SG 183 has only three EFP roots $\bar{\Gamma}_7 + \bar{K}_6 + \bar{M}_5$, $\bar{\Gamma}_8 + \bar{K}_4 + \bar{K}_5 + \bar{M}_5$, $\bar{\Gamma}_9 + \bar{K}_4 + \bar{K}_5 + \bar{M}_5$. Here Γ , K , M stand for the high symmetry momenta $(0, 0, 0)$, $(\frac{2\pi}{3}, \frac{2\pi}{3}, 0)$, $(\pi, 0, 0)$, respectively. Due to compatibility relations, the irreps in the $k_z = \pi$ -plane are completely determined by the irreps in the $k_z = 0$ -plane. The irreps are defined in Table II. For the first root, the C_3 representation matrices at Γ and K can be written as $-\sigma_0$ and $e^{-i\frac{\pi}{3}\sigma_z}$, respectively. And, for the second and third roots, the C_3 representation matrices at Γ and K can be written as $e^{-i\frac{\pi}{3}\sigma_z}$ and $-\sigma_0$, respectively. Due to the correspondence between C_3 eigenvalues and Wilson loop winding in Refs. [55, 56], one can find that the Wilson loop winding in all the three cases are $3n \pm 1$ for n some integer, showing the topological nature of the state.

VI. MATERIALS

Armed with our new complete classification, we set out to discover examples of topological bands in existing materials. This is a particularly challenging task, as one recent catalogue of high-throughput topological materials [46] searched and found that *no materials are topologically fragile at the Fermi level*, due to the fact that there are usually enough occupied EBR to turn any fragile set of bands into trivial. Hence, we have to settle for finding fragile sets of *bands* hopefully close to the Fermi level. We have performed thousands of ab-initio calculations and have produced a list of 100 good materials which exhibit fragile topological bands close to the Fermi level (Table III). We showcase some of them in Fig. 5: CsAu_3S_2 , $\text{Bi}_2\text{Ru}_2\text{O}_7$, RbNiF_3 , and AlSiTe_3 have the fragile band right at or immediately below the Fermi level, well separated in the whole k -space sampled, from both the conduction and the valence bands. We computed our new fragile indices of these materials and confirmed them to be topological. This is the first time fragile topological bands have been predicted in crystalline systems. The (relatively) flat fragile bands in RbNiF_3 may have interesting interacting physics since the bandwidths are smaller than the on-site Hubbard interaction of Ni, which is usually 8-10eV.

Fragile topological bands have in-gap boundary states (the “filling anomaly” [83]) if the boundary cuts through

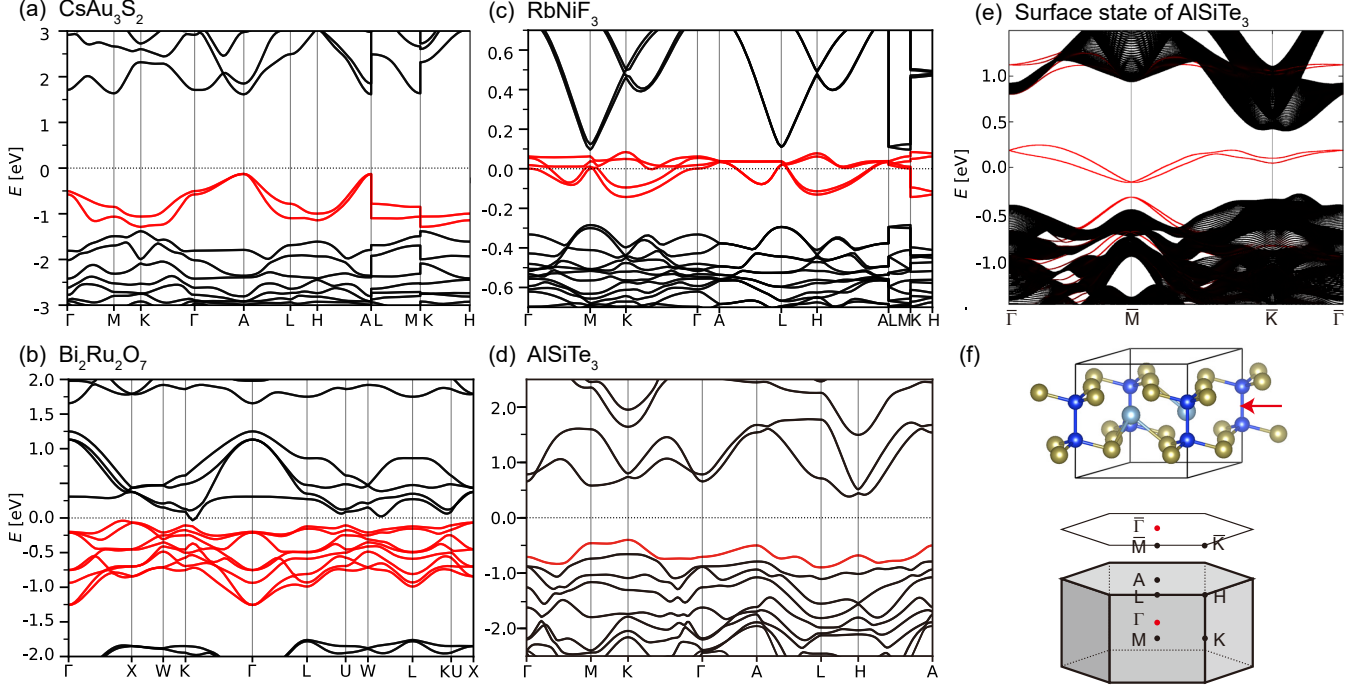


FIG. 5. Fragile bands in materials. (a) the band structure of CsAu_3S_2 (ICSD=82540) in SG 164 ($P\bar{3}m1$). (b) $\text{Bi}_2\text{Ru}_2\text{O}_7$ (ICSD=166566) in SG 227 ($Fd\bar{3}m$). (c) RbNiF_3 (ICSD=15090) in SG 194 ($P6_3/mmc$). (d) AlSiTe_3 (ICSD=75001) in SG 147 ($P\bar{3}$). (e) Top surface state of AlSiTe_3 . (f) The crystal structure of AlSiTe_3 and the bulk/surface BZ. The red arrow shows the position of surface termination. Here the fragile bands are colored as red, and the upper and lower bands are colored as black, and the Fermi-levels are represented by the horizontal dotted lines. More information about the fragile bands, such as irreps and gaps from lower and upper bands as well as a hundred more band structures with fragile topology, can be found in [74].

empty Wyckoff positions which have nonzero coefficients in the EBR decomposition. Here we take AlSiTe_3 as an example to show such in-gap states. The SG 147 $P\bar{3}$ has four types of maximal Wyckoff positions: $1a$ (000), $1b$ ($00\frac{1}{2}$), $3e$ ($\frac{1}{2}00$) ($0\frac{1}{2}0$) ($\frac{1}{2}\frac{1}{2}0$), $3f$ ($\frac{1}{2}0\frac{1}{2}$) ($0\frac{1}{2}\frac{1}{2}$) ($\frac{1}{2}\frac{1}{2}\frac{1}{2}$), and three types of non-maximal Wyckoff positions $2c$ (0,0, z) (0,0, $-z$), $2d$ ($\frac{1}{3}, \frac{2}{3}, z$) ($\frac{2}{3}, \frac{1}{3}, -z$), $6g$ (x, y, z) ($-y, x-y, z$) ($-x+y, -x, z$) ($-x, -y, -z$) ($y, -x+y, -z$) ($x-y, x, -z$). The Al, Si, and Te atoms occupy the $2d$, $2c$, and $6g$ positions, respectively. The BZ of SG 147 $P\bar{3}$, as shown in Fig. 5f, has six high symmetry momenta: Γ , K, M, A, H, L. The irreps formed by the fragile band shown in Fig. 5d are

$$\bar{\Gamma}_4\bar{\Gamma}_4 + \bar{K}_5\bar{K}_6 + \bar{M}_3\bar{M}_3 + \bar{A}_7\bar{A}_7 + \bar{H}_5\bar{H}_6 + \bar{L}_2\bar{L}_2. \quad (21)$$

These irreps decompose into EBRs as

$$\begin{aligned} &({}^1\bar{E}_g^2\bar{E}_g)_b \uparrow SG \oplus ({}^1\bar{E}_u^2\bar{E}_u)_b \uparrow SG \\ &\oplus (\bar{E}_u\bar{E}_u)_b \uparrow SG \ominus ({}^1\bar{E}^2\bar{E})_{2d} \uparrow SG, \end{aligned} \quad (22)$$

where $(\rho)_w \uparrow SG$ represent the EBR induced from the irrep ρ of the site-symmetry-group of the Wyckoff position w . Therefore, the fragile band is equivalent (in terms of irreps) to a combination of 3 Wannier functions at the b position and “-1” Wannier functions at the $2d$ position. We have checked that the trivial bands below the fragile band do not cancel the Wannier functions at $1b$. Now

we consider a surface terminating at the b position (as shown in Fig. 5f). Since the 3 Wannier states cannot be symmetrically divided into the two sides, there must be in-gap states on the surface. We confirm the existence of such in-gap states by a first-principle calculation of a slab (Fig. 5e).

We hope new experiments and predictions of responses in fragile states will follow our exciting discovery of fragile bands.

TABLE III: Fragile bands in materials. Fragile bands in materials. In the first three columns the chemical formulae, the space group numbers, and the ICSD numbers of the materials are tabulated. The fourth column gives the number of fragile branches in the band structure of the corresponding material. In the fifth to tenth columns the information of the fragile branch closest to the Fermi level are tabulated. “Bands” gives the band indices of the fragile branch. Here we refer the highest occupied band as the 0th band, and the lowest empty band as the 1st band, *etc.* “Irreps” gives the irreps formed by the fragile bands at high symmetry momenta. Δ_l (Δ_u) is the indirect gap between the fragile bands and the lower (upper) bands. Δ'_l (Δ'_u) is the direct gap between the fragile bands and the lower (upper) bands.

Formula	SG	ICSD	NF	Bands	Irreps	Δ_l (eV)	Δ_u (eV)	Δ'_l (eV)	Δ'_u (eV)
Cs(Au ₃ S ₂)	164	82540	2	-3 ~ 0	A ₄ A ₅ +A ₈ +Γ ₄ Γ ₅ +Γ ₈ +H ₄ H ₅ +H ₆ +K ₄ K ₅ +K ₆ +2L ₅ L ₆ +2M ₅ M ₆	0.0946	1.7424	0.0946	1.7424
RbNiF ₃	194	15090	3	-3 ~ 4	A ₄ A ₅ +A ₆ +2Γ ₁₀ +Γ ₁₁ +Γ ₁₂ +2H ₈ +2H ₉ +2K ₈ +2K ₉ +2L ₃ L ₄ +4M ₆	0.1416	0.0121	0.2149	0.0336
Rb ₆ Ni ₆ F ₁₈	194	410391	1	-3 ~ 4	A ₄ A ₅ +A ₆ +2Γ ₁₀ +Γ ₁₁ +Γ ₁₂ +2H ₈ +2H ₉ +2K ₈ +2K ₉ +2L ₃ L ₄ +4M ₆	0.1561	0.012	0.2329	0.0121
Bi ₂ (Ru ₂ O ₇)	227	166566	2	-15 ~ 0	Γ ₆ +Γ ₇ +3Γ ₁₀ +4X ₅ +3L ₆ L ₇ +5L ₉ +2W ₃ W ₄ +2W ₅ W ₆ +4W ₇	0.5048	0.0065	0.771	0.0865
Bi ₂ O ₃	164	186365	1	1 ~ 2	A ₈ +Γ ₈ +H ₄ H ₅ +K ₄ K ₅ +L ₃ L ₄ +M ₃ M ₄	0.4934	0.0	1.1165	0.2286
Pb ₄ Se ₄	225	238502	1	-3 ~ 0	Γ ₁₁ +X ₈ +X ₉ +L ₄ L ₅ +L ₉ +2W ₇	0.0	0.3062	0.2209	0.3085
PbSe	225	248492	1	-3 ~ 0	Γ ₁₁ +X ₈ +X ₉ +L ₄ L ₅ +L ₉ +2W ₇	0.0	0.224	0.2056	0.224
PbSe	225	62195	1	-3 ~ 0	Γ ₁₁ +X ₈ +X ₉ +L ₆ L ₇ +L ₈ +2W ₆	0.0	0.1305	0.212	0.1305
BiScO ₃	221	181115	1	-15 ~ 0	Γ ₈ +Γ ₉ +3Γ ₁₁ +2R ₉ +3R ₁₁ +3M ₆ +3M ₇ +2M ₈ +3X ₆ +3X ₇ +X ₈ +X ₉	0.0	0.6693	0.1211	0.8368
Ge	227	44841	1	-3 ~ 4	Γ ₈ +Γ ₉ +Γ ₁₀ +2X ₅ +L ₄ L ₅ +L ₈ +2L ₉ +W ₃ W ₄ +W ₅ W ₆ +2W ₇	0.0	0.0	0.2548	0.0874
MgCl ₂	166	26157	1	-3 ~ 0	Γ ₆ Γ ₇ +Γ ₉ +T ₆ Γ ₇ +T ₉ +2F ₃ F ₄ +2L ₃ L ₄	0.0	5.9915	0.085	6.1919
LiCdAs	216	609966	2	-1 ~ 2	Γ ₈ +2X ₇ +L ₄ L ₅ +L ₆ +2W ₆ +W ₇ +W ₈	0.0	0.0	0.1502	0.0849
Bi ₂ (Ru ₂ O ₇)	227	161102	2	-15 ~ 0	Γ ₆ +Γ ₇ +3Γ ₁₀ +4X ₅ +3L ₆ L ₇ +5L ₉ +2W ₃ W ₄ +2W ₅ W ₆ +4W ₇	0.5238	0.0	0.7923	0.0842
PbTe	225	648615	1	-3 ~ 0	Γ ₁₁ +X ₈ +X ₉ +L ₄ L ₅ +L ₉ +2W ₇	0.0	0.2613	0.0836	0.3544
Bi(ScO ₃)	221	158759	1	-15 ~ 0	Γ ₈ +Γ ₉ +3Γ ₁₁ +2R ₉ +3R ₁₀ +3M ₆ +3M ₇ +2M ₉ +X ₆ +X ₇ +3X ₈ +3X ₉	0.0	0.422	0.0765	0.6957
AlSiTe ₃	147	75001	4	-1 ~ 0	A ₇ A ₇ +Γ ₄ Γ ₄ +H ₅ H ₆ +K ₅ K ₆ +L ₂ L ₂ +M ₃ M ₃	0.0	0.6883	0.0669	0.8923
CuIn	194	180112	1	1 ~ 8	A ₄ A ₅ +A ₆ +Γ ₇ +Γ ₈ +Γ ₉ +Γ ₁₀ +2H ₆ H ₇ +2H ₈ +2K ₇ +K ₈ +K ₉ +2L ₃ L ₄ +3M ₅ +M ₆	0.0	0.0	0.131	0.0669
PtO ₂	164	24922	4	1 ~ 2	A ₄ A ₅ +Γ ₄ Γ ₅ +H ₆ +K ₆ +L ₃ L ₄ +M ₃ M ₄	1.5328	0.0	1.757	0.0619
Hf ₃ Al ₃ C ₅	194	161587	3	-1 ~ 6	A ₄ A ₅ +A ₆ +2Γ ₇ +Γ ₈ +Γ ₉ +H ₄ H ₅ +H ₆ H ₇ +H ₈ +H ₉ +2K ₇ +K ₈ +K ₉ +2L ₃ L ₄ +4M ₆	0.0	0.0	0.0594	0.1486
SrAl ₂ Si ₂	164	419886	3	-3 ~ 0	A ₄ A ₅ +A ₈ +Γ ₆ Γ ₇ +Γ ₉ +H ₄ H ₅ +H ₆ +K ₄ K ₅ +K ₆ +2L ₅ L ₆ +2M ₃ M ₄	0.0	0.0	0.0559	0.3243
SnAs	225	611424	1	-2 ~ 1	Γ ₁₁ +X ₈ +X ₉ +L ₆ L ₇ +L ₈ +2W ₆	0.0	0.0	0.0518	0.1985
Bi ₂ (Os ₂ O ₇)	227	161105	1	-15 ~ 0	Γ ₆ +Γ ₇ +3Γ ₁₀ +4X ₅ +3L ₆ L ₇ +5L ₉ +2W ₃ W ₄ +2W ₅ W ₆ +4W ₇	0.8702	0.0	0.9833	0.0512
BaZr(PO ₄) ₂	164	173842	9	1 ~ 2	A ₉ +Γ ₈ +H ₄ H ₅ +K ₄ K ₅ +L ₅ L ₆ +M ₃ M ₄	3.905	0.0	3.9474	0.0502
SnS	225	52107	1	-3 ~ 0	Γ ₁₁ +X ₈ +X ₉ +L ₆ L ₇ +L ₈ +2W ₆	0.0	0.1121	0.0484	0.1328
NbSbSi	129	646436	1	-5 ~ 2	2A ₅ +Γ ₈ +3Γ ₉ +2M ₅ +Z ₈ +3Z ₉ +2R ₃ R ₄ +2X ₃ X ₄	0.0	0.0	0.0465	0.0639
Na ₂ BaMgP ₂ O ₈	147	262716	10	1 ~ 2	A ₈ A ₉ +Γ ₅ Γ ₆ +H ₄ H ₄ +K ₄ K ₄ +L ₂ L ₂ +M ₃ M ₃	5.2768	0.0	5.312	0.0458
BiTe	156	79364	5	-1 ~ 0	A ₄ A ₅ +Γ ₄ Γ ₅ +H ₅ +H ₅ +K ₅ +K ₆ +L ₃ L ₄ +M ₃ M ₄	0.0	0.0447	0.0879	0.0447
Zr(MoO ₄) ₂	164	59999	10	1 ~ 2	A ₄ A ₅ +Γ ₄ Γ ₅ +H ₆ +K ₆ +L ₃ L ₄ +M ₃ M ₄	3.1215	0.0	3.135	0.0431
MoGe ₂	139	76139	1	-3 ~ 2	2Γ ₆ +Γ ₉ +M ₆ +M ₇ +M ₈ +2P ₆ +P ₇ +2X ₅ +X ₆ +3N ₃ N ₄	0.0	0.0	0.0389	0.0832
PbMg ₂	225	151361	1	-1 ~ 6	Γ ₁₀ +Γ ₁₁ +X ₆ +X ₇ +X ₈ +X ₉ +L ₄ L ₅ +L ₆ L ₇ +2L ₈ +3W ₆ +W ₇	0.0	0.0	0.1356	0.0338
Ni(OH) ₂	164	28101	4	-1 ~ 0	A ₄ A ₅ +Γ ₄ Γ ₅ +H ₆ +K ₆ +L ₃ L ₄ +M ₃ M ₄	0.4417	0.0	0.494	0.0336
KSc(MoO ₄) ₂	164	28019	7	1 ~ 2	A ₄ A ₅ +Γ ₄ Γ ₅ +H ₆ +K ₆ +L ₃ L ₄ +M ₃ M ₄	2.9384	0.0	2.9384	0.0331
PbS	225	250762	1	-3 ~ 0	Γ ₁₁ +X ₈ +X ₉ +L ₄ L ₅ +L ₉ +2W ₇	0.0	0.1131	0.0328	0.1131
SrSi ₂ Al ₂	164	609338	3	-3 ~ 0	A ₄ A ₅ +A ₈ +Γ ₆ Γ ₇ +Γ ₉ +H ₄ H ₅ +H ₆ +K ₄ K ₅ +K ₆ +2L ₅ L ₆ +2M ₃ M ₄	0.0	0.0	0.0327	0.3753
PtB	194	615210	1	-1 ~ 10	A ₄ A ₅ +2A ₆ +Γ ₇ +Γ ₈ +Γ ₁₀ +Γ ₁₁ +2Γ ₁₂ +H ₄ H ₅ +2H ₆ H ₇ +2H ₈ +H ₉ +3K ₇ +K ₈ +2K ₉ +3L ₃ L ₄ +6M ₅	0.0	0.0	0.0321	0.2012
CaGaGeH	156	173567	1	-1 ~ 0	A ₄ A ₅ +Γ ₄ Γ ₅ +H ₄ +H ₆ +K ₄ +K ₆ +L ₃ L ₄ +M ₃ M ₄	0.0	0.4363	0.0314	0.7898
MgCl ₂	164	17063	2	-3 ~ 0	A ₆ A ₇ +A ₉ +Γ ₆ Γ ₇ +Γ ₉ +H ₄ H ₅ +H ₆ +K ₄ K ₅ +K ₆ +2L ₃ L ₄ +2M ₃ M ₄	0.0	5.5186	0.0299	5.5186
Mg ₂ Al ₂ Se ₅	164	41928	7	-1 ~ 0	A ₄ A ₅ +Γ ₆ Γ ₇ +H ₆ +K ₆ +L ₃ L ₄ +M ₅ M ₆	0.0	0.7281	0.0292	0.7281
K ₃ V(VO ₄) ₂	164	100782	7	-1 ~ 0	A ₆ A ₇ +Γ ₄ Γ ₅ +H ₆ +K ₆ +L ₅ L ₆ +M ₃ M ₄	2.1516	0.0	2.1663	0.0289
PtS ₂	164	41375	4	1 ~ 2	A ₄ A ₅ +Γ ₄ Γ ₅ +H ₆ +K ₆ +L ₃ L ₄ +M ₃ M ₄	0.4445	0.0	1.1335	0.0278
PbS	225	62190	1	-3 ~ 0	Γ ₁₁ +X ₈ +X ₉ +L ₆ L ₇ +L ₈ +2W ₆	0.0	0.0277	0.0338	0.0277
Cd(OH) ₂	164	165225	4	-1 ~ 0	A ₈ +Γ ₈ +H ₄ H ₅ +K ₄ K ₅ +L ₃ L ₄ +M ₃ M ₄	0.0	1.747	0.0262	1.9915
Mg ₂ Pb	225	642745	1	-1 ~ 6	Γ ₁₀ +Γ ₁₁ +X ₆ +X ₇ +X ₈ +X ₉ +L ₄ L ₅ +L ₆ L ₇ +2L ₈ +3W ₆ +W ₇	0.0	0.0	0.2433	0.0259
K(Ag(CN) ₂)	163	30275	2	-3 ~ 0	A ₄ A ₄ +Γ ₄ Γ ₅ +Γ ₆ Γ ₇ +H ₄ H ₅ +H ₆ +K ₄ K ₅ +K ₆ +L ₂ L ₂ +M ₃ M ₄ +M ₅ M ₆	0.0	3.1161	0.0251	3.1161
SnP	225	77786	1	-2 ~ 1	Γ ₁₁ +X ₈ +X ₉ +L ₆ L ₇ +L ₈ +2W ₆	0.0	0.0	0.0251	0.3066
MgO(OH) ₂	164	95472	1	-1 ~ 0	A ₆ A ₇ +Γ ₆ Γ ₇ +H ₆ +K ₆ +L ₅ L ₆ +M ₅ M ₆	0.0	3.6627	0.0242	3.6242
Cu ₄ O ₃	141	100566	1	-7 ~ 0	2Γ ₆ +2Γ ₇ +2M ₅ +2F ₃ F ₆ +2P ₇ +2X ₃ X ₄ +N ₃ N ₄ +3N ₅ N ₆	0.0	0.0	0.0466	0.0242
BaSr ₂ Mg(SiO ₄) ₂	164	247861	4	1 ~ 2	A ₉ +Γ ₈ +H ₄ H ₅ +K ₄ K ₅ +L ₅ L ₆ +M ₃ M ₄	5.0528	0.0	5.1228	0.0236
CuI	156	84217	5	-1 ~ 0	A ₄ A ₅ +Γ ₄ Γ ₅ +H ₄ +H ₆ +K ₄ +K ₅ +L ₃ L ₄ +M ₃ M ₄	0.0	1.367	0.0234	1.367
Ag ₂ O	164	20368	5	-1 ~ 0	A ₆ A ₇ +Γ ₆ Γ ₇ +H ₆ +K ₆ +L ₅ L ₆ +M ₅ M ₆	0.0	0.0	0.0542	0.0233
Nb ₃ Au ₂	139	54403	1	0 ~ 3	Γ ₆ +Γ ₉ +M ₇ +M ₈ +2P ₇ +X ₅ +X ₆ +2N ₅ N ₆	0.0	0.0	0.0212	0.0369
W ₂ Zr	227	653435	1	-15 ~ 4	Γ ₇ +Γ ₈ +2Γ ₁₀ +2Γ ₁₁ +5X ₅ +L ₄ L ₅ +3L ₆ L ₇ +2L ₈ +4L ₉ +3W ₃ W ₄ +2W ₅ W ₆ +5W ₇	0.0	0.0	0.021	0.0702
ZrW ₂	227	151401	1	-15 ~ 4	Γ ₇ +Γ ₈ +2Γ ₁₀ +2Γ ₁₁ +5X ₅ +L ₄ L ₅ +3L ₆ L ₇ +2L ₈ +4L ₉ +3W ₃ W ₄ +2W ₅ W ₆ +5W ₇	0.0	0.0	0.021	0.0702
MgSiN ₂	166	186509	1	-3 ~ 0	Γ ₆ Γ ₇ +Γ ₉ +T ₄ T ₅ +T ₈ +2F ₃ F ₄ +2L ₅ L ₆	0.0	4.2025	0.0206	5.0508
Ba(Ag ₂ S ₂)	164	50183	5	1 ~ 2	A ₈ +Γ ₈ +H ₄ H ₅ +K ₄ K ₅ +L ₃ L ₄ +M ₃ M ₄	0.9298	0.0	0.9298	0.0201
In ₂ Se ₃	164	602266	5	1 ~ 2	A ₈ +Γ ₈ +H ₄ H ₅ +K ₄ K ₅ +L ₃ L ₄ +M ₃ M ₄	0.0	0.0	0.4934	0.0199
PbTe	225	153711	1	-3 ~ 0	Γ ₁₁ +X ₈ +X ₉ +L ₆ L ₇ +L ₈ +2W ₆	0.0	0.0199	0.0597	0.0199
RbYTe ₂	194	419996	3	-3 ~ 0	A ₄ A ₅ +2Γ ₁₀ +H ₈ +H ₉ +K ₈ +K ₉ +L ₃ L ₄ +2M ₆	0.0	0.9207	0.0196	1.604
W ₂ Zr	227	106218	1	-15 ~ 4	Γ ₇ +Γ ₈ +2Γ ₁₀ +2Γ ₁₁ +5X ₅ +3L ₄ L ₅ +L ₆ L ₇ +4L ₈ +2L ₉ +2W ₃ W ₄ +3W ₅ W ₆ +5W ₇	0.0	0.0	0.0191	0.0676
Li ₂ CuSn ₂	141	426084	1	-1 ~ 6	2Γ ₆ +				

TABLE III (Continued.)

Formula	SG	ICSD	NF	Bands	Irreps	Δ_l (eV)	Δ_u (eV)	Δ'_l (eV)	Δ'_u (eV)
Ba(Sb ₂ O ₆)	162	74541	5	-1 ~ 0	$A_6A_7 + \Gamma_6\Gamma_7 + H_6 + K_6 + L_5L_6 + M_5M_6$	0.0	3.3497	0.0119	3.4314
Ca(Al ₁₂ Si ₄ O ₂₇)	147	91233	6	1 ~ 2	$A_5A_6 + \Gamma_5\Gamma_6 + H_4H_4 + K_4K_4 + L_3L_3 + M_3M_3$	5.4299	0.0	5.5036	0.0119
Al ₃ In ₂	164	612019	2	0 ~ 1	$A_9 + \Gamma_8 + H_4H_5 + K_4K_5 + L_5L_6 + M_3M_4$	0.0	0.0	0.0116	0.1515
Tl(Mo ₆ O ₁₇)	164	62699	9	0 ~ 1	$A_8 + \Gamma_8 + H_4H_5 + K_4K_5 + L_3L_4 + M_3M_4$	0.0	0.0	0.0188	0.0115
NbSe ₂	164	76576	6	0 ~ 1	$A_4A_5 + \Gamma_4\Gamma_5 + H_6 + K_6 + L_3L_4 + M_3M_4$	0.0	0.0	0.011	0.0667
CdLi ₂ Ge	225	52803	2	-1 ~ 2	$\Gamma_{11} + X_8 + X_9 + L_6L_7 + L_8 + 2W_6$	0.0	0.0	0.0109	0.1314
Sr(As ₂ O ₆)	162	420296	3	-1 ~ 0	$A_6A_7 + \Gamma_4\Gamma_5 + H_6 + K_6 + L_5L_6 + M_3M_4$	0.0	3.9384	0.0106	4.2275
Mg(Cr ₂ O ₄)	227	167459	1	-7 ~ 0	$\Gamma_6 + \Gamma_7 + \Gamma_{10} + 2X_5 + L_6L_7 + L_8 + 2L_9 + 2W_5W_6 + 2W_7$	0.0	0.0	0.0132	0.0101
YRe ₂	194	150517	1	-15 ~ 0	$2A_4A_5 + 2A_6 + 2\Gamma_7 + \Gamma_8 + 2\Gamma_{10} + \Gamma_{11} + 2\Gamma_{12} + 2H_6H_7 + 4H_8 + 2H_9 + 2K_7 + 4K_8 + 2K_9 + 4L_3L_4 + 3M_5 + 5M_6$	0.0	0.0	0.0099	0.0238
HfMo ₂	227	638607	1	-11 ~ 8	$\Gamma_7 + \Gamma_8 + 2\Gamma_{10} + 2\Gamma_{11} + 5X_5 + 3L_4L_5 + L_6L_7 + 4L_8 + 2L_9 + 2W_3W_4 + 3W_5W_6 + 5W_7$	0.0	0.0	0.0168	0.0097
Ba ₃ Si ₆ O ₁₂ N ₂	147	421322	3	-1 ~ 0	$A_8A_9 + \Gamma_8\Gamma_9 + H_4H_4 + K_4K_4 + L_2L_2 + M_2M_2$	0.0	4.766	0.0095	5.0373
MgCr ₂ O ₄	227	290599	1	-7 ~ 0	$\Gamma_6 + \Gamma_7 + \Gamma_{10} + 2X_5 + L_6L_7 + L_8 + 2L_9 + 2W_5W_6 + 2W_7$	0.0	0.0	0.013	0.0095
Al ₃ Pd ₂	164	58117	1	0 ~ 1	$A_6A_7 + \Gamma_4\Gamma_5 + H_6 + K_6 + L_5L_6 + M_3M_4$	0.0	0.0	0.0093	0.1289
Zr ₃ Al ₃ C ₅	194	159412	2	-1 ~ 6	$A_4A_5 + A_6 + 2\Gamma_7 + \Gamma_8 + \Gamma_9 + H_4H_5 + H_6H_7 + H_8 + H_9 + 2K_7 + K_8 + K_9 + 2L_3L_4 + 4M_6$	0.0	0.0	0.017	0.0093
Ca(As ₂ O ₆)	162	81064	1	-1 ~ 0	$A_6A_7 + \Gamma_4\Gamma_5 + H_6 + K_6 + L_5L_6 + M_3M_4$	0.0	3.9469	0.0093	4.2667
CaSi ₂	166	248517	1	1 ~ 4	$\Gamma_6\Gamma_7 + \Gamma_9 + \Gamma_6\Gamma_7 + \Gamma_9 + 2F_3F_4 + 2L_3L_4$	0.0	0.0	0.0153	0.0092
CuV ₂ S ₄	227	628953	1	-5 ~ 6	$\Gamma_7 + \Gamma_8 + \Gamma_{10} + \Gamma_{11} + 3X_5 + 2L_6L_7 + L_8 + 3L_9 + 2W_3W_4 + W_5W_6 + 3W_7$	0.0	0.0	0.0105	0.009
SiC	156	43827	10	-1 ~ 0	$A_4A_5 + \Gamma_4\Gamma_5 + H_4 + H_6 + K_4 + K_6 + L_3L_4 + M_3M_4$	0.0	1.6239	0.0087	2.733
CsSnI ₃	127	69995	1	1 ~ 12	$3A_6A_7 + \Gamma_6 + 3\Gamma_7 + \Gamma_8 + \Gamma_9 + 3M_5M_9 + 2Z_6 + 4Z_7 + 3R_3R_4 + 3X_3X_4$	0.1877	0.0	0.1877	0.0086
ZnCr ₂ S ₄	227	42019	2	-11 ~ 0	$\Gamma_7 + \Gamma_8 + \Gamma_{10} + \Gamma_{11} + 3X_5 + 2L_6L_7 + L_8 + 3L_9 + 2W_3W_4 + W_5W_6 + 3W_7$	0.0	0.0	0.0083	0.0099
LiSr(AlF ₆)	163	68905	1	1 ~ 4	$A_5A_6 + 2\Gamma_8 + H_4H_5 + H_6 + K_4K_5 + K_6 + L_2L_2 + 2M_3M_4$	7.6262	0.0	7.6405	0.0083
Ba ₂ NiOsO ₆	164	16406	11	-1 ~ 0	$A_6A_7 + \Gamma_4\Gamma_5 + H_6 + K_6 + L_5L_6 + M_3M_4$	0.0	0.0	0.0079	0.0096
BaSrFe ₄ O ₈	162	37011	11	-1 ~ 0	$A_9 + \Gamma_9 + H_4H_5 + K_4K_5 + L_5L_6 + M_5M_6$	0.0	0.0	0.0299	0.0079
SiC	156	107204	2	-1 ~ 0	$A_4A_5 + \Gamma_4\Gamma_5 + H_5 + H_6 + K_5 + K_6 + L_3L_4 + M_3M_4$	0.0	1.7191	0.0079	2.8422
BC ₇	156	181953	3	0 ~ 1	$A_4A_5 + \Gamma_4\Gamma_5 + H_4 + H_6 + K_4 + K_6 + L_3L_4 + M_3M_4$	0.0	2.7989	0.0077	3.7572
Sn ₂ (Ta ₂ O ₇)	227	27119	4	-11 ~ 0	$\Gamma_7 + \Gamma_8 + \Gamma_{10} + \Gamma_{11} + 3X_5 + 2L_6L_7 + L_8 + 3L_9 + 2W_3W_4 + W_5W_6 + 3W_7$	0.0	0.8308	0.0077	0.8798
Fe(Cr ₂ O ₄)	227	183963	2	1 ~ 8	$\Gamma_6 + \Gamma_7 + \Gamma_{10} + 2X_5 + L_4L_5 + 3L_9 + W_3W_4 + W_5W_6 + 2W_7$	0.0	0.0	0.0085	0.0075
Zn(Cr ₂ S ₄)	227	166481	1	-11 ~ 0	$\Gamma_7 + \Gamma_8 + \Gamma_{10} + \Gamma_{11} + 3X_5 + 2L_6L_7 + L_8 + 3L_9 + 2W_3W_4 + W_5W_6 + 3W_7$	0.0	0.0	0.0075	0.0141
BC ₅	156	180770	3	0 ~ 1	$A_4A_5 + \Gamma_4\Gamma_5 + H_5 + H_6 + K_5 + K_6 + L_3L_4 + M_3M_4$	0.0	2.9665	0.0074	4.2867

Γ_1	Γ_2	Γ_3	M_1	M_2	K_1	K_2K_3		
E	1	1	2		E	1	1	2
$2C_3$	1	1	-1		C'_2	1	-1	
$3C'_2$	1	-1	0		C_3^{-1}	1	-1	

TABLE IV. Character table of irreps at high symmetry momenta in magnetic space group $P6'2'2$ (#177.151 in BNS settings) [51]. For the little group of Γ , E , C_3 , and C'_2 represent the conjugation classes generated from identity, C_{3z} , and C_{2x} , respectively. The number before each conjugate class represents the number of operations in this class. Conjugate class symbols at M and K are defined in similar ways.

VII. DISCUSSION

In this section we discuss two examples related to our classification. The first is the TBG [55, 58, 59, 69, 70], and the second is Fu's topological crystalline insulator [24]. TBG can be successfully diagnosed through our framework; while Fu's model is beyond the symmetry eigenvalue classification. Nevertheless, we develop a generalized symmetry eigenvalue criterion for Fu's state.

A. Twisted bilayer graphene

TBG has an approximate valley-U(1) symmetry [63] and the single-valley Hamiltonian has the magnetic SG $P6'2'2$ (#177.151 in the BNS notation). The irreps of $P6'2'2$ are tabulated in Table IV. The nearly flat bands around the Fermi level form the irreps [55]

$$\Gamma_1 + \Gamma_2 + M_1 + M_2 + K_2K_3. \quad (23)$$

Ref. [55] found that these irreps cannot be obtained as a difference of EBRs and proved that bands having these irreps have C_2T -protected Wilson loop winding, with the winding number $3n \pm 1$ ($n \in \mathbb{Z}$). Another EFP having Wilson loop winding given in the supplementary material of Ref. [55] is

$$\Gamma_3 + M_1 + M_2 + 2K_1. \quad (24)$$

We apply the polyhedron method (Section IV) to the magnetic SG $P6'2'2$ and obtain the complete eigenvalue criteria for the EFPs. The details of calculations are given in Appendix D. Here we briefly describe the results. We obtain a single inequality-type criterion

$$2m(K_2K_3) < m(\Gamma_3), \quad (25)$$

and a single \mathbb{Z}_2 -type criterion

$$\begin{aligned} m(\Gamma_1) + m(\Gamma_2) + 2m(\Gamma_3) - 2m(K_2K_3) &= 0, \\ m(\Gamma_2) &= 1 \pmod{2}. \end{aligned} \quad (26)$$

The EFP (23) is diagnosed by the \mathbb{Z}_2 -type criterion, and the other EFP (24) is diagnosed by the inequality-type criterion. We emphasize that Eqs. (25) and (26) go beyond the two-band eigenvalue criteria derived in Ref. [55] because they apply to many-band systems. Applying the method introduced in Section V, we find that $P6'2'2$ has only two EFP roots and the two roots are just Eqs. (23) and (24).

B. Fu's topological crystalline insulator and a generalized symmetry eigenvalue criterion

Fu's state is spinless and is protected by C_4 rotation and TRS. The topological invariant is well defined only if the Hilbert space is restricted to $p_{x,y}$ orbitals. Correspondingly, the topological surface state is stable only if the model consists of $p_{x,y}$ orbitals. Therefore, this state has the defining character of fragile topology. Recently, Alexandradinata *et al.* proved that the topology of Fu's model is indeed fragile [84].

This model has an accidental inversion symmetry. In Appendix E1 we show that the fragile topology cannot be diagnosed through the C_4 and inversion eigenvalues. Nevertheless, we develop a "generalized symmetry eigenvalue criterion" for this state (Appendix E3). Usually, the diagnosis of topology involves additional symmetries. For example, diagnosis of strong topological insulator, which is protected by TRS, involves the inversion symmetry. We find that the additional symmetries diagnosing Fu's state are inversion and C_{2x} rotation. With these additional symmetries, a \mathbb{Z}_2 invariant can be defined in terms of the symmetry eigenvalues. However, the \mathbb{Z}_2 non-trivial phase is indeed a topological nodal ring semimetal, where the nodal rings are stabilized by inversion (and/or M_z). After the inversion is broken, the nodal rings are gapped. If the inversion symmetry is broken in such a way that no gap closing happens at the high symmetry points, the obtained insulating phase has the topology of Fu's model. Since the additional symmetries for diagnosis enforces the topological state to be semimetal, we call this eigenvalue criterion as "generalized".

VIII. SUMMARY

In this paper, we have obtained three major progresses in the field of topological phases. We have, for the

first time, entirely mathematically classified the fragile topological states indicated by symmetry eigenvalues - EFPs. We found an extremely rich structure of these phases, linked to the mathematical classification of affine monoids, which surpasses the richness of stable topological phases. We have then, for the first time, provided examples of fragile bands in more than a hundred of realistic materials, showcasing some of the best, well-separated sets of bands. Our work finishes one other important sub-field of topological states of matter. It would be remarkably interesting to find a clear experimental consequence of the well-separated fragile sets of bands we have discovered. One such fragile band is the wonder-material of twisted bilayer graphene.

ACKNOWLEDGMENTS

We acknowledge Maia G. Vergniory, Zhijun Wang, and Claudia Felser for collaboration on previous related works. Z.S. and B.B. are supported by the Department of Energy Grant No. desc-0016239, the National Science Foundation EAGER Grant No. DMR 1643312, Simons Investigator Grants No. 404513, No. ONR N00014-14-1-0330, No. NSF-MRSEC DMR 1420541, the Packard Foundation No. 2016-65128, the Schmidt Fund for Development of Majorama Fermions funded by the Eric and Wendy Schmidt Transformative Technology Fund. L.E. is supported by the Government of the Basque Country (project IT779-13), the Spanish Ministry of Economy and Competitiveness (MINECO), and the European Fund for Economic and Regional Development (FEDER; project MAT2015-66441-P). We are mostly grateful to the MPG computing center for allowing us access to the Cobra and Draco Supercomputers. This research also used resources of the National Energy Research Scientific Computing Center (NERSC), a U.S. Department of Energy Office of Science User Facility operated under Contract No. DE-AC02-05CH11231.

-
- [1] C. L. Kane and E. J. Mele, "Quantum spin hall effect in graphene," *Phys. Rev. Lett.* **95**, 226801 (2005).
 - [2] C. L. Kane and E. J. Mele, " \mathbb{Z}_2 Topological Order and the Quantum Spin Hall Effect," *Phys. Rev. Lett.* **95**, 146802 (2005).
 - [3] B Andrei Bernevig, Taylor L Hughes, and Shou-Cheng Zhang, "Quantum spin hall effect and topological phase transition in hgte quantum wells," *Science* **314**, 1757–1761 (2006).
 - [4] Markus König, Steffen Wiedmann, Christoph Brüne, Andreas Roth, Hartmut Buhmann, Laurens W Molenkamp, Xiao-Liang Qi, and Shou-Cheng Zhang, "Quantum spin hall insulator state in hgte quantum wells," *Science* **318**, 766–770 (2007).
 - [5] Liang Fu, C. L. Kane, and E. J. Mele, "Topological insulators in three dimensions," *Phys. Rev. Lett.* **98**, 106803 (2007).
 - [6] Haijun Zhang, Chao-Xing Liu, Xiao-Liang Qi, Xi Dai, Zhong Fang, and Shou-Cheng Zhang, "Topological insulators in bi 2 se 3, bi 2 te 3 and sb 2 te 3 with a single dirac cone on the surface," *Nature physics* **5**, 438 (2009).
 - [7] YL Chen, James G Analytis, J-H Chu, ZK Liu, S-K Mo, Xiao-Liang Qi, HJ Zhang, DH Lu, Xi Dai, Zhong Fang, *et al.*, "Experimental realization of a three-dimensional topological insulator, bi2te3," *science* **325**, 178–181 (2009).
 - [8] Yuqi Xia, Dong Qian, David Hsieh, L Wray, Arijeet Pal, Hsin Lin, Arun Bansil, DHYS Grauer, Yew San Hor, Robert Joseph Cava, *et al.*, "Observation of a large-gap topological-insulator class with a single dirac cone on the surface," *Nature physics* **5**, 398 (2009).

- [9] Alexei Kitaev, “Periodic table for topological insulators and superconductors,” *AIP Conference Proceedings* **1134**, 22–30 (2009).
- [10] Xiao-Liang Qi and Shou-Cheng Zhang, “Topological insulators and superconductors,” *Rev. Mod. Phys.* **83**, 1057–1110 (2011).
- [11] M. Z. Hasan and C. L. Kane, “Colloquium: Topological insulators,” *Rev. Mod. Phys.* **82**, 3045–3067 (2010).
- [12] Joel E Moore, “The birth of topological insulators,” *Nature* **464**, 194 (2010).
- [13] Shuichi Murakami, “Phase transition between the quantum spin hall and insulator phases in 3d: emergence of a topological gapless phase,” *New Journal of Physics* **9**, 356–356 (2007).
- [14] Xiangang Wan, Ari M. Turner, Ashvin Vishwanath, and Sergey Y. Savrasov, “Topological semimetal and fermiarc surface states in the electronic structure of pyrochlore iridates,” *Phys. Rev. B* **83**, 205101 (2011).
- [15] Gang Xu, Hongming Weng, Zhijun Wang, Xi Dai, and Zhong Fang, “Chern semimetal and the quantized anomalous hall effect in HgCr_2Se_4 ,” *Phys. Rev. Lett.* **107**, 186806 (2011).
- [16] AA Burkov, “Topological semimetals,” *Nature materials* **15**, 1145 (2016).
- [17] Hongming Weng, Chen Fang, Zhong Fang, B. Andrei Bernevig, and Xi Dai, “Weyl Semimetal Phase in Noncentrosymmetric Transition-Metal Monophosphides,” *Physical Review X* **5**, 011029 (2015).
- [18] Su-Yang Xu, Ilya Belopolski, Nasser Alidoust, Madhab Neupane, Guang Bian, Chenglong Zhang, Raman Sankar, Guoqing Chang, Zhujun Yuan, Chi-Cheng Lee, Shin-Ming Huang, Hao Zheng, Jie Ma, Daniel S. Sanchez, BaoKai Wang, Arun Bansil, Fangcheng Chou, Pavel P. Shibayev, Hsin Lin, Shuang Jia, and M. Zahid Hasan, “Discovery of a Weyl Fermion semimetal and topological Fermi arcs,” *Science*, aaa9297 (2015).
- [19] Lexian Yang, Zhongkai Liu, Yan Sun, Han Peng, Haifeng Yang, Teng Zhang, Bo Zhou, Yi Zhang, Yanfeng Guo, Marein Rahn, Dharmalingam Prabhakaran, Zahid Husain, Sung-Kwan Mo, Claudia Felser, Binghai Yan, and Yulin Chen, “Discovery of a Weyl Semimetal in non-Centrosymmetric Compound TaAs ,” *arXiv:1507.00521 [cond-mat]* (2015), arXiv: 1507.00521.
- [20] Zhijun Wang, Yan Sun, Xing-Qiu Chen, Cesare Franchini, Gang Xu, Hongming Weng, Xi Dai, and Zhong Fang, “Dirac semimetal and topological phase transitions in $A_3\text{Bi}$ ($a = \text{Na, k, rb}$),” *Phys. Rev. B* **85**, 195320 (2012).
- [21] S. M. Young, S. Zaheer, J. C. Y. Teo, C. L. Kane, E. J. Mele, and A. M. Rappe, “Dirac semimetal in three dimensions,” *Phys. Rev. Lett.* **108**, 140405 (2012).
- [22] Bohm-Jung Yang and Naoto Nagaosa, “Classification of stable three-dimensional dirac semimetals with nontrivial topology,” *Nature communications* **5**, 4898 (2014).
- [23] Jeffrey C. Y. Teo, Liang Fu, and C. L. Kane, “Surface states and topological invariants in three-dimensional topological insulators: Application to $\text{Bi}_{1-x}\text{Sb}_x$,” *Phys. Rev. B* **78**, 045426 (2008).
- [24] Liang Fu, “Topological crystalline insulators,” *Phys. Rev. Lett.* **106**, 106802 (2011).
- [25] Timothy H Hsieh, Hsin Lin, Junwei Liu, Wenhui Duan, Arun Bansil, and Liang Fu, “Topological crystalline insulators in the snite material class,” *Nature communications* **3**, 982 (2012).
- [26] Robert-Jan Slager, Andrej Mesaros, Vladimir Juričić, and Jan Zaanen, “The space group classification of topological band-insulators,” *Nature Physics* **9**, 98–102 (2013).
- [27] Ken Shiozaki and Masatoshi Sato, “Topology of crystalline insulators and superconductors,” *Phys. Rev. B* **90**, 165114 (2014).
- [28] Chao-Xing Liu, Rui-Xing Zhang, and Brian K. Van Leeuwen, “Topological nonsymmorphic crystalline insulators,” *Phys. Rev. B* **90**, 085304 (2014).
- [29] Chen Fang and Liang Fu, “New classes of three-dimensional topological crystalline insulators: Nonsymmorphic and magnetic,” *Phys. Rev. B* **91**, 161105 (2015).
- [30] Wladimir A Benalcazar, B Andrei Bernevig, and Taylor L Hughes, “Quantized electric multipole insulators,” *Science* **357**, 61–66 (2017).
- [31] Wladimir A. Benalcazar, B. Andrei Bernevig, and Taylor L. Hughes, “Electric multipole moments, topological multipole moment pumping, and chiral hinge states in crystalline insulators,” *Phys. Rev. B* **96**, 245115 (2017).
- [32] Frank Schindler, Ashley M Cook, Maia G Vergniory, Zhijun Wang, Stuart SP Parkin, B Andrei Bernevig, and Titus Neupert, “Higher-order topological insulators,” *Science advances* **4**, eaat0346 (2018).
- [33] Josias Langbehn, Yang Peng, Luka Trifunovic, Felix von Oppen, and Piet W. Brouwer, “Reflection-symmetric second-order topological insulators and superconductors,” *Phys. Rev. Lett.* **119**, 246401 (2017).
- [34] Zhida Song, Zhong Fang, and Chen Fang, “ $(d - 2)$ -dimensional edge states of rotation symmetry protected topological states,” *Phys. Rev. Lett.* **119**, 246402 (2017).
- [35] Chen Fang and Liang Fu, “Rotation anomaly and topological crystalline insulators,” *arXiv preprint arXiv:1709.01929* (2017).
- [36] Motohiko Ezawa, “Higher-order topological insulators and semimetals on the breathing kagome and pyrochlore lattices,” *Phys. Rev. Lett.* **120**, 026801 (2018).
- [37] Barry Bradlyn, L. Elcoro, Jennifer Cano, M. G. Vergniory, Zhijun Wang, C. Felser, M. I. Aroyo, and B. Andrei Bernevig, “Topological quantum chemistry,” *Nature* **547**, 298–305 (2017).
- [38] Hoi Chun Po, Ashvin Vishwanath, and Haruki Watanabe, “Complete theory of symmetry-based indicators of band topology,” *Nature Communications* **8**, 50 (2017).
- [39] Jorrit Kruthoff, Jan de Boer, Jasper van Wezel, Charles L. Kane, and Robert-Jan Slager, “Topological Classification of Crystalline Insulators through Band Structure Combinatorics,” *Physical Review X* **7**, 041069 (2017).
- [40] Luis Elcoro, Barry Bradlyn, Zhijun Wang, Maia G. Vergniory, Jennifer Cano, Claudia Felser, B. Andrei Bernevig, Danel Orobengoa, Gemma de la Flor, and Mois I. Aroyo, “Double crystallographic groups and their representations on the Bilbao Crystallographic Server,” *Journal of Applied Crystallography* **50**, 1457–1477 (2017), arXiv: 1706.09272.
- [41] M. G. Vergniory, L. Elcoro, Zhijun Wang, Jennifer Cano, C. Felser, M. I. Aroyo, B. Andrei Bernevig, and Barry Bradlyn, “Graph Theory Data for Topological Quantum Chemistry,” *Physical Review E* **96** (2017), 10.1103/PhysRevE.96.023310, arXiv: 1706.08529.
- [42] Jennifer Cano, Barry Bradlyn, Zhijun Wang, L. Elcoro, M. G. Vergniory, C. Felser, M. I. Aroyo, and B. Andrei Bernevig, “Topology of disconnected elementary band

- representations,” *Phys. Rev. Lett.* **120**, 266401 (2018).
- [43] Eslam Khalaf, Hoi Chun Po, Ashvin Vishwanath, and Haruki Watanabe, “Symmetry indicators and anomalous surface states of topological crystalline insulators,” *Phys. Rev. X* **8**, 031070 (2018).
- [44] Zhida Song, Tiantian Zhang, Zhong Fang, and Chen Fang, “Quantitative mappings between symmetry and topology in solids,” *Nature Communications* **9**, 3530 (2018).
- [45] Zhida Song, Tiantian Zhang, and Chen Fang, “Diagnosis for Nonmagnetic Topological Semimetals in the Absence of Spin-Orbital Coupling,” *Physical Review X* **8**, 031069 (2018).
- [46] MG Vergniory, L Elcoro, Claudia Felser, Nicolas Regnault, B Andrei Bernevig, and Zhijun Wang, “A complete catalogue of high-quality topological materials,” *Nature* **566**, 480 (2019).
- [47] Tiantian Zhang, Yi Jiang, Zhida Song, He Huang, Yuqing He, Zhong Fang, Hongming Weng, and Chen Fang, “Catalogue of topological electronic materials,” *Nature* **566**, 475 (2019).
- [48] Feng Tang, Hoi Chun Po, Ashvin Vishwanath, and Xiang-gang Wan, “Comprehensive search for topological materials using symmetry indicators,” *Nature* **566**, 486 (2019).
- [49] Feng Tang, Hoi Chun Po, Ashvin Vishwanath, and Xiang-gang Wan, “Efficient topological materials discovery using symmetry indicators,” *Nature Physics* , 1 (2019).
- [50] Jennifer Cano, Barry Bradlyn, Zhijun Wang, L. Elcoro, M. G. Vergniory, C. Felser, M. I. Aroyo, and B. Andrei Bernevig, “Building blocks of topological quantum chemistry: Elementary band representations,” *Physical Review B* **97**, 035139 (2018).
- [51] Mois I Aroyo, JM Perez-Mato, D Orobengoa, E Tasci, G De La Flor, and A Kirov, “Crystallography online: Bilbao crystallographic server,” *Bulg. Chem. Commun* **43**, 183–197 (2011); Mois Ilia Aroyo, Juan Manuel Perez-Mato, Cesar Capillas, Eli Kroumova, Svetoslav Ivantchev, Gotzon Madariaga, Asen Kirov, and Hans Wondratschek, “Bilbao crystallographic server: I. databases and crystallographic computing programs,” *Zeitschrift für Kristallographie-Crystalline Materials* **221**, 15–27 (2006); Mois I Aroyo, Asen Kirov, Cesar Capillas, JM Perez-Mato, and Hans Wondratschek, “Bilbao crystallographic server. ii. representations of crystallographic point groups and space groups,” *Acta Crystallographica Section A: Foundations of Crystallography* **62**, 115–128 (2006).
- [52] Rui Yu, Xiao Liang Qi, Andrei Bernevig, Zhong Fang, and Xi Dai, “Equivalent expression of \mathbb{Z}_2 topological invariant for band insulators using the non-Abelian Berry connection,” *Phys. Rev. B* **84**, 075119 (2011).
- [53] A. Alexandradinata, Xi Dai, and B. Andrei Bernevig, “Wilson-loop characterization of inversion-symmetric topological insulators,” *Physical Review B* **89**, 155114 (2014).
- [54] Adrien Bouhon, Annica M Black-Schaffer, and Robert-Jan Slager, “Wilson loop approach to topological crystalline insulators with time reversal symmetry,” *arXiv preprint arXiv:1804.09719* (2018).
- [55] Zhida Song, Zhijun Wang, Wujun Shi, Gang Li, Chen Fang, and B. Andrei Bernevig, “All Magic Angles in Twisted Bilayer Graphene are Topological,” *Physical Review Letters* **123**, 036401 (2019).
- [56] Barry Bradlyn, Zhijun Wang, Jennifer Cano, and B. Andrei Bernevig, “Disconnected elementary band representations, fragile topology, and wilson loops as topological indices: An example on the triangular lattice,” *Phys. Rev. B* **99**, 045140 (2019).
- [57] Hoi Chun Po, Haruki Watanabe, and Ashvin Vishwanath, “Fragile topology and wannier obstructions,” *Phys. Rev. Lett.* **121**, 126402 (2018).
- [58] Junyeong Ahn, Sungjoon Park, and Bohm-Jung Yang, “Failure of nielsen-ninomiya theorem and fragile topology in two-dimensional systems with space-time inversion symmetry: application to twisted bilayer graphene at magic angle,” *arXiv preprint arXiv:1808.05375* (2018), arXiv: 1808.05375v3.
- [59] Hoi Chun Po, Liujun Zou, T Senthil, and Ashvin Vishwanath, “Faithful tight-binding models and fragile topology of magic-angle bilayer graphene,” *arXiv preprint arXiv:1808.02482* (2018).
- [60] María Blanco de Paz, Maia G. Vergniory, Dario Bercioux, Aitzol García-Etxarri, and Barry Bradlyn, “Engineering Fragile Topology in Photonic Crystals: Topological Quantum Chemistry of Light,” *arXiv:1903.02562 [cond-mat, physics:physics]* (2019), arXiv: 1903.02562.
- [61] Juan L. Mañes, “Fragile Phonon Topology on the Time-Reversal Symmetric Honeycomb,” *arXiv:1904.06997 [cond-mat]* (2019), arXiv: 1904.06997.
- [62] Dominic V. Else, Hoi Chun Po, and Haruki Watanabe, “Fragile topological phases in interacting systems,” *Phys. Rev. B* **99**, 125122 (2019).
- [63] Rafi Bistritzer and Allan H. MacDonald, “Moiré bands in twisted double-layer graphene,” *Proceedings of the National Academy of Sciences* **108**, 12233–12237 (2011).
- [64] Kyoungwan Kim, Ashley DaSilva, Shengqiang Huang, Babak Fallahazad, Stefano Larentis, Takashi Taniguchi, Kenji Watanabe, Brian J. LeRoy, Allan H. MacDonald, and Emanuel Tutuc, “Tunable moiré bands and strong correlations in small-twist-angle bilayer graphene,” *Proceedings of the National Academy of Sciences* **114**, 3364–3369 (2017).
- [65] Yuan Cao, Valla Fatemi, Ahmet Demir, Shiang Fang, Spencer L Tomarken, Jason Y Luo, Javier D Sanchez-Yamagishi, Kenji Watanabe, Takashi Taniguchi, Efthimios Kaxiras, *et al.*, “Correlated insulator behaviour at half-filling in magic-angle graphene superlattices,” *Nature* **556**, 80 (2018).
- [66] Yuan Cao, Valla Fatemi, Shiang Fang, Kenji Watanabe, Takashi Taniguchi, Efthimios Kaxiras, and Pablo Jarillo-Herrero, “Unconventional superconductivity in magic-angle graphene superlattices,” *Nature* **556**, 43 (2018).
- [67] Shengqiang Huang, Kyoungwan Kim, Dmitry K. Efimkin, Timothy Lovorn, Takashi Taniguchi, Kenji Watanabe, Allan H. MacDonald, Emanuel Tutuc, and Brian J. LeRoy, “Topologically protected helical states in minimally twisted bilayer graphene,” *Phys. Rev. Lett.* **121**, 037702 (2018).
- [68] Matthew Yankowitz, Shaowen Chen, Hryhorii Polshyn, Yuxuan Zhang, K. Watanabe, T. Taniguchi, David Graf, Andrea F. Young, and Cory R. Dean, “Tuning superconductivity in twisted bilayer graphene,” *Science* **363**, 1059–1064 (2019).
- [69] Grigory Tarnopolsky, Alex Jura Kruchkov, and Ashvin Vishwanath, “Origin of magic angles in twisted bilayer graphene,” *Phys. Rev. Lett.* **122**, 106405 (2019).

- [70] Jianpeng Liu, Junwei Liu, and Xi Dai, “A complete picture for the band topology in twisted bilayer graphene,” [arXiv preprint arXiv:1810.03103](#) (2018).
- [71] J. Zak, “Band representations of space groups,” *Phys. Rev. B* **26**, 3010–3023 (1982).
- [72] L. Michel and J. Zak, “Elementary energy bands in crystals are connected,” *Physics Reports* **341**, 377 – 395 (2001), symmetry, invariants, topology.
- [73] Luis Elcoro, Zhida Song, and B. Andrei Bernevig, “Application of the induction procedure and the Smith Decomposition in the calculation and topological classification of electronic band structures in the 230 space groups” in preparation.
- [74] Song and et al., “[Supplementary Materials: tables about materials, parameterization of band irreps, fragile criteria, and fragile roots.](#)”
- [75] The Sage Developers, *SageMath, the Sage Mathematics Software System (Version 8.4)* (2018).
- [76] D. J. Thouless, M. Kohmoto, M. P. Nightingale, and M. den Nijs, “Quantized Hall Conductance in a Two-Dimensional Periodic Potential,” *Physical Review Letters* **49**, 405–408 (1982).
- [77] F. D. M. Haldane, “Model for a Quantum Hall Effect without Landau Levels: Condensed-Matter Realization of the “Parity Anomaly,”” *Physical Review Letters* **61**, 2015–2018 (1988).
- [78] Yasuhiro Hatsugai, “Chern number and edge states in the integer quantum Hall effect,” *Physical Review Letters* **71**, 3697–3700 (1993).
- [79] Winfried Bruns and Bogdan Ichim, “Normaliz: algorithms for affine monoids and rational cones,” *Journal of Algebra* **324**, 1098–1113 (2010).
- [80] Raymond Hemmecke, “On the computation of hilbert bases of cones,” in *Mathematical software* (World Scientific, 2002) pp. 307–317.
- [81] Liang Fu and C. L. Kane, “Topological insulators with inversion symmetry,” *Phys. Rev. B* **76**, 045302 (2007).
- [82] Taylor L. Hughes, Emil Prodan, and B. Andrei Bernevig, “Inversion-symmetric topological insulators,” *Phys. Rev. B* **83**, 245132 (2011).
- [83] Benjamin J Wieder and B Andrei Bernevig, “The axion insulator as a pump of fragile topology,” [arXiv preprint arXiv:1810.02373](#) (2018).
- [84] A. Alexandradinata, Chen Fang, Matthew J. Gilbert, and B. Andrei Bernevig, “Spin-orbit-free topological insulators without time-reversal symmetry,” *Phys. Rev. Lett.* **113**, 116403 (2014).
- [85] Wikipedia contributors, “[Wikipedia, smith normal form,](#)” (2019).
- [86] Komei Fukuda, *Lecture: Polyhedral computation* (Institute for Operations Research and Institute of Theoretical Computer Science. ETH Zurich., 2013).
- [87] Lex E Renner, *Linear algebraic monoids*, Vol. 134 (Springer Science & Business Media, 2006).
- [88] Winfried Bruns and Joseph Gubeladze, *Polytopes, rings, and K-theory*, Vol. 27 (Springer, 2009).

Appendix A: Diagnosis for fragile phases: the inequality method

Fragile topological states [37, 42, 57], also referred to as fragile phases in this paper, are defined to be non-Wannierizable insulating states, where the Wannier obstruction can be removed by coupling the state to a particular set of trivial (Wannierizable) bands. (A band structure is Wannierizable if a set of *symmetric* Wannier functions can be constructed from the bands.) In other words, if the number of Wannier functions is fixed to be the number of bands, the fragile phase is not Wannierizable; however, if more Wannier functions are allowed, the fragile bands can be realized as a subset of the bands constructed from all the Wannier functions; the bands outside of this subset are completely trivial (Wannierizable). Physically, the bands outside the subset correspond to the trivial bands that are added to remove the Wannier obstruction. In this paper, we restrict ourself to the fragile phases that can be diagnosed from symmetry eigenvalues. These fragile phases cannot be diagnosed from the indicators introduced in Ref. [38, 43–45], but they can be written in terms of EBRs [37, 54, 55, 57–59].

Thus we need a new framework to understand the symmetry data vector (B) of fragile phases. Generally speaking, if the symmetry eigenvalues have the following property

$$\exists p \in \mathbb{Z}^{N_{EBR}}, \text{ s.t. } B = EBR \cdot p, \quad \text{and} \quad \forall p \in \mathbb{N}^{N_{EBR}}, B \neq EBR \cdot p, \quad (\text{A1})$$

then we say that the corresponding band structure has at least a fragile topology diagnosable by the symmetry eigenvalues or EBRs. (It could also have robust/strong topology undiagnosable by symmetry eigenvalues.) In other words, the symmetry data vector B of a fragile phase cannot be written as a sum of EBRs, but only as a difference of two sums of EBRs, *i.e.*, $B = \sum_i p_i EBR_i - \sum_j q_j EBR_j$, where $p_i, q_j \geq 0$ and $p_i q_i = 0$ for all i . Here and after we use A_i to represent the i -th column of the matrix A . Then adding the BR written as $\sum_i q_i EBR_i$ to the fragile phase makes the total symmetry data vector completely trivial.

1. An example: SG 150

To familiarize ourselves with the symmetry data of fragile phases, here we take an example SG 150 ($P321$) in presence of SOC and TRS. The EBR matrix of is given by

$$EBR = \begin{pmatrix} 0 & 1 & 2 & 0 \\ 1 & 0 & 0 & 2 \\ 0 & 1 & 2 & 0 \\ 1 & 0 & 0 & 2 \\ 0 & 1 & 0 & 1 \\ 0 & 1 & 0 & 1 \\ 1 & 0 & 2 & 1 \\ 0 & 1 & 0 & 1 \\ 0 & 1 & 0 & 1 \\ 1 & 0 & 2 & 1 \\ 0 & 1 & 0 & 1 \\ 0 & 1 & 0 & 1 \\ 1 & 0 & 2 & 1 \\ 0 & 1 & 0 & 1 \\ 0 & 1 & 0 & 1 \\ 1 & 0 & 2 & 1 \\ 1 & 1 & 2 & 2 \\ 1 & 1 & 2 & 2 \end{pmatrix} = \begin{pmatrix} 1 & 0 & -1 & 0 & 0 & 0 & 1 & 0 & 0 & 0 & 0 & 0 & 0 & 0 & 0 & 0 & 0 & 0 & 0 & 0 \\ 0 & 0 & 1 & 0 & 0 & 0 & 0 & 1 & 0 & 0 & 0 & 0 & 0 & 0 & 0 & 0 & 0 & 0 & 0 & 0 \\ 1 & 0 & -1 & 0 & 0 & 0 & 0 & 0 & 0 & 0 & 0 & 0 & 0 & 0 & 0 & 0 & 0 & 0 & 0 & 0 \\ 0 & 0 & 1 & 0 & 0 & 1 & 0 & 0 & 0 & 0 & 0 & 0 & 0 & 0 & 0 & 0 & 0 & 0 & 0 & 0 \\ 1 & -1 & 0 & 0 & 0 & 0 & 0 & 0 & 1 & 0 & 0 & 0 & 0 & 0 & 0 & 0 & 0 & 0 & 0 & 0 \\ 1 & -1 & 0 & 0 & 0 & 0 & 0 & 0 & 0 & 1 & 0 & 0 & 0 & 0 & 0 & 0 & 0 & 0 & 0 & 0 \\ 0 & 1 & 0 & 0 & 0 & 0 & 0 & 0 & 0 & 1 & 0 & 0 & 0 & 0 & 0 & 0 & 0 & 0 & 0 & 0 \\ 1 & -1 & 0 & 0 & 0 & 0 & 0 & 0 & 0 & 0 & 1 & 0 & 0 & 0 & 0 & 0 & 0 & 0 & 0 & 0 \\ 1 & -1 & 0 & 0 & 0 & 0 & 0 & 0 & 0 & 0 & 0 & 1 & 0 & 0 & 0 & 0 & 0 & 0 & 0 & 0 \\ 0 & 1 & 0 & 0 & 0 & 0 & 0 & 0 & 0 & 0 & 0 & 0 & 1 & 0 & 0 & 0 & 0 & 0 & 0 & 0 \\ 1 & -1 & 0 & 0 & 0 & 0 & 0 & 0 & 0 & 0 & 0 & 0 & 0 & 1 & 0 & 0 & 0 & 0 & 0 & 0 \\ 1 & -1 & 0 & 0 & 0 & 0 & 0 & 0 & 0 & 0 & 0 & 0 & 0 & 0 & 1 & 0 & 0 & 0 & 0 & 0 \\ 0 & 1 & 0 & 0 & 0 & 0 & 0 & 0 & 0 & 0 & 0 & 0 & 0 & 0 & 0 & 1 & 0 & 0 & 0 & 0 \\ 1 & -1 & 0 & 0 & 0 & 0 & 0 & 0 & 0 & 0 & 0 & 0 & 0 & 0 & 0 & 0 & 1 & 0 & 0 & 0 \\ 1 & -1 & 0 & 0 & 0 & 0 & 0 & 0 & 0 & 0 & 0 & 0 & 0 & 0 & 0 & 0 & 0 & 1 & 0 & 0 \\ 0 & 1 & 0 & 0 & 1 & 0 & 0 & 0 & 0 & 0 & 0 & 0 & 0 & 0 & 0 & 0 & 0 & 0 & 0 & 0 \\ 1 & 0 & 0 & 0 & 0 & 0 & 0 & 0 & 0 & 0 & 0 & 0 & 0 & 0 & 0 & 0 & 0 & 0 & 0 & 0 \\ 1 & 0 & 0 & 1 & 0 & 0 & 0 & 0 & 0 & 0 & 0 & 0 & 0 & 0 & 0 & 0 & 0 & 0 & 0 & 0 \\ 1 & 0 & 0 & 0 & 1 & 0 & 0 & 0 & 0 & 0 & 0 & 0 & 0 & 0 & 0 & 0 & 0 & 0 & 0 & 0 \end{pmatrix} \begin{pmatrix} 1 & 0 & 0 & 0 \\ 0 & 1 & 0 & 0 \\ 0 & 0 & 1 & 0 \\ 0 & 0 & 0 & 1 \\ 0 & 0 & 0 & 0 \\ 0 & 0 & 0 & 0 \\ 0 & 0 & 0 & 0 \\ 0 & 0 & 0 & 0 \\ 0 & 0 & 0 & 0 \\ 0 & 0 & 0 & 0 \\ 0 & 0 & 0 & 0 \\ 0 & 0 & 0 & 0 \\ 0 & 0 & 0 & 0 \\ 0 & 0 & 0 & 0 \\ 0 & 0 & 0 & 0 \\ 0 & 0 & 0 & 0 \\ 0 & 0 & 0 & 0 \\ 0 & 0 & 0 & 0 \\ 0 & 0 & 0 & 0 \\ 0 & 0 & 0 & 0 \end{pmatrix} \begin{pmatrix} 1 & 1 & 2 & 2 \\ 1 & 0 & 2 & 1 \\ 1 & 0 & 0 & 2 \\ 0 & 0 & -1 & 0 \end{pmatrix}, \quad (\text{A2})$$

where the Smith Decomposition $L\Lambda R$ is given after the second equal-sign. Here each column of the matrix EBR represents an EBR, and the irreps represented by the rows of the EBR matrix are $\overline{A}_4\overline{A}_5, \overline{A}_6, \overline{\Gamma}_4\overline{\Gamma}_5, \overline{\Gamma}_6, \overline{H}_4, \overline{H}_5, \overline{H}_6, \overline{HA}_4, \overline{HA}_5, \overline{HA}_6, \overline{K}_4, \overline{K}_5, \overline{K}_6, \overline{KA}_4, \overline{KA}_5, \overline{KA}_6, \overline{L}_3\overline{L}_4, \overline{M}_3\overline{M}_4$, in the notation of the *Bilbao Crystallographic Server* (BCS) [40, 51]. (One can find the definitions of these irreps at the *Irreducible representations of the Double Space Groups* section of the BCS [40].) Since the diagonal elements of Λ are either 1 or 0, there is no indicator in this SG. As described in Ref. [37, 38, 40, 73], the space of compatibility-relation-allowed symmetry data can be generated from the first r columns of the L matrix, with r the rank of Λ (here $r = 3$). In other words, we can always write the symmetry data vector as $B = EBR \cdot p = L\Lambda R \cdot p$. Thus, we can introduce the parameter's $y_i = (Rp)_i$ ($i = 1, 2 \dots r$) and write the symmetry data as

$$B = \sum_{i=1}^3 (L\Lambda)_i y_i = (y_1 - y_3, y_3, y_1 - y_3, y_3, y_1 - y_2, y_1 - y_2, y_2, y_1 - y_2, y_1 - y_2, y_2, y_1 - y_2, y_1 - y_2, y_2, y_1 - y_2, y_1 - y_2, y_2, y_1, y_1)^T. \quad (\text{A3})$$

For the number of irreps to be nonnegative, *i.e.*, $B \geq 0$, the following inequalities should be satisfied

$$y_1 \geq y_3 \geq 0, \quad y_1 \geq y_2 \geq 0. \quad (\text{A4})$$

Therefore, only the y 's that satisfy Eq. (A4) correspond to physical band structures. In the following we will use y to represent the band structures.

Now we decompose the symmetry data vector in Eq. (A3) as a combination of EBRs, *i.e.*, $B = \sum_i p_i EBR_i$ (Eq. (A1)). On one hand, as $y_i = (R \cdot p)_i$ ($i = 1, 2, 3$) and $\Lambda = \text{diag}(1 \ 1 \ 1 \ 0)$ (Eq. (A2)), we can always write p as $p = y_1 R_1^{-1} + y_2 R_2^{-1} + y_3 R_3^{-1}$. (R_i^{-1} is the i -th column of the matrix R^{-1} .) On the other hand, if p is a solution of $y_i = (Rp)_i$ ($i = 1, 2, 3$), $p + kR_4^{-1}$ is also a solution, where k is a free parameter, because $(RR_4^{-1})_{1,2,3} = 0$. Therefore, the general solution of the equation $B = EBR \cdot p$ or $y_i = (\Lambda Rp)_i$ ($i = 1, 2, 3$) takes the form of

$$p = y_1 R_1^{-1} + y_2 R_2^{-1} + y_3 R_3^{-1} + k R_4^{-1}. \quad (\text{A5})$$

Substituting the R matrix into Eq. (A5), we obtain

$$p = (2y_2 - y_3 - 4k, y_1 - y_3 - 2k, k, -y_2 + y_3 + 2k)^T. \quad (\text{A6})$$

For p to be an integer, vector k need to be integer because $p_3 = k$. For a given y vector, if there exists some integer k such that each element of p is nonnegative, then the corresponding symmetry data vector can be written as a sum positive EBRs, and so can be a trivial phase; otherwise, the corresponding band structure necessarily has a fragile topology. Therefore we conclude that the equivalent condition for symmetry data associated with y to be trivial is

$$\exists k \in \mathbb{Z}, \quad \text{s.t.} \quad 2y_2 - y_3 - 4k \geq 0, \quad y_1 - y_3 - 2k \geq 0, \quad k \geq 0, \quad -y_2 + y_3 + 2k \geq 0. \quad (\text{A7})$$

Solving the inequalities in Eq. (A7), we rewrite the trivial condition as

$$\exists k \in \mathbb{Z}, \quad s.t. \quad \max \left(0, \frac{1}{2}y_2 - \frac{1}{2}y_3 \right) \leq k \leq \min \left(\frac{1}{2}y_2 - \frac{1}{4}y_3, \frac{1}{2}y_1 - \frac{1}{2}y_3 \right). \quad (\text{A8})$$

There are two possible cases where Eq. (A8) has no solution: (type-I) Eq. (A8) has no solution even where k is allowed to be a rational number; (type-II) Eq. (A8) has rational solutions but no integer solution. The two cases correspond to the inequality-type index and the \mathbb{Z}_2 -type index defined in the main text, respectively. Here we first consider type-I. We directly see that type-I happens when any of the following four inequalities is satisfied (A) $0 > \frac{1}{2}y_2 - \frac{1}{4}y_3$, (B) $\frac{1}{2}y_2 - \frac{1}{2}y_3 > \frac{1}{2}y_2 - \frac{1}{4}y_3$, (C) $0 > \frac{1}{2}y_1 - \frac{1}{2}y_3$, (D) $\frac{1}{2}y_2 - \frac{1}{2}y_3 > \frac{1}{2}y_1 - \frac{1}{2}y_3$. For example $0 > \frac{1}{2}y_2 - \frac{1}{4}y_3$ (A) and Eq. (A8) implies $0 \leq k < 0$, which has no solution. Actually, (B), (C) and (D) cannot be satisfied by real band structures because they conflict with $B \geq 0$ (Eq. (A4)). Therefore the only left possibility is (A), for which we get the fragile criterion as

$$y_3 - 2y_2 > 0. \quad (\text{A9})$$

In this paper we refer to $y_3 - 2y_2$ as an *inequality-type fragile index*. A key difference between the inequality-type index for fragile phase and the symmetry-based indicator for stable/strong phase is that the latter can become trivial upon stacking, whereas the former cannot. For example, double of the generator state of a \mathbb{Z}_2 indicator becomes a trivial state, whereas stacking of any positive number of the inequality-type fragile phase, for example, the $y_3 - 2y_2 = 1$ state, is still a fragile phase, because the inequality is still satisfied.

Now we consider type-II, where Eq. (A8) has solutions only if k is allowed to be rational number. Type-II happens if the interval set by Eq. (A8) is nonzero but does not contain any integer. We notice that the solution of Eq. (A8) can be written as the intersection of the following three intervals

$$0 \leq k \leq \min \left(\frac{1}{2}y_2 - \frac{1}{4}y_3, \frac{1}{2}y_1 - \frac{1}{2}y_3 \right), \quad (\text{A10})$$

$$\frac{1}{2}y_2 - \frac{1}{2}y_3 \leq k \leq \frac{1}{2}y_2 - \frac{1}{4}y_3, \quad (\text{A11})$$

$$\frac{1}{2}y_2 - \frac{1}{2}y_3 \leq k \leq \frac{1}{2}y_1 - \frac{1}{2}y_3. \quad (\text{A12})$$

If Eq. (A10) has solutions, the solutions must include the lower bound 0, which violates our request that the interval does not contain integers. Thus Eq. (A10) does not bring new indices. Therefore we only need to consider the case where Eq. (A11) or (A12) has only fractional solutions but no integer solution. For Eq. (A11) to have no integer solution, we set $y_2 - y_3$ to be an odd integer such that the lower bound $\frac{1}{2}y_2 - \frac{1}{2}y_3$ is fractional, and, at the same time, set the interval to be smaller than $\frac{1}{2}$, *i.e.*, $0 \leq \frac{1}{2}y_2 - \frac{1}{4}y_3 - (\frac{1}{2}y_2 - \frac{1}{2}y_3) < \frac{1}{2}$. Considering y 's are integers, this condition can be realized when (A) $y_2 - y_3 = 1 \pmod{2}$ and $\frac{1}{2}y_2 - \frac{1}{4}y_3 - (\frac{1}{2}y_2 - \frac{1}{2}y_3) = 0$, or (B) $y_2 - y_3 = 1 \pmod{2}$ and $\frac{1}{2}y_2 - \frac{1}{4}y_3 - (\frac{1}{2}y_2 - \frac{1}{2}y_3) = \frac{1}{4}$. For Eq. (A12) to have no integer solution, we set $y_2 - y_3$ to be an odd integer such that the lower bound $\frac{1}{2}y_2 - \frac{1}{2}y_3$ is fractional, and, at the same time, set the interval to be smaller than $\frac{1}{2}$, *i.e.*, $0 \leq \frac{1}{2}y_1 - \frac{1}{2}y_3 - (\frac{1}{2}y_2 - \frac{1}{2}y_3) < \frac{1}{2}$. Considering y 's are integers, this condition can be realized when (C) $y_2 - y_3 = 1 \pmod{2}$ and $\frac{1}{2}y_1 - \frac{1}{2}y_3 - (\frac{1}{2}y_2 - \frac{1}{2}y_3) = 0$. Since all the three cases (A,B,C) are not inconsistent with Eq. (A4), all of them can be realized by some physical band structures. Therefore, we obtain fragile criteria for the three cases as

$$y_3 = 0 \quad \text{and} \quad \delta_1 = y_2 - y_3 = 1 \pmod{2}, \quad (\text{A13})$$

$$y_3 = 1 \quad \text{and} \quad \delta_2 = y_2 - y_3 = 1 \pmod{2}, \quad (\text{A14})$$

$$y_1 - y_2 = 0 \quad \text{and} \quad \delta_3 = y_2 - y_3 = 1 \pmod{2}. \quad (\text{A15})$$

In this paper we refer to $\delta_{1,2,3}$ as \mathbb{Z}_2 -type fragile indices, which are similar with the symmetry-based indicators in the sense that they also will become trivial upon stacking. For example, the double of the state $y = (1, 1, 0)$, where $y_3 = 0$ and $\delta_1 = 1$, is a trivial state, because it reads $2y = (2, 2, 0)$ and has trivial indices.

2. The inequality method to get the fragile criteria

The above method can be generalized to any SG. In this paper we refer to this method as the inequality method. Here we present a summary of the inequality method. First, making use of the Smith Decomposition of the EBR matrix ($EBR = L\Lambda R$), we parameterize the symmetry data as $B = \sum_{i=1}^r (L\Lambda)_i y_i$, with r the rank of Λ and $y = (y_1 \cdots y_r)^T$ an integer vector, such that B has vanishing indicators. For the numbers of irreps to be nonnegative, there should be

$$B = \sum_{i=1}^r (L\Lambda)_i y_i \geq 0. \quad (\text{A16})$$

Second, we decompose the symmetry data vector associated with y as a combination of EBRs, *i.e.*, $B = EBR \cdot p$ or $y_i = (Rp)_i$ ($i = 1 \cdots r$), where $p = (p_1 \cdots p_{N_{EBR}})^T$ is the combination coefficient. Clearly, the decomposition

$$B = \sum_{i=1}^r (L\Lambda)_i y_i + \sum_{i=1}^{N_{EBR}-r} (L\Lambda)_{r+i} k_i, \quad (\text{A17})$$

where k_i 's are free (integer) parameters, gives the same symmetry data vector than Eq. (A16) because $\Lambda_i = 0$ for $i > r$. Thus the general solution of $B = EBR \cdot p$ can be written as $p = R^{-1} \begin{pmatrix} y \\ k \end{pmatrix}$. As both R and R^{-1} are integer matrices, p is integer vector iff k is integer vector. Therefore, the condition for the symmetry data to be trivial is equivalent to the existence of integer solutions of k for the inequalities $p \geq 0$ subject to the constraints $B \geq 0$ (Eq. (A16)): If there exists such k such that $p \geq 0$, then the symmetry data can be written as a sum of EBRs. Now we describe the solution of $p \geq 0$. At the first step, we consider k_1 as a variable and $k_2 \cdots k_{N_{EBR}-1}$ and y as fixed parameters. Then the solution of $p \geq 0$ takes the form

$$\max \left(f_1^{(-1)}(k_2 \cdots y_r), f_1^{(-2)}(k_2 \cdots y_r), \dots \right) \leq k_1 \leq \min \left(f_1^{(1)}(k_2 \cdots y_r), f_1^{(2)}(k_2 \cdots y_r), \dots \right) \quad (\text{A18})$$

Here f 's are linear functions of k and y with rational coefficients. At the second step, by requiring $f_1^{(i)} \leq f_1^{(j)}$, where $i < 0$ and $j > 0$, such that k_1 has a nontrivial solution, we obtain a set of constraints about $k_2 \cdots k_{N_{EBR}-r}$ and y . Solving these constraints by regarding k_2 as the variable and $k_3 \cdots k_{N_{EBR}-1}$ and y as fixed parameters, we can obtain the solution as

$$\max \left(f_2^{(-1)}(k_3 \cdots y_r), f_2^{(-2)}(k_3 \cdots y_r), \dots \right) \leq k_2 \leq \min \left(f_2^{(1)}(k_3 \cdots y_r), f_2^{(2)}(k_3 \cdots y_r), \dots \right) \quad (\text{A19})$$

...

At the $(N_{EBR} - r)$ -th step, solving the constraints that guarantee $k_{N_{EBR}-r-1}$ to have a nontrivial solution by considering $k_{N_{EBR}-r}$ as the variable and y as fixed parameter, we obtain the solution

$$\max \left(h_0^{(-1)}(y_1 \cdots y_r), h_0^{(-2)}(y_1 \cdots y_r), \dots \right) \leq k_{N_{EBR}-r} \leq \min \left(h_0^{(1)}(y_1 \cdots y_r), h_0^{(2)}(y_1 \cdots y_r), \dots \right), \quad (\text{A20})$$

Here h 's are linear functions of y with rational coefficients. At the next step, we regard y_1 as the variable and $y_2 \cdots y_r$ as fixed parameters. By requiring $k_{N_{EBR}-r}$ to have a nontrivial solution, we obtain the constraints satisfied by y_1 as

$$\max \left(h_1^{(-1)}(y_2 \cdots y_r), h_1^{(-2)}(y_2 \cdots y_r), \dots \right) \leq y_1 \leq \min \left(h_1^{(1)}(y_2 \cdots y_r), h_1^{(2)}(y_2 \cdots y_r), \dots \right), \quad (\text{A21})$$

Following the procedure, we can successfully obtain the constraints satisfied by $y_2 \cdots y_r$ as

$$\max \left(h_2^{(-1)}(y_3 \cdots y_r), h_2^{(-2)}(y_3 \cdots y_r), \dots \right) \leq y_2 \leq \min \left(h_2^{(1)}(y_3 \cdots y_r), h_2^{(2)}(y_3 \cdots y_r), \dots \right), \quad (\text{A22})$$

...

$$\max \left(h_{r-1}^{(-1)}(y_r), h_{r-1}^{(-2)}(y_r), \dots \right) \leq y_{r-1} \leq \min \left(h_{r-1}^{(1)}(y_r), h_{r-1}^{(2)}(y_r), \dots \right). \quad (\text{A23})$$

Eqs. (A18) to (A23) can be thought as an algorithm, where the $(n+1)$ -th step is obtained by requiring that the n -th step has a nontrivial (rational) solution. Therefore, to ensure $k_1 \cdots k_{N_{EBR}}$ to have a nontrivial (rational) solution,

we need and only need the constraints in Eq. (A21) to (A23) to be satisfied. In other words, if $h_l^{(i)} > h_l^{(j)}$ for any $i < 0, j > 0$ ($l = 0, 1 \dots r$), the constraints Eq. (A21) to (A23) are violated, this would imply the non-existence of k satisfying Eqs. (A18) to (A20). Hence we can define the inequality-type indices as $h_l^{(i)} - h_l^{(j)}$ ($i < 0, j > 0, l = 0, 1 \dots r$), the positive values of which imply Eqs. (A18) to (A20) not having a solution and hence $k_1 \dots k_{N_{EBR-r}}$ not having a solution and hence imply to a fragile topology. In practice, we need to check whether $h_l^{(i)} - h_l^{(j)} > 0$ is consistent with the positivity of B (Eq. (A16)). If not, then there is no need to introduce such an index, as it cannot be realized by real band structure. As discussed in the paragraph below in Eq. (A8) in the example of SG 150, $h_l^{(i)}$ and $h_l^{(j)}$ pairs set four possible inequality-type indices, but only one of them is consistent with Eq. (A16). By this method we can obtain all the inequality-type fragile indices in principle. However, we emphasize that the computational time of solving $p \geq 0$ in form of Eqs. (A18) to (A21) and (A23) increases exponentially with the number of variables. Therefore, it is very hard to solve SGs where r is very large by the inequality method; several these groups are solved in Ref. [73].

Finding $\mathbb{Z}_{n=2,3,\dots}$ -type fragile indices is more complicated: one needs to check whether the solution of k contains integer points. For simplicity, let us first check whether the $k_{N_{EBR-r}}$ component has integer solutions. For a given $y = (y_1 \dots y_r)^T$, if there exist fractional $h_0^{(i)}$ and $h_0^{(j)}$ ($i < 0, j > 0$), then the conditions for $k_{N_{EBR-r}}$ to have no integer solutions are (i) $h_0^{(i)} \in \mathbb{Q} - \mathbb{Z}$ (non-integer rational) and (ii) $h_0^{(j)} < [h_0^{(i)}]$ such that $h_0^{(i)} \leq k_{N_{EBR-r}} \leq h_0^{(j)} < [h_0^{(i)}]$ has no integer solution sitting between a non-integer rational and the smallest integer larger or equal to this non-integer rational. Here $[x]$ represents the smallest integer larger or equal to x . Now let us write the condition (i) and (ii) more explicitly to get the \mathbb{Z}_n -type indices. As $h_0^{(i)}$ is a rational linear function of y , there exist a minimal integer κ such that $\kappa h_0^{(i)} \in \mathbb{Z}$ for arbitrary $y \in \mathbb{Z}^r$. Therefore, for given y , condition-(i) is equivalent to

$$\delta = \kappa h_0^{(i)}(y) \neq 0 \pmod{\kappa}. \quad (\text{A24})$$

When Eq. (A24) is satisfied, $[h_0^{(i)}]$ can be written as $h_0^{(i)} + 1 - \frac{1}{\kappa}(\kappa h_0^{(i)} \pmod{\kappa})$, and thus condition-(ii) is equivalent to

$$h_0^{(j)} - h_0^{(i)} < 1 - \frac{1}{\kappa}(\kappa h_0^{(i)} \pmod{\kappa}). \quad (\text{A25})$$

In the example of SG 150, picking $h_0^{(i)}$ as $\frac{1}{2}y_2 - \frac{1}{2}y_3$, $h_0^{(j)}$ as $\frac{1}{2}y_2 - \frac{1}{4}y_3$, and $\kappa = 2$, Eq. (A24) and Eq. (A25) are given as $\delta = y_2 - y_3 = 1 \pmod{2}$ and $\frac{1}{4}y_3 < \frac{1}{2}$, respectively, which implies Eqs. (A13) and (A14).

So far we have derived the \mathbb{Z}_n -type fragile indices given by the $k_{N_{EBR-r}}$ component. Now we consider the \mathbb{Z}_n -type fragile indices given by the $k_{N_{EBR-r-1}}$ component. We can re-derive Eqs. (A18) to (A20) in a different order of k 's components, where the last-solved component is $k_{N_{EBR-r-1}}$. Then following Eqs. (A24) and (A25) we can derive the \mathbb{Z}_n -type fragile criteria given by $k_{N_{EBR-r-1}}$. In Appendix A3 we present an example of interchanging the order of $k_{N_{EBR-r}}$ and $k_{N_{EBR-r-1}}$. By setting each k_i as the last-solved component, we can get all the \mathbb{Z}_n -type fragile criteria given by *individual* k components. We present a case by case study of this method in Ref. [73].

3. Another example: SG 143

Here we present the calculation of fragile indices in SG 143 ($P3$) as a nontrivial example of the the \mathbb{Z}_n -type indices. The Smith Decomposition of the EBR matrix is given by

$$EBR = \begin{pmatrix} 1 & 0 & 0 & -1 & 0 & 0 & 0 & 0 & 1 & 0 & 0 & 0 & 0 & 0 & 0 & 0 & 0 & 0 & 0 & 0 \\ 0 & 0 & 0 & 1 & 0 & 0 & 0 & 0 & 0 & 1 & 0 & 0 & 0 & 0 & 0 & 0 & 0 & 0 & 0 & 0 \\ 1 & 0 & 0 & -1 & 0 & 0 & 0 & 0 & 0 & 0 & 0 & 0 & 0 & 0 & 0 & 0 & 0 & 0 & 0 & 0 \\ 0 & 0 & 0 & 1 & 0 & 0 & 0 & 0 & 1 & 0 & 0 & 0 & 0 & 0 & 0 & 0 & 0 & 0 & 0 & 0 \\ 2 & -1 & -1 & 0 & 0 & 0 & 0 & 0 & 0 & 1 & 0 & 0 & 0 & 0 & 0 & 0 & 0 & 0 & 0 & 0 \\ 0 & 0 & 1 & 0 & 0 & 0 & 0 & 0 & 0 & 0 & 1 & 0 & 0 & 0 & 0 & 0 & 0 & 0 & 0 & 0 \\ 0 & 1 & 0 & 0 & 0 & 0 & 0 & 0 & 0 & 0 & 1 & 0 & 0 & 0 & 0 & 0 & 0 & 0 & 0 & 0 \\ 2 & -1 & -1 & 0 & 0 & 0 & 0 & 0 & 0 & 0 & 0 & 1 & 0 & 0 & 0 & 0 & 0 & 0 & 0 & 0 \\ 0 & 0 & 1 & 0 & 0 & 0 & 0 & 0 & 0 & 0 & 0 & 0 & 1 & 0 & 0 & 0 & 0 & 0 & 0 & 0 \\ 0 & 1 & 0 & 0 & 0 & 0 & 0 & 0 & 0 & 0 & 0 & 0 & 0 & 0 & 0 & 0 & 0 & 0 & 0 & 0 \\ 2 & -1 & -1 & 0 & 0 & 0 & 0 & 0 & 0 & 0 & 0 & 0 & 0 & 0 & 0 & 0 & 0 & 0 & 0 & 0 \\ 0 & 0 & 1 & 0 & 0 & 0 & 1 & 0 & 0 & 0 & 0 & 0 & 0 & 0 & 0 & 0 & 0 & 0 & 0 & 0 \\ 0 & 1 & 0 & 0 & 0 & 1 & 0 & 0 & 0 & 0 & 0 & 0 & 0 & 0 & 0 & 0 & 0 & 0 & 0 & 0 \\ 1 & 0 & 0 & 0 & 0 & 0 & 0 & 0 & 0 & 0 & 0 & 0 & 0 & 0 & 0 & 0 & 0 & 0 & 0 & 0 \\ 1 & 0 & 0 & 0 & 1 & 0 & 0 & 0 & 0 & 0 & 0 & 0 & 0 & 0 & 0 & 0 & 0 & 0 & 0 & 0 \end{pmatrix} \begin{pmatrix} 1 & 0 & 0 & 0 & 0 & 0 \\ 0 & 1 & 0 & 0 & 0 & 0 \\ 0 & 0 & 1 & 0 & 0 & 0 \\ 0 & 0 & 0 & 1 & 0 & 0 \\ 0 & 0 & 0 & 0 & 1 & 0 \\ 0 & 0 & 0 & 0 & 0 & 1 \\ 0 & 0 & 0 & 0 & 0 & 0 \\ 0 & 0 & 0 & 0 & 0 & 0 \\ 0 & 0 & 0 & 0 & 0 & 0 \\ 0 & 0 & 0 & 0 & 0 & 0 \\ 0 & 0 & 0 & 0 & 0 & 0 \\ 0 & 0 & 0 & 0 & 0 & 0 \\ 0 & 0 & 0 & 0 & 0 & 0 \\ 0 & 0 & 0 & 0 & 0 & 0 \\ 0 & 0 & 0 & 0 & 0 & 0 \\ 0 & 0 & 0 & 0 & 0 & 0 \\ 0 & 0 & 0 & 0 & 0 & 0 \\ 0 & 0 & 0 & 0 & 0 & 0 \\ 0 & 0 & 0 & 0 & 0 & 0 \\ 0 & 0 & 0 & 0 & 0 & 0 \end{pmatrix} \begin{pmatrix} 1 & 1 & 1 & 1 & 1 & 1 \\ 2 & 0 & 0 & 0 & 1 & 1 \\ 0 & 2 & 0 & 1 & 0 & 1 \\ 0 & 0 & 0 & 1 & 1 & 1 \\ -1 & -1 & 0 & 0 & 0 & 0 \\ 1 & 0 & 0 & 0 & 0 & 0 \end{pmatrix}, \quad (\text{A26})$$

where the order of irreps is $\overline{A}_4\overline{A}_4, \overline{A}_5\overline{A}_6, \overline{\Gamma}_4\overline{\Gamma}_4, \overline{\Gamma}_5\overline{\Gamma}_6, \overline{H}_4, \overline{H}_5, \overline{H}_6, \overline{HA}_4, \overline{HA}_5, \overline{HA}_6, \overline{K}_4, \overline{K}_5, \overline{K}_6, \overline{KA}_4, \overline{KA}_5, \overline{KA}_6, \overline{L}_2\overline{L}_2, \overline{M}_2\overline{M}_2$, in the BCS notation [40, 51]. The rank of the EBR matrix is $r = 4$, and the number of EBRs is $N_{EBR} = 6$, thus y has four components and k has two components. From Eq. (A26), it is direct to see that the solution of $B = \sum_{i=1}^r (L\Lambda)_i y_i \geq 0$ is

$$y_1 \geq y_4 \geq 0, \quad y_2 \geq 0, \quad y_3 \geq 0, \quad 2y_1 - y_2 - y_3 \geq 0. \quad (\text{A27})$$

Relying on the discussion in Appendix A 2, we can write the p -vector as

$$p = R^{-1} \begin{pmatrix} y \\ k \end{pmatrix} = \begin{pmatrix} k_2 \\ -k_1 - k_2 \\ y_1 - y_4 + k_1 \\ -y_2 + y_4 + 2k_2 \\ -y_3 + y_4 - 2k_1 - 2k_2 \\ y_2 + y_3 - y_4 + 2k_1 \end{pmatrix}. \quad (\text{A28})$$

Now we solve the inequality by the method described in Eqs. (A18) to (A23). At the first step, we take k_1 as the variable, then $p \geq 0$ gives

$$-k_1 - k_2 \geq 0, \quad y_1 - y_4 + k_1 \geq 0, \quad -y_3 + y_4 - 2k_1 - 2k_2 \geq 0, \quad y_2 + y_3 - y_4 + 2k_1 \geq 0. \quad (\text{A29})$$

(For now we temporarily omit the first and fourth components of p , *i.e.*, k_2 and $-y_2 + y_4 + 2k_2$, where k_1 is not involved.) The four constraints in Eq. (A29) should be satisfied at the same time, so we obtain

$$\max \left(-\frac{1}{2}y_2 - \frac{1}{2}y_3 + \frac{1}{2}y_4, -y_1 + y_4 \right) \leq k_1 \leq \min \left(-k_2, -k_2 - \frac{1}{2}y_3 + \frac{1}{2}y_4 \right), \quad (\text{A30})$$

At the second step, we regard k_2 as the variable and find the constraints satisfied by k_2 that guarantee (i) $p_1 \geq 0$, $p_4 \geq 0$, and (ii) k_1 has a nontrivial solution. On one hand, for p_1 and p_4 to be nonnegative, we have

$$k_2 \geq 0, \quad -y_2 + y_4 + 2k_2 \geq 0. \quad (\text{A31})$$

On the other hand, for k_1 to have nontrivial solutions, we should satisfy the inequalities

$$\begin{aligned} -\frac{1}{2}y_2 - \frac{1}{2}y_3 + \frac{1}{2}y_4 &\leq -k_2 \\ -\frac{1}{2}y_2 - \frac{1}{2}y_3 + \frac{1}{2}y_4 &\leq -k_2 - \frac{1}{2}y_3 + \frac{1}{2}y_4 \\ -y_1 + y_4 &\leq -k_2 \\ -y_1 + y_4 &\leq -k_2 - \frac{1}{2}y_3 + \frac{1}{2}y_4 \end{aligned} \quad (\text{A32})$$

Regarding k_2 as the variable, the constraints in Eqs. (A31) and (A32) can be equivalently written as

$$\max \left(0, \frac{1}{2}y_2 - \frac{1}{2}y_4 \right) \leq k_2 \leq \min \left(\frac{1}{2}y_2, \frac{1}{2}y_2 + \frac{1}{2}y_3 - \frac{1}{2}y_4, y_1 - \frac{1}{2}y_3 - \frac{1}{2}y_4, y_1 - y_4 \right). \quad (\text{A33})$$

Eq. (A33) guarantees that (i) $p_{1,4}$ are nonnegative, and (ii) Eq. (A30) has a nontrivial solution, which guarantees that $p_{2,3,5,6}$ are nonnegative. Thus, the sufficient and necessary condition for p to be nonnegative is that Eq. (A33) has nontrivial solutions. And, Eq. (A33) has nontrivial solutions if and only if the two lower bounds are smaller than the four upper bounds, *i.e.*, the eight inequalities

$$\begin{aligned} y_2 \geq 0, \quad y_2 + y_3 - y_4 \geq 0, \quad 2y_1 - y_3 - y_4 \geq 0, \quad y_1 - y_4 \geq 0, \\ y_4 \geq 0, \quad y_3 \geq 0, \quad 2y_1 - y_2 - y_3 \geq 0, \quad 2y_1 - y_2 - y_4 \geq 0. \end{aligned} \quad (\text{A34})$$

Now we are ready to work out the fragile indices. First we look at the inequality-type. We notice that the first, fourth, fifth, sixth, and seventh inequalities in Eq. (A34) are identical to the inequalities in Eq. (A27) obtained from $B \geq 0$ and hence do not bring any new index. But the second, third, and last inequalities are not included in Eq. (A27). Therefore we can get three inequality-type fragile criteria as the second, third and last inequalities in Eq. (A27) (for which k_2 solutions do not exist.)

$$y_4 - y_2 - y_3 > 0, \quad (\text{A35})$$

$$y_3 + y_4 - 2y_1 > 0, \quad (\text{A36})$$

$$y_2 + y_4 - 2y_1 > 0. \quad (\text{A37})$$

$$(\text{A38})$$

Now we look at the \mathbb{Z}_n -type indices. First let us derive the condition for k_2 to have fractional solutions but no integer solution. Eq. (A33) can be thought as the intersection of the following five equations

$$0 \leq k_2 \leq \min \left(\frac{1}{2}y_2, \frac{1}{2}y_2 + \frac{1}{2}y_3 - \frac{1}{2}y_4, y_1 - \frac{1}{2}y_3 - \frac{1}{2}y_4, y_1 - y_4 \right), \quad (\text{A39})$$

$$\frac{1}{2}y_2 - \frac{1}{2}y_4 \leq k_2 \leq \frac{1}{2}y_2, \quad (\text{A40})$$

$$\frac{1}{2}y_2 - \frac{1}{2}y_4 \leq k_2 \leq \frac{1}{2}y_2 + \frac{1}{2}y_3 - \frac{1}{2}y_4, \quad (\text{A41})$$

$$\frac{1}{2}y_2 - \frac{1}{2}y_4 \leq k_2 \leq y_1 - \frac{1}{2}y_3 - \frac{1}{2}y_4, \quad (\text{A42})$$

$$\frac{1}{2}y_2 - \frac{1}{2}y_4 \leq k_2 \leq y_1 - y_4. \quad (\text{A43})$$

If Eq. (A39) has solutions, the solutions must contain the integer 0, which would *not* be a fractional solution of k_2 but an integer solution. Similarly, if Eq. (A43) has solutions, the solutions must contain the integer $y_1 - y_4$. Thus neither Eq. (A39) nor Eq. (A43) can bring new indices, since the bounds of these equations are integers, and we are looking for non-integer solutions but no integer solutions. Therefore we only need to consider the cases where Eq. (A40) or Eq. (A41) or Eq. (A42) has only fractional solutions but no integer solution. For Eq. (A40) to have no integer solution, we set the lower bound as half integer and set the interval to be smaller than $\frac{1}{2}$, *i.e.*, $y_2 - y_4 = 1 \pmod 2$ and $0 \leq \frac{1}{2}y_2 - (\frac{1}{2}y_2 - \frac{1}{2}y_4) < \frac{1}{2}$. Considering y 's are integers, we can rewrite this condition as (A).

$$y_2 - y_4 = 1 \pmod 2, \quad y_4 = 0. \quad (\text{A44})$$

Similarly, for Eqs. (A41) and (A42) to have no integer solution, we get (B)

$$y_2 - y_4 = 1 \pmod 2, \quad y_3 = 0, \quad (\text{A45})$$

and (C)

$$y_2 - y_4 = 1 \pmod 2, \quad 2y_1 - y_2 - y_3 = 0, \quad (\text{A46})$$

respectively. Then we consider the case where k_2 can be integer but k_1 cannot. The solution Eq. (A30) can be thought as the intersection of the following three solutions

$$-\frac{1}{2}y_2 - \frac{1}{2}y_3 + \frac{1}{2}y_4 \leq k_1 \leq -k_2, \quad (\text{A47})$$

$$-\frac{1}{2}y_2 - \frac{1}{2}y_3 + \frac{1}{2}y_4 \leq k_1 \leq -k_2 - \frac{1}{2}y_3 + \frac{1}{2}y_4, \quad (\text{A48})$$

$$-y_1 + y_4 \leq k_1 \leq \min \left(-k_2, -k_2 - \frac{1}{2}y_3 + \frac{1}{2}y_4 \right). \quad (\text{A49})$$

Since we are looking for non-integer solutions, Eqs. (A47) and (A49) cannot bring new indices because if they have solutions, they must have integer solutions. (If there is an integer solution, then there is always at least one way of writing the B as a sum of EBRs with nonnegative coefficients.) For example, when Eq. (A47) has solutions, $-k_2$ must be a solution; when Eq. (A49) has solutions, $-y_1 + y_4$ must be a solution. Thus we only need to consider the case where Eq. (A48) has no integer solution. We set the lower bound of Eq. (A48) as half integer, *i.e.*, $-y_2 - y_3 + y_4 = 1 \pmod 2$, and set the interval to be smaller than $\frac{1}{2}$, *i.e.*, $-k_2 - \frac{1}{2}y_3 + \frac{1}{2}y_4 - (-\frac{1}{2}y_2 - \frac{1}{2}y_3 + \frac{1}{2}y_4) = -k_2 + \frac{1}{2}y_2 < \frac{1}{2}$ for arbitrary integer k_2 allowed by Eq. (A33). The interval smaller than $\frac{1}{2}$ condition can be equivalently written as $\frac{1}{2}y_2 - \frac{1}{2} < \min(k_2)$.

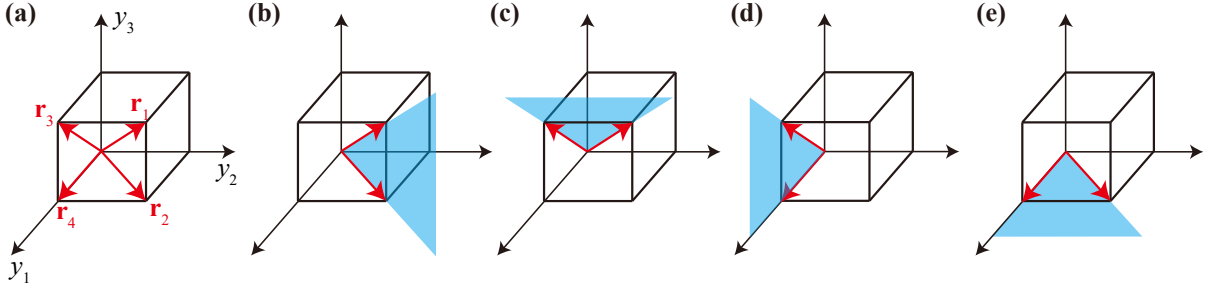


FIG. 6. The rays and boundary planes in of the polyhedral cone Y in SG 150. (a) $\mathbf{r}_1 = (1, 1, 1)^T$, $\mathbf{r}_2 = (1, 1, 0)^T$, $\mathbf{r}_3 = (1, 0, 1)^T$, $\mathbf{r}_4 = (1, 0, 0)^T$. (b) the $y_1 - y_2 = 0$ plane. (c) the $y_1 - y_3 = 0$ plane. (d) the $y_2 = 0$ plane. (e) the $y_3 = 0$ plane.

Due to Eq. (A33), $\min(k_2)$ can be either 0 or $\lceil \frac{y_2 - y_4}{2} \rceil$. There are three cases: (D) if $y_2 - y_4 \leq 0$, then $\min(k_2) = 0$, (E) if $y_2 - y_4 \geq 0$ and $y_2 - y_4 = 0 \pmod{2}$, then $\min(k_2) = \frac{1}{2}(y_2 - y_4)$, and (F) if $y_2 - y_4 \geq 0$ and $y_2 - y_4 = 1 \pmod{2}$, then $\min(k_2) = \frac{1}{2}(y_2 - y_4) + \frac{1}{2}$. (D) with the condition $\frac{1}{2}y_2 - \frac{1}{2} < \min(k_2)$ implies $y_2 < 1$ and $y_4 \geq 0$ ($y_4 \geq 0$ is already contained in Eq. (A27)). Since $y_2 \geq 0$ (Eq. (A27)) we have $y_2 = 0$ and the fragile criterion

$$-y_2 - y_3 + y_4 = 1 \pmod{2}, \quad y_2 = 0. \quad (\text{A50})$$

(E) with the condition $\frac{1}{2}y_2 - \frac{1}{2} < \min(k_2)$ implies $y_4 < 1$ and $y_2 \geq y_4$. Since $y_4 \geq 0$ (Eq. (A27)) have $y_4 = 0$ and $y_2 \geq 0$ ($y_2 \geq 0$ is already contained in Eq. (A27)). Thus the fragile criterion is

$$-y_2 - y_3 + y_4 = 1 \pmod{2}, \quad y_2 - y_4 = 0 \pmod{2}, \quad y_4 = 0. \quad (\text{A51})$$

(F) with the condition $\frac{1}{2}y_2 - \frac{1}{2} < \min(k_2)$ implies $y_4 < 2$ and $y_2 \geq y_4$. Since $y_4 \geq 0$ (Eq. (A27)), we have $y_4 = 0, 1$. For $y_4 = 0$, we have $y_2 \geq 0$, and the fragile criterion

$$-y_2 - y_3 + y_4 = 1 \pmod{2}, \quad y_2 - y_4 = 1 \pmod{2}, \quad y_4 = 0. \quad (\text{A52})$$

For $y_4 = 1$, we have $y_2 \geq 1$, and the fragile criterion

$$-y_2 - y_3 + y_4 = 1 \pmod{2}, \quad y_2 - y_4 = 1 \pmod{2}, \quad y_4 = 1. \quad (\text{A53})$$

Therefore, Eqs. (A44) to (A46) and (A50) to (A53) are all the \mathbb{Z}_2 -type criteria in SG 143.

Appendix B: Fragile phases as affine monoids

1. Examples of Y and X

Here we take Y of SG 150 as an example to show the two representations of the polyhedral cone. Due to Eq. (A4), the H-representation of Y can be written as

$$Y = \{y \in \mathbb{R}^3 \mid y_1 \geq y_2, y_1 \geq y_3, y_2 \geq 0, y_3 \geq 0\}. \quad (\text{B1})$$

As shown in Fig. 6, the 2-dimensional faces of the polyhedral cone are the subsets of Y where a single inequality is saturated, and the 1-dimensional faces, or the rays, of the polyhedral cone are where two of the inequalities are saturated. To be specific, the six pairs of the four inequalities in Eq. (B1) set (i) $y_1 = y_2 = y_3$ and $y_1 \geq 0$, (ii) $y_1 = y_2 = 0$ and $0 \geq y_3 \geq 0$ (or $y_3 = 0$), (iii) $y_1 = y_2$ and $y_3 = 0$ and $y_2 \geq 0$ (iv) $y_1 = y_3$ and $y_2 = 0$ and $y_1 \geq 0$, (v) $y_1 = y_3 = 0$ and $0 \geq y_2 \geq 0$, (vi) $y_2 = y_3 = 0$ and $y_1 \geq 0$; we find that (i), (iii), (iv) and (vi) are rays and (ii) and (v) are points. Therefore, the ray matrix in the V-representation of Y is given by

$$\text{Ray} = \begin{pmatrix} 1 & 1 & 1 & 1 \\ 1 & 1 & 0 & 0 \\ 1 & 0 & 1 & 0 \end{pmatrix}. \quad (\text{B2})$$

Here we take X in SG 150 as another example to show the two representations of the polyhedral cone. The rays of X are given by the first r rows of each column of the R matrix in Eq. (A2), as shown in Fig. 7a. Due to Theorem 4, there will be an H-representation of X . Let us work out the H-representation. As $R_{1:r, \cdot}$ is a 3×4 matrix (Eq. (A2)),

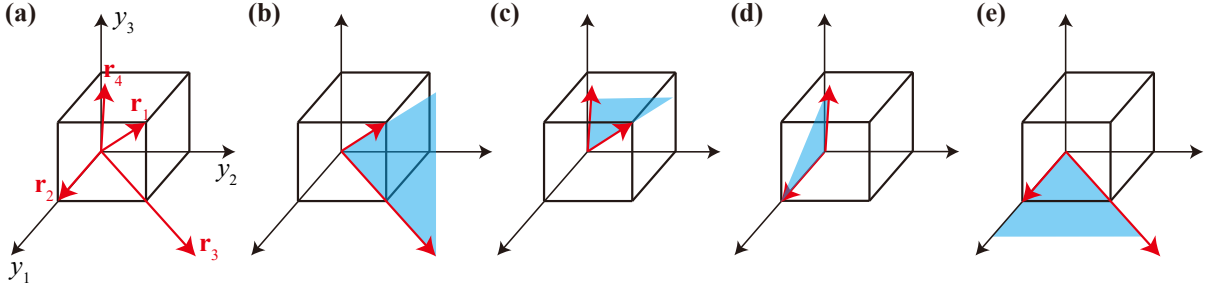


FIG. 7. The rays and boundary planes in of the polyhedral cone X in SG 150. (a) $\mathbf{r}_1 = (1, 1, 1)^T$, $\mathbf{r}_2 = (1, 0, 0)^T$, $\mathbf{r}_3 = (2, 2, 0)^T$, $\mathbf{r}_4 = (2, 1, 2)^T$. (b) the $y_1 - y_2 = 0$ plane. (c) the $y_1 - y_3 = 0$ plane. (d) the $2y_2 - y_3 = 0$ plane. (e) the $y_3 = 0$ plane.

X has four rays, where each pair sets a plane: (i) the first two rays set the plane $y_2 - y_3 = 0$, (ii) the first and the third set $y_1 - y_2 = 0$ (Fig. 7b), (iii) the first and the last set $y_1 - y_3 = 0$ (Fig. 7c), (iv) the second and the third set $y_3 = 0$ (Fig. 7d), (v) the second and the last set $2y_2 - y_3 = 0$ (Fig. 7e), and (vi) the last two set $2y_1 - 2y_2 + y_3 = 0$. It is direct to verify that (ii)-(v) are boundaries of X , whereas (i) and (vi) are not. For example, all points (except origin) on the third ray and the fourth ray satisfy $y_2 - y_3 > 0$ and $y_2 - y_3 < 0$, respectively; because the points on the rays are on different sides of the $y_2 - y_3 = 0$, $y_2 - y_3 = 0$ is not a boundary. On the other hand, all the rays satisfy $y_1 - y_2 \geq 0$, thus $y_1 - y_2 = 0$ is a boundary. Therefore, we obtain

$$X = \{y \in \mathbb{R}^3 \mid y_1 \geq y_2, y_1 \geq y_3, 2y_2 - y_3 \geq 0, y_3 \geq 0\}. \quad (\text{B3})$$

2. Hilbert bases of \bar{Y} and EFP roots

An affine monoid M is called *positive* if $\forall a, b \in M - \{0\} \Rightarrow a + b \neq 0$. Theorem 7 in Appendix F tells us that the intersection of a pointed polyhedral cone and the integer lattice is a positive monoid. Therefore, \bar{Y} is indeed a positive affine monoid. Since \bar{X} is a subset of \bar{Y} , \bar{X} is also a positive affine monoid.

Due to Theorem 6, any positive affine monoid has a unique minimal set of generators, called the Hilbert bases. All the elements in the monoid can be written as sum of the Hilbert bases with positive coefficients. It should be noticed that any of the Hilbert basis cannot be written as a sum of other nonzero elements in the positive affine monoid with positive coefficients. As shown in the following examples, in some cases the vectors of the Hilbert bases are linearly dependent on each other, but writing anyone of them as a linear combination of others will involve negative coefficients. Here we divide the Hilbert bases into two parts: the fragile phase bases and the trivial bases. The trivial bases actually correspond to EBRs because they are trivial (BR) and cannot be written as a sum of other elements with positive coefficients (elementary basis). We call the fragile phase bases as *EFP roots*. From the aspect of symmetry data, the fragile roots are the “representative” phases of EFPs, as any EFP can be obtained by either stacking the roots or stacking the roots with EBRs (trivial bands).

Example. We take Y in SG 150 as an example to derive the Hilbert bases. The Y polyhedron is given in Eq. (B1). To derive the Hilbert bases, we further divide the points in \bar{Y} into two cases: (i) $0 \leq y_3 \leq y_2 \leq y_1$, (ii) $0 \leq y_2 \leq y_3 \leq y_1$. For case-(i), we can rewrite the y -vector as

$$y = \begin{pmatrix} y_1 \\ y_2 \\ y_3 \end{pmatrix} = y_3 \begin{pmatrix} 1 \\ 1 \\ 1 \end{pmatrix} + (y_2 - y_3) \begin{pmatrix} 1 \\ 0 \\ 0 \end{pmatrix} + (y_1 - y_2) \begin{pmatrix} 1 \\ 0 \\ 0 \end{pmatrix}. \quad (\text{B4})$$

For case-(ii), we can rewrite the y -vector as

$$y = \begin{pmatrix} y_1 \\ y_2 \\ y_3 \end{pmatrix} = y_2 \begin{pmatrix} 1 \\ 1 \\ 1 \end{pmatrix} + (y_3 - y_2) \begin{pmatrix} 1 \\ 0 \\ 0 \end{pmatrix} + (y_1 - y_3) \begin{pmatrix} 1 \\ 0 \\ 0 \end{pmatrix}. \quad (\text{B5})$$

Therefore there are four Hilbert bases

$$b_1 = \begin{pmatrix} 1 \\ 1 \\ 1 \end{pmatrix}, \quad b_2 = \begin{pmatrix} 1 \\ 0 \\ 0 \end{pmatrix}, \quad b_3 = \begin{pmatrix} 1 \\ 0 \\ 0 \end{pmatrix}, \quad b_4 = \begin{pmatrix} 1 \\ 0 \\ 1 \end{pmatrix}. \quad (\text{B6})$$

b_1, b_2, b_3, b_4 are also the rays of the polyhedral cone Y (Eq. (B2)). The four bases are linearly dependent, but they are not redundant for the monoid as none of them can be written as a sum of the other three with positive coefficients.

To be specific, $b_1 = b_3 + b_4 - b_2$, $b_2 = b_3 + b_4 - b_1$, $b_3 = b_1 + b_2 - b_4$, $b_4 = b_1 + b_2 - b_3$. Applying the fragile criteria of SG 150, *i.e.*, Eqs. (A9) and (A13) to (A15) to be four bases, we find that b_1 and b_2 are trivial, b_3 satisfies the \mathbb{Z}_2 -type criterion Eq. (A13), and b_4 satisfies the inequality-type criterion Eq. (A9). In fact, b_1 and b_3 are the first and second columns of the right transformation matrix R (the first three rows) in the Smith Decomposition of the EBR matrix (Eq. (A2)), respectively, and thus present two EBRs of SG 150. Therefore SG 150 has only two EFP roots: b_3 and b_4 .

There are two commonly used algorithms to calculate the Hilbert bases of positive affine monoid, *i.e.*, the Normaliz algorithm [79] and the Hemmecke algorithm [80], which are available in the *Normaliz* package and the *4ti2* package, respectively. In this work, we mainly use the 4ti2 package to solve the Hilbert bases. Applying this algorithm for each \bar{Y} , we are able to calculate all the fragile roots in all SGs, as tabulated in Table S3 of [74]. In Table 1 in the main text, we summarized the numbers of fragile roots in all the SGs.

3. Hilbert bases of $\mathbb{Z}^r \cap X$

As introduced in Section IV A, $\bar{X} = \{y \in \mathbb{Z}^r \mid y_i = (Rp)_i, p \in \mathbb{N}^{N_{EBR}}\}$ represent all the trivial points in Y . Thus the fragile phases are represented by points in $\bar{Y} - \bar{X}$. For convenience we introduced the auxillary polyhedral cone $X = \{y \in \mathbb{R}^r \mid y_i = (Rp)_i, p \in \mathbb{R}^{N_{EBR}}\}$ and divide the points in $\bar{Y} - \bar{X}$ into $\bar{Y} - \mathbb{Z}^r \cap X$ and $\mathbb{Z}^r \cap X - \bar{X}$. Here we discuss a special issue of the Hilbert bases of $\mathbb{Z}^r \cap X$, which will be used in deriving the fragile indices in Appendix C 2. A basis $b_l \in \text{Hil}(\mathbb{Z}^r \cap X)$ is either trivial ($\in \bar{X}$) or nontrivial ($\notin \bar{X}$), depending whether it can be written as a sum of columns of $R_{1:r,:}$, *i.e.*, $\exists q_l \in \mathbb{N}^{N_{EBR}}$ s.t. $b_l = R_{1:r,:}q_l$. Now we define the order of b_l as the smallest positive integer κ_l that makes $\kappa_l b_l \in \bar{X}$. We first consider the solutions of the equation $b_l = R_{1:r,:}q_l$, where q_l is vector with N_{EBR} components. The general solution of $b_l = R_{1:r,:}q_l$ is given as $q_l = \sum_i^r (b_l)_i R_i^{-1} + \sum_{j=1}^{N_{EBR}-r} k_j R_{j+r}^{-1}$, where R_i^{-1} is the i -th column of R^{-1} , r is the rank of the EBR matrix, and k 's are free parameters. For convenience, we introduce the auxillary polyhedron

$$K_l = \left\{ k \in \mathbb{Q}^{N_{EBR}} \mid \sum_i^r (b_l)_i R_i^{-1} + \sum_{j=1}^{N_{EBR}-r} k_j R_{j+r}^{-1} \geq 0 \right\}. \quad (\text{B7})$$

Notice that R is a unimodular matrix, thus $q_l \in \mathbb{N}^r \Leftrightarrow k \in \mathbb{Z}^{N_{EBR}-r}$. If K_l contains integer points, we can take an integer point in it, k , such that the corresponding $q_l \in \mathbb{N}^r$ and hence $b_l = R_{1:r,:}q_l$ is a combination with nonnegative coefficients of columns in $R_{1:r,:}$. If K_l contains only fractional points but no integer point, the corresponding q_l 's are nonnegative but fractional, and hence b_l can be only be written as a combination with nonnegative fractional coefficients of columns in $R_{1:r,:}$. For this second case we can introduce a (minimal) positive integer κ_l such that $\kappa_l K_l$, *i.e.*,

$$\kappa_l K_l = \{ \kappa_l k \mid k \in K_l \}, \quad (\text{B8})$$

contains at least one integer point. Such a κ_l always exists: suppose k is a fractional vector in K_l , then we can take κ_l as the least common multiplier of the denominators of the components of k such that $\kappa_l k$ is an integer vector. We always choose κ_l as the minimal integer that makes $\kappa_l K_l$ contains at least one integer point. κ_l can be thought as the ‘‘order’’ of a nontrivial Hilbert basis because $\kappa_l b_l$ can be written as a combination with nonnegative integer coefficients of columns in $R_{1:r,:}$ and hence belongs to \bar{X} .

Example. Now we derive the Hilbert bases of $\mathbb{Z}^3 \cap X$ in SG 150. X is shown in Fig. 7, and its H-representation is derived in Eq. (B3). To derive the Hilbert bases, we further divide the points in $\mathbb{Z}^3 \cap X$ into two cases: (i) $y_2 - y_3 \geq 0$, (ii) $y_2 - y_3 \leq 0$. For case-(i), we can rewrite the y -vector as

$$y = \begin{pmatrix} y_1 \\ y_2 \\ y_3 \end{pmatrix} = y_3 \begin{pmatrix} 1 \\ 1 \\ 1 \end{pmatrix} + (y_2 - y_3) \begin{pmatrix} 1 \\ 0 \\ 0 \end{pmatrix} + (y_1 - y_2) \begin{pmatrix} 1 \\ 0 \\ 0 \end{pmatrix}. \quad (\text{B9})$$

The three bases in case-(i) are same with the bases in case-(i) of \bar{Y} (Eq. (B4)). For case-(ii), where $y_2 - y_3 \leq 0$, we can rewrite the y -vector as

$$y = \begin{pmatrix} y_1 \\ y_2 \\ y_3 \end{pmatrix} = (y_1 - y_3) \begin{pmatrix} 1 \\ 1 \\ 1 \end{pmatrix} + (2y_2 - y_3) \begin{pmatrix} 1 \\ 0 \\ 0 \end{pmatrix} + (y_3 - y_2) \begin{pmatrix} 2 \\ 1 \\ 1 \end{pmatrix}. \quad (\text{B10})$$

The three bases in case-(ii), where $y_2 - y_3 \leq 0$, are different with the bases in case-(ii) of \bar{Y} (Eq. (B5)) because here we cannot decompose y into $(1, 0, 1)^T$ since $(1, 0, 1)^T \notin \bar{X}$. Therefore there are four Hilbert bases

$$b_1 = \begin{pmatrix} 1 \\ 1 \\ 1 \end{pmatrix}, \quad b_2 = \begin{pmatrix} 1 \\ 0 \\ 0 \end{pmatrix}, \quad b_3 = \begin{pmatrix} 1 \\ 1 \\ 0 \end{pmatrix}, \quad b_4 = \begin{pmatrix} 2 \\ 1 \\ 2 \end{pmatrix}. \quad (\text{B11})$$

b_1, b_2, b_4 are the (first three rows of) columns of R (Eq. (A2)) and hence are trivial. b_3 , on the other hand, is half of the (first three rows of) third column in R . Thus we obtain $\kappa_1 = \kappa_2 = \kappa_4 = 1$, and $\kappa_3 = 2$. To check, we calculate κ_3 using the algorithm described in the last paragraph. The inverse of the R matrix (Eq. (A2)) is

$$R^{-1} = \begin{pmatrix} 0 & 2 & -1 & 4 \\ 1 & 0 & -1 & 2 \\ 0 & 0 & 0 & -1 \\ 0 & -1 & 1 & -2 \end{pmatrix}, \quad (\text{B12})$$

and hence due to Eq. (B7) we obtain

$$K_3 = \left\{ k \in \mathbb{Q} \mid 2 + 4k \geq 0, 1 + 2k \geq 0, -k \geq 0, -1 - 2k \geq 0 \right\} = \left\{ -\frac{1}{2} \right\}. \quad (\text{B13})$$

Therefore, $\kappa_3 = 2$ is the minimal integer that makes $\kappa_3 K_3$ to have an integer point.

Appendix C: Fragile indices

1. Removing un-allowed inequality-type indices

In Section IV B we have introduced the general method to derive inequality-type criteria in form of $ay < 0$. Here we describe how to judge whether $ay < 0$ is allowed. For a given row a in A , we define $Y' = \{y \in \mathbb{R}^r \mid L\Lambda_{:,1:r}y \geq 0 \text{ and } ay < 0\}$. Notice that Y' is an open set (due to the condition $ay < 0$). (A set is open if it does not contain any of its boundary points.) Clearly, $Y' = \emptyset$ implies that $ay < 0$ is not allowed in Y . However, we do not use Y' in practical calculation because it is complicated to store and process an open set in our group calculations; instead, we make use of the closed extension of Y' , *i.e.*, $Y'' = \left\{ y \in \mathbb{R}^r \mid \begin{pmatrix} L\Lambda_{:,1:r} \\ -a \end{pmatrix} y \geq 0 \right\}$. Since Y'' is a superset of Y' , obviously, $Y'' = \emptyset \Rightarrow Y' = \emptyset$. Thus $Y'' = \emptyset$ implies $ay < 0$ is forbidden by the $B \geq 0$ condition. Now we show how to detect the case $Y' = \emptyset$ but $Y'' \neq \emptyset$. We notice that $Y' = \emptyset$ implies that $Y'' = Y'' - Y' = \{y \in \mathbb{R}^r \mid L\Lambda_{:,1:r}y \geq 0 \text{ and } ay = 0\} \neq \emptyset$. The presence of equation $ay = 0$ will reduce the dimension of the polyhedron. Thus this case can be diagnosed by $\dim(Y'') < r$.

Example. In the paragraphs above we have described a general algorithm to derive the inequality-type fragile criteria. As an example, here we re-derive the inequality-type fragile criteria of SG 150 using the polyhedron method. The polyhedral cone Y is given by Eq. (B1), and the polyhedral cone X is given by Eq. (B3). We rewrite Eq. (B3) in terms of the A matrix as

$$X = \{y \in \mathbb{R}^3 \mid Ay \geq 0\}, \quad A = \begin{pmatrix} 1 & -1 & 0 \\ 1 & 0 & -1 \\ 0 & 2 & -1 \\ 0 & 0 & 1 \end{pmatrix}, \quad (\text{C1})$$

The four rows in A correspond to four possible inequality-type fragile indices, *i.e.*, $y_2 - y_1$, $y_3 - y_1$, $y_3 - 2y_2$, and $-y_3$, the positive values of which imply fragile phases. However, the first, second, and last inequalities are not allowed in Y . For the first index $y_2 - y_1$, the auxiliary polyhedral cone $Y'' = \{y_1 \geq y_2, y_1 \geq y_3, y_2 \geq 0, y_3 \geq 0, y_2 - y_1 \geq 0\} = \{y_1 = y_2, y_1 \geq y_3, y_2 \geq 0, y_3 \geq 0\}$ has a dimension 2 (< 3), implying $y_2 - y_1 > 0$ is not allowed in Y . For the second index $y_3 - y_1$, the auxiliary polyhedral cone $Y'' = \{y_1 \geq y_2, y_1 = y_3, y_2 \geq 0, y_3 \geq 0\}$ has a dimension 2 (< 3), implying $y_3 - y_1 > 0$ is not allowed in Y . For the last index $-y_3$, the auxiliary polyhedral cone $Y'' = \{y_1 \geq y_2, y_1 \geq y_3, y_2 \geq 0, y_3 = 0\}$ has a dimension 2 (< 3), implying $-y_3 > 0$ is not allowed in Y , so the corresponding fragile index is not necessary. Therefore, the only inequality-type index is $y_3 - 2y_2$, consistent with the result (Eq. (A9)) in Appendix A 1.

2. \mathbb{Z}_2 -type fragile indices

In this subsection we consider the type-II fragile phases, *i.e.*, symmetry data vectors represented by points in $\mathbb{Z}^r \cap X - \bar{X}$, and derive the corresponding \mathbb{Z}_n -type fragile criteria. It turns out that all the \mathbb{Z}_n -type criteria are of \mathbb{Z}_2 -type.

a. $\mathbb{Z}^r \cap X - \bar{X}$ is close to the boundary of X

A key property allowing us to derive the general \mathbb{Z}_n -indices is that the points in $\mathbb{Z}^r \cap X - \bar{X}$ are all close to the boundaries of X , as will be explained more clearly below. Here we present a heuristic description of this conclusion and leave the proof for the following paragraphs. As we will prove, there always exists a finite integer vector $\Delta y \in \bar{X}$ such that for $\forall y \in \mathbb{Z}^r \cap X - \bar{X}$, $y + \Delta y \in \bar{X}$. In other words, the shifted monoid $\Delta y + \mathbb{Z}^r \cap X = \{y + \Delta y | y \in \mathbb{Z}^r \cap X\}$ is a subset of \bar{X} and hence

$$\begin{aligned} \Delta y + \mathbb{Z}^r \cap X &\subset \bar{X} \\ \Rightarrow \mathbb{Z}^r \cap X - \bar{X} &\subset \mathbb{Z}^r \cap X - (\Delta y + \mathbb{Z}^r \cap X) = \mathbb{Z}^r \cap (X - (\Delta y + X)), \end{aligned} \quad (\text{C2})$$

i.e., $X - (\Delta y + X)$ is superset of $\mathbb{Z}^r \cap X - \bar{X}$. We show that $X - (\Delta y + X)$ is close to the boundary of X . We assume that X has the H-representation $X = \{y \in \mathbb{R}^r \mid Ay \geq 0\}$, then if $x \in \Delta y + X$, there is $x - \Delta y \in X$ and hence $A(x - \Delta y) \geq 0$. Thus we obtain the H-representation of $\Delta y + X$

$$\Delta y + X = \{y \in \mathbb{R}^r \mid A(y - \Delta y) \geq 0\}. \quad (\text{C3})$$

and hence obtain $X - (\Delta y + X)$ as

$$X - (\Delta y + X) = \{y \in \mathbb{R}^r \mid Ay \geq 0, \text{ and } \exists i, \text{ s.t. } (Ay)_i < (A\Delta y)_i\}. \quad (\text{C4})$$

Since the i -th boundary of X is given by $(Ay)_i = 0$, for a given point y , $(Ay)_i$ can be thought as the distance from y to the i -th boundary of X . Eq. (C4) means that for $\forall y \in X - (\Delta y + X)$, there always exists some boundary of X such that the distance from y to this boundary is smaller than the distance from Δy (the existence of which we will prove) to this boundary. That means the points $X - (\Delta y + X)$ is close to the boundary of X .

Before going to prove the existence of Δy , here we first study the property of points in $\mathbb{Z}^r \cap X$. $\mathbb{Z}^r \cap X$ is generated from the so-called Hilbert bases, denoted as $\text{Hil}(\mathbb{Z}^r \cap X)$ (Theorem 6 in Appendix F). To be specific, we can rewrite $\mathbb{Z}^r \cap X$ as

$$\mathbb{Z}^r \cap X = \{y = b_1 p_1 + b_2 p_2 + \dots + b_{N_H} p_{N_H} \mid b_1, b_2 \dots b_{N_H} \in \text{Hil}(\mathbb{Z}^r \cap X), p_1, p_2 \dots p_{N_H} \in \mathbb{N}\}, \quad (\text{C5})$$

where N_H is the number of Hilbert bases. As shown in Appendix B3, for each basis b_l , there is a positive integer κ_l - the order of b_l - such that $\kappa_l b_l \in \bar{X}$ (a trivial point). With the concept of order κ_l of Hilbert basis, we can decompose a general point in $\mathbb{Z}^r \cap X$ in Eq. (C5) into two parts

$$y = \sum_l (p_l \bmod \kappa_l) b_l + \sum_l \lfloor p_l / \kappa_l \rfloor \kappa_l b_l, \quad (\text{C6})$$

where $\lfloor a \rfloor$ is the largest integer equal or smaller to a . The second part in this decomposition belongs to \bar{X} by construction, since $\kappa_l b_l \in \bar{X}$ and $\lfloor p_l / \kappa_l \rfloor \in \mathbb{N}$. Therefore, to shift y to \bar{X} , we only need to shift the first part to \bar{X} .

Now we prove the existence of Δy . As shown in Eq. (C6), the nontrivial part of any point in $\mathbb{Z}^r \cap X - \bar{X}$ is of the form $\sum_l (p_l \bmod \kappa_l) b_l$, thus to shift it to \bar{X} , we only Δy to satisfy

$$\forall p \in \mathbb{N}^{N_H}, \quad \Delta y + \sum_l (p_l \bmod \kappa_l) b_l \in \bar{X}. \quad (\text{C7})$$

As b_l represent either a trivial state (EBR) or an EFP, both of which can be written as an integer combination of EBRs, we can write b_l as $b_l = R_{1:r,:} q_l$ for some $q_l \in \mathbb{Z}^{N_H}$. If $b_l \in \bar{X}$, q_l can be a nonnegative vector; whereas if $b_l \notin \bar{X}$, at least one component of q_l is negative. The choice of q_l is not unique. In general q_l can be written as $\sum_{i=1}^r R_i^{-1} (b_l)_i + \sum_{j=1}^{N_{EBR}-r} R_j^{-1} k_j$, where R_i^{-1} is the i -th column of the R^{-1} matrix, and k 's are free parameters. For now, for each b_l we just pick a specific q_l . We decompose q_l into two parts: the nonnegative part q_l^+ and the negative part q_l^- , *i.e.*,

$$(q_l^+)_i = \begin{cases} (q_l)_i, & \text{if } (q_l)_i \geq 0 \\ 0, & \text{if } (q_l)_i < 0 \end{cases}, \quad (q_l^-)_i = \begin{cases} 0, & \text{if } (q_l)_i \geq 0 \\ (q_l)_i, & \text{if } (q_l)_i < 0 \end{cases}. \quad (\text{C8})$$

Then we have

$$\Delta y + \sum_l (p_l \bmod \kappa_l) b_l = \Delta y + \sum_l (p_l \bmod \kappa_l) R_{1:r,:} q_l^+ + \sum_l (p_l \bmod \kappa_l) R_{1:r,:} q_l^-. \quad (\text{C9})$$

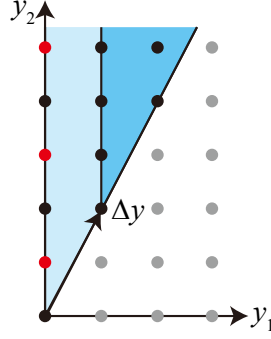


FIG. 8. The shift vector Δy in SG 199. Points in \bar{X} is represented by the black dots, the polyhedral cone X is shaded by light blue, the shifted polyhedral cone $\Delta y + X$ is shaded by blue, points in $\mathbb{Z}^2 \cap X - \bar{X}$ are represented by red dots. All the points in $\mathbb{Z}^2 \cap X - \bar{X}$ are in $X - (\Delta y + X)$ and are close to the boundary of X .

Notice that p_l is a number, q_l , q_l^+ , and q_l^- are vectors. The second term in the right hand side of Eq. (C9) is already in \bar{X} as it is a nonnegative integer combination of columns of $R_{1:r,:}$. Hence Δy only need to shift the third term in Eq. (C9) to \bar{X} . We can choose Δy as

$$\Delta y = - \sum_l (\kappa_l - 1) R_{1:r,:} q_l^- \quad (\text{C10})$$

such that

$$\Delta y + \sum_l (p_l \bmod \kappa_l) R_{1:r,:} q_l^- = \sum_l ((p_l \bmod \kappa_l) - \kappa_l + 1) R_{1:r,:} q_l^- \quad (\text{C11})$$

is always a nonnegative integer combination of columns of $R_{1:r,:}$, because $(p_l \bmod \kappa_l) - \kappa_l + 1 \leq 0$ and hence $((p_l \bmod \kappa_l) - \kappa_l + 1) q_l^- \geq 0$. Therefore Δy defined Eq. (C10) satisfies the condition in Eq. (C7).

Example. Here we take SG 199 as an example to show how to determine Δy . As discussed in the main text (Eq. (8)) and shown in Fig. 8, \bar{X} is given as

$$\bar{X} = \{p_1(0, 2)^T + p_2(1, 2)^T + p_3(1, 3)^T \mid p_{1,2,3} \in \mathbb{N}\} = \{R_{1:r,:} p \mid p \in \mathbb{N}^3\}, \quad (\text{C12})$$

where $R_{1:r,:}$ is given by (Eq. (4) in the main text)

$$R_{1:r,:} = \begin{pmatrix} 0 & 1 & 1 \\ 2 & 2 & 3 \end{pmatrix}. \quad (\text{C13})$$

On the other hand, the polyhedron cone X , which is identical to Y (Eq. (6) in the main text), is given as

$$X = \{y \in \mathbb{R}^2 \mid y_2 \geq 2y_1 \geq 0\}. \quad (\text{C14})$$

The inequality $y_1 \geq 0$ can be rewritten as $(1, 0)y \geq 0$, and the inequality $y_2 \geq 2y_1$ can be rewritten as $(-2, 1)y \geq 0$. Thus X can be rewritten as

$$X = \{y \in \mathbb{R}^2 \mid Ay \geq 0\}, \quad A = \begin{pmatrix} 1 & 0 \\ -2 & 1 \end{pmatrix}. \quad (\text{C15})$$

For any point y in $\mathbb{Z}^2 \cap X$, we can decompose it as $y = y_1(1, 2)^T + (y_2 - 2y_1)(0, 1)^T$. Thus the Hilbert bases of $\mathbb{Z}^2 \cap X$ are $b_1 = (0, 1)^T$ and $b_2 = (1, 2)^T$ and the monoid $\mathbb{Z}^r \cap X$ is

$$\mathbb{Z} \cap X = \{p_1(0, 1)^T + p_2(1, 2)^T \mid p_{1,2} \in \mathbb{N}\}, \quad (\text{C16})$$

On the other hand, \bar{X} can be obtained by adding the (first two rows of) columns of R in Eq. (C13), *i.e.*, $\bar{X} = \{p_1(0, 2)^T + p_2(1, 2)^T + p_3(1, 3)^T \mid p_{1,2,3} \in \mathbb{N}\}$ (Fig. 8). As shown in Fig. 8 and proved in the main text (around Eq. (9)), the set $\mathbb{Z}^r \cap X - \bar{X}$ is given as

$$\mathbb{Z}^r \cap X - \bar{X} = \{(0, 2p + 1)^T \mid p \in \mathbb{N}\} = \{(0, 1)^T, (0, 3)^T, (0, 5)^T \dots\}. \quad (\text{C17})$$

One can immediately observe that the vector $\Delta y = (1, 2)^T$ shift all the points in $\mathbb{Z}^r \cap X - \bar{X}$ to \bar{X} , *e.g.*, $(0, 1) \rightarrow (1, 3)^T$, $(0, 3) \rightarrow (1, 5)^T$, $(0, 5) \rightarrow (1, 7)^T$, *etc.*

Now let us pretend that we do not know Δy and use the algorithm described in last paragraph to determine Δy . Twice of b_1 belongs to \bar{X} (Eq. (C12)) and hence $\kappa_1 = 2$; b_2 is already in \bar{X} and hence $\kappa_2 = 1$. To obtain the q_1^+ and q_1^- (Eq. (C8)), which will be used to determine Δy , we write b_1 b_2 in terms of columns of $R_{1:r,:}$ with integer coefficients as

$$b_1 = (1, 3)^T - (1, 2)^T = R_{1:r,1}(0, -1, 1)^T, \quad b_2 = (1, 2)^T = R_{1:r,1}(0, 1, 0)^T, \quad (\text{C18})$$

i.e., $q_1 = (0, -1, 1)^T$ and $q_2 = (0, 1, 0)^T$. Due to Eq. (C8), $q_1^- = (0, -1, 0)^T$, $q_2^- = 0$. Then according to Eq. (C9), we obtain

$$\Delta y = -(\kappa_1 - 1)R_{1:r,:}q_1^- = (1, 2)^T \quad (\text{C19})$$

which is identical with direct observation. In the end let us verify Eq. (C4). Since the distances from Δy to the first and second boundaries are $(A\Delta y)_1 = 1$ and $(A\Delta y)_2 = 0$, respectively. Thus Eq. (C4) can be written as $X - (\Delta y + X) = \{y \in \mathbb{R}^4 \mid Ay \geq 0, (Ay)_1 < 1\} = \{y \in \mathbb{R}^4 \mid 0 \leq y_1 < 1, -2y_1 + y_2 \geq 0\}$, which is consistent with Fig. 8.

Example. We take SG 150 as a nontrivial example to show how to determine Δy . The $R_{1:r,:}$ matrix can be directly read from Eq. (A2). Thus we can write \bar{X} as

$$\bar{X} = \{R_{1:r,:}p \mid p \in \mathbb{N}^4\}, \quad R_{1:r,:} = \begin{pmatrix} 1 & 1 & 2 & 2 \\ 1 & 0 & 2 & 1 \\ 1 & 0 & 0 & 2 \end{pmatrix}. \quad (\text{C20})$$

On the other hand, from the example analyses in Sections IV A and IV B and Appendix B 3, we obtain the H-representation of X as Eqs. (B3) and (C1), and the four Hilbert bases of $\mathbb{Z}^3 \cap X$ as $b_1 = (1, 1, 1)^T$, $b_2 = (1, 0, 0)$, $b_3 = (1, 1, 0)^T$, and $b_4 = (2, 1, 2)^T$ (Eq. (B11)), respectively. b_1, b_2, b_4 are the first, second, and fourth column of $R_{1:r,:}$ shown in Eq. (C20), and hence belong to \bar{X} . So we have the order $\kappa_1 = \kappa_2 = \kappa_4 = 1$. b_3 is half of the second column of $R_{1:r,:}$ and thus the order $\kappa_3 = 2$. To obtain the q_3^+ and q_3^- (Eq. (C8)), which will be used to determine Δy , we write b_3 as an integer combination of the columns of $R_{1:r,:}$ as

$$b_3 = 2 \begin{pmatrix} 1 \\ 1 \\ 1 \end{pmatrix} + \begin{pmatrix} 1 \\ 0 \\ 0 \end{pmatrix} - \begin{pmatrix} 2 \\ 1 \\ 2 \end{pmatrix} = R_{1:r,:}q_3, \quad (\text{C21})$$

with

$$q_3 = (2, 1, 0, -1)^T. \quad (\text{C22})$$

Due to Eq. (C8), we have $q_3^- = (0, 0, 0, -1)^T$. According to Eq. (C10) we have

$$\Delta y = -(\kappa_3 - 1)R_{1:r,:}q_3^- = (2, 1, 2)^T. \quad (\text{C23})$$

Now we calculate the distances from Δy to the boundaries of X . Using the A matrix in Eq. (C1), we obtain (i) distance from Δy to the boundary $y_1 - y_2 = 0$ is $(Ay)_1 = 2 - 1 = 1$, (ii) distance from Δy to the boundary $y_1 - y_3 = 0$ is $(Ay)_2 = 2 - 2 = 0$, (iii) distance from Δy to the boundary $2y_2 - y_3 = 0$ is $(Ay)_3 = 2 - 2 = 0$, and (iv) distance from Δy to the boundary $y_3 = 0$ is $(Ay)_4 = 2$. This means the points in $\mathbb{Z}^r \cap X - \bar{X}$ satisfy either $y_1 - y_2 = 0$ or $y_3 = 0, 1$, which is consistent with Eqs. (A13) to (A15).

b. Determining the \mathbb{Z}_2 -type indices

We emphasize that in general $X - (\Delta y + X)$ defined in Eq. (C4) is *not* a polyhedron, because the Eq. (C4) does not match the definition of polyhedron in Theorem 3. For example if we take X as $X = \{y \in \mathbb{R}^2 \mid y_1 \geq 0, y_2 \geq 0\}$ and $\Delta y = (1, 1)$. Then $X - (\Delta y + X) = \{y \in \mathbb{R}^2 \mid 0 \leq y_1 \leq 1, y_2 \geq 0\} + \{y \in \mathbb{R}^2 \mid 0 \leq y_2 \leq 1, y_1 \geq 0\}$ is obviously not a polyhedron. Nevertheless, the integer points in $X - (\Delta y + X)$ belong to some lower-dimensional polyhedra, *i.e.*,

$$\mathbb{Z}^r \cap (X - (\Delta y + X)) = \bigoplus_i \bigoplus_{d=0}^{(A\Delta y)_i - 1} \mathbb{Z}^r \cap W^{(i,d)}, \quad (\text{C24})$$

with

$$W^{(i,d)} = \{x \in \mathbb{R}^r \mid (Ax)_i = d \text{ and } Ax \geq 0\} \quad (\text{C25})$$

a $(r-1)$ -dimensional polyhedron. Since Δy shifts all the points in $\mathbb{Z}^r \cap X$ into \bar{X} , Eq. (C24) sums over all the lower-dimensional polyhedra close to the boundaries with distances up to the distances from Δy to the boundaries. By definition (Theorem 4 in Appendix F), the H-representation of a polyhedral cone consists of a set of inequalities and a set of homogeneous equations, *i.e.*, $P = \{x \in \mathbb{R}^r \mid Ax \geq 0, Cx = 0\}$, with A some $n \times r$ matrix and C some $m \times r$ matrix for some n and m . Thus $W^{(i,0)}$ is a polyhedral cone in the $d = 0$ subspace, but in general, $W^{(i,d)}$ ($d > 0$) is neither polyhedral cone nor a shifted polyhedral cone, *i.e.*, $v + P = \{A(x-v) \geq 0, C(x-v) = 0\}$. $W^{(i,d)}$ is a shifted polyhedral cone only if we can find some $v \in \mathbb{R}^r$ such that $(Av)_j = \delta_{ij}d$ and hence $W^{(i,d)}$ can be written as $\{(A(x-v))_i = 0 \text{ and } A(x-v) \geq 0\}$. However, such v does not exist in general case where $d > 0$. For example, if $A_{j\cdot}$ ($j = 1 \cdots, i-1, i+1, \cdots, r+1$) are all linearly independent, then $v = 0$ due to $(Av)_j = 0$ ($j \neq i$), which is in contradiction with the condition $(Av)_i = d$. In the example discussed in the end of this section, as shown in Fig. 9c, the $W^{(4,1)}$ is not a shifted polyhedral cone.

The trivial integer points in $W^{(i,d)}$ are given by

$$\bar{W}^{(i,d)} = \bar{X} \cap W^{(i,d)} = \{R_{1:r,:}p \mid p \in \mathbb{N}^{N_{EBR}} \text{ and } (AR_{1:r,:}p)_i = d \text{ and } AR_{1:r,:}p \geq 0\} \quad (\text{C26})$$

As each column in $R_{1:r,:}$ represents a point in X and hence certainly satisfies the inequalities of X , *i.e.*, $\forall j, AR_{1:r,j} \geq 0$, and hence $AR_{1:r,:}p \geq 0$ is redundant, we can rewrite $\bar{W}^{(i,d)}$ as

$$\bar{W}^{(i,d)} = \{R_{1:r,:}p \mid p \in \mathbb{N}^{N_{EBR}} \text{ and } (AR_{1:r,:}p)_i = d\}. \quad (\text{C27})$$

In the following we will derive the criterion for a point $x \in \mathbb{Z}^r \cap W^{(i,d)}$ to not belong to $\bar{W}^{(i,d)}$ (such that x represents a fragile state). We first consider the case $d = 0$. Due to Eq. (C27), the monoid $\bar{W}^{(i,0)}$ is generated from the columns of $R_{1:r,:}$ that satisfy $(Ax)_i = 0$. We denote the columns of $R_{1:r,:}$ satisfying $(Ac)_i = 0$ columns as $\{C_1^{(i)}, C_2^{(i)}, \dots\}$. In principle, there are two kinds of points in $\mathbb{Z}^r \cap W^{(i,0)} - \bar{W}^{(i,0)}$, which include the points representing EFPs: (i) points that cannot be written as any integer combinations of $\{C_1^{(i)}, C_2^{(i)}, \dots\}$ but can only written as fractional combinations of $\{C_1^{(i)}, C_2^{(i)}, \dots\}$, and (ii) points can be written as some integer combinations of $\{C_1^{(i)}, C_2^{(i)}, \dots\}$ but cannot be written as nonnegative integer combinations of $\{C_1^{(i)}, C_2^{(i)}, \dots\}$. However, as will be explained in Appendix C3, case-(ii) does not exist in practice. Thus we only need to consider case-(i). We denote the matrix consisting of the columns $\{C_1^{(i)}, C_2^{(i)}, \dots\}$ as $C^{(i)}$, *i.e.*, $C^{(i)} = (C_1^{(i)}, C_2^{(i)}, \dots)$. Then a point $x \in \mathbb{Z}^r \cap W^{(i,0)}$ belongs to case-(i) only if $x = C^{(i)}p$ has *no* integer solution, where p is regarded as the variable. To see whether such integer solutions exist, here we apply the Smith Decomposition technique again. We write $C^{(i)}$ as $C^{(i)} = L^{(i)}\Lambda^{(i)}R^{(i)}$, where $L^{(i)}$, $R^{(i)}$ are unimodular integer matrices, and $\Lambda^{(i)}$ is a diagonal integer matrix. Here we assume the rank of C is $r^{(i)}$, and thus the first $r^{(i)}$ diagonal elements of $\Lambda^{(i)}$ are nonzero. (The Smith Decomposition matrices of $C^{(i)}$ are indexed by i . One should not confuse them with the Smith Decomposition matrices of the EBR matrix, *i.e.*, $L\Lambda R$.) Then the equation $x = C^{(i)}p$ has integer solutions only if

$$(L^{(i)-1}x)_j = 0 \pmod{\Lambda_{jj}^{(i)}}, \quad \text{for } j \leq r^{(i)} \quad (\text{C28})$$

because when Eq. (C28) is true we can write the integer solution as

$$p_j = \sum_{k=1}^{r^{(i)}} R_{jk}^{(i)-1} \frac{1}{\Lambda_{kk}^{(i)}} (L^{(i)-1}x)_k. \quad (\text{C29})$$

Therefore, we conclude that the fragile criterion to diagnose points in $\mathbb{Z}^r \cap W^{(i,0)} - \bar{W}^{(i,0)}$ is

$$(Ax)_i = 0, \quad \text{and } \delta^{(i)}(x) \neq 0 \quad (\text{for } \Lambda_{jj}^{(i)} > 0). \quad (\text{C30})$$

where $\delta^{(i)}(x)$ is a vector consisting of the \mathbb{Z}_n -type fragile indices

$$\delta_j^{(i)}(x) = (L^{(i)-1}x)_j \pmod{\Lambda_{jj}^{(i)}} \quad (\text{C31})$$

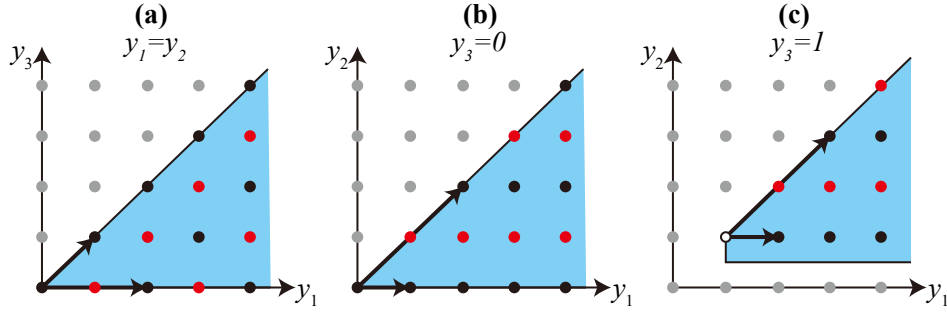


FIG. 9. $W^{(i,d)}$'s in SG 150. (a) $W^{(1,0)}$ in the $y_1 = y_2$ plane. (b) $W^{(4,0)}$ in the $y_3 = 0$ plane. In (a)-(b) the polyhedral cone $W^{(i,0)}$ is represented by the shaded area, the generators of $\overline{W}^{(i,0)}$ are represented by the bold black arrows, the points in $\overline{W}^{(i,0)}$ are represented by black dots, and the points in $\mathbb{Z}^3 \cap W^{(i,0)} - \overline{W}^{(i,0)}$ are represented by red dots. (c) $W^{(4,1)}$ in the $y_3 = 1$ plane. The polyhedron $W^{(4,1)}$ is represented by the shaded area, the points (only one) in the set $\overline{W}^{(4,1)}$ are represented by the hollow circle, the points in $\overline{W}^{(4,1)}$ are represented by black dots, and the points in $\mathbb{Z}^3 \cap W^{(4,1)} - \overline{W}^{(4,1)}$ are represented by red dots.

As the components where the corresponding $\Lambda_{jj}^{(i)} = 1$ always vanish ($0 \bmod 1 = 0$, $1 \bmod 1 = 0$), in the following we only keep the components where the corresponding $\Lambda_{jj}^{(i)} > 1$. In practice, $\Lambda_{jj}^{(i)} = 2$ is the only case where $\Lambda_{jj}^{(i)} > 1$. Thus all the \mathbb{Z}_n -type indices are \mathbb{Z}_2 -type indices.

Example. Here we take SG 199 as an example to show the algorithm described above. First as discussed in the example in Appendix C 2 a and shown in Fig. 8, Δy is $(1, 2)^T$. Its distance to the first boundary $y_1 = 0$ is $(A\Delta y)_1 = 1$, and its distance to the second boundary $y_2 - 2y_1 = 0$ is $(A\Delta y)_2 = 0$, where A is given in Eq. (C15). Due to Eq. (C24) we only need to consider the sub-polyhedron $W^{(1,0)} = \{y \in \mathbb{R}^2 \mid (Ay)_1 = 0, (Ay)_2 \geq 0\}$, which, due to A in Eqs. (C15) and (C25), is given as

$$W^{(1,0)} = \{y \in \mathbb{R}^2 \mid y_1 = 0, y_2 \geq 0\}. \quad (\text{C32})$$

It contains the integer points

$$\mathbb{Z}^2 \cap W^{(1,0)} = \{(0, 0), (0, 1), (0, 2), \dots\}. \quad (\text{C33})$$

Among the three columns of $R_{1:r,:}$ (Eq. (C13)), only the first column satisfies $(Ac)_1 = 0$. Thus, due to Eq. (C27), $\overline{W}^{(1,0)}$, which represent trivial points in $W^{(1,0)}$, is given as

$$\overline{W}^{(1,0)} = \{p(0, 2)^T \mid p \in \mathbb{N}\}, \quad (\text{C34})$$

and the $C^{(1)}$ matrix is given as $C^{(1)} = (0, 2)^T$. Following the algorithm described in last paragraph, we calculate the Smith Decomposition of $C^{(1)}$

$$C^{(1)} = L^{(1)}\Lambda^{(1)}R^{(1)} = \begin{pmatrix} 0 & 1 \\ 1 & 0 \end{pmatrix} \begin{pmatrix} 2 \\ 0 \end{pmatrix} (1). \quad (\text{C35})$$

Substituting $L^{(1)}$, $\Lambda^{(1)}$, and Eq. (C15) into Eqs. (C30) and (C31), we obtain the fragile criterion as

$$y_1 = 0, \quad \text{and} \quad \delta^{(1)}(y) = y_2 \neq 0 \bmod 2, \quad (\text{C36})$$

which is identical with Eq. (9) in the main text.

Example. We take SG 150 as another example to show the criteria to diagnose points in $\mathbb{Z}^r \cap W^{(i,0)} - \overline{W}^{(i,0)}$. According to Eq. (C24), we only need to analyse the $W^{(i,d)}$'s with $(A\Delta y)_i - 1 \geq d$. As discussed in the example in Appendix C 2 a, the shift vector is $\Delta y = (2, 1, 2)^T$ (Eq. (C23)), and its distances to the four boundaries defined by A in Eq. (C1) (Fig. 7b-e) are $(A\Delta y)_1 = 1$, $(A\Delta y)_2 = 0$, $(A\Delta y)_3 = 0$, $(A\Delta y)_4 = 2$, respectively. Thus, we only need to consider the subpolyhedron $W^{(1,0)}$, $W^{(4,0)}$, $W^{(4,1)}$. Here we only calculate the criteria in $W^{(1,0)}$ and $W^{(4,0)}$. Due to the A matrix for SG 150 in Eq. (C1), $(Ay)_1 = 0$ gives the equation $y_1 = y_2$, and $(Ay)_4 = 0$ gives the condition $y_3 = 0$. Then, following the definition of $W^{(i,d)}$ in Eq. (C25), we obtain

$$W^{(1,0)} = \{y \in \mathbb{R}^3 \mid y_1 = y_2, y_1 \geq y_3, y_3 \geq 0\}, \quad (\text{C37})$$

$$W^{(4,0)} = \{y \in \mathbb{R}^3 \mid y_3 = 0, y_1 \geq y_2, y_2 \geq 0\}. \quad (\text{C38})$$

Now let us determine the trivial point monoids $\overline{W}^{(1,0)}$ and $\overline{W}^{(4,0)}$ due to Eq. (C27). For $\overline{W}^{(1,0)}$, among the four columns of $R_{1:r,:}$ (Eq. (C20)), only the first $(1, 1, 1)^T$ and third $(2, 2, 0)^T$ satisfy $(Ac)_1 = 0$. For $\overline{W}^{(4,0)}$, among the four columns of $R_{1:r,:}$, only the second $(1, 0, 0)^T$ and third $(2, 2, 0)^T$ satisfy $(Ac)_4 = 0$. Thus

$$\overline{W}^{(1,0)} = \{p_1(1, 1, 1)^T + p_2(2, 2, 0)^T \mid p_1, p_2 \in \mathbb{N}\}, \quad (\text{C39})$$

$$\overline{W}^{(4,0)} = \{p_1(1, 0, 0)^T + p_2(2, 2, 0)^T \mid p_1, p_2 \in \mathbb{N}\}. \quad (\text{C40})$$

From Fig. 9a, where $W^{(1,0)}$ and $\overline{W}^{(1,0)}$ are plotted, one can conclude the criterion in $W^{(1,0)}$ is $y_1 = y_2$ and $y_1 - y_3 = 1 \pmod{2}$, which is identical with Eq. (A15). Similarly, from Fig. 9b, where $W^{(4,0)}$ and $\overline{W}^{(4,0)}$ are plotted, we can conclude the criterion in $W^{(4,0)}$ is $y_3 = 0$ and $y_2 = 1 \pmod{2}$, which is identical to Eq. (A13). In the following we show how to get these criteria by following the algorithm from Eq. (C27) to Eq. (C30). For $W^{(1,0)}$, the $C^{(1)}$ matrix and its Smith Decomposition are

$$C^{(1)} = \begin{pmatrix} 1 & 2 \\ 1 & 2 \\ 1 & 0 \end{pmatrix} = \begin{pmatrix} 1 & 1 & 0 \\ 1 & 1 & 1 \\ 1 & 0 & 0 \end{pmatrix} \begin{pmatrix} 1 & 0 \\ 0 & 2 \end{pmatrix} \begin{pmatrix} 1 & 0 \\ 0 & 1 \end{pmatrix}. \quad (\text{C41})$$

The inversion of $L^{(1)}$ is

$$L^{(1)-1} = \begin{pmatrix} 0 & 0 & 1 \\ 1 & 0 & -1 \\ -1 & 1 & 0 \end{pmatrix}. \quad (\text{C42})$$

Substituting $L^{(1)-1}$ and $\Lambda^{(1)}$ into Eqs. (C30) and (C31) we obtain

$$y_1 - y_2 = 0, \quad \text{and} \quad \delta^{(1)}(y) = y_1 - y_3 \neq 0 \pmod{2}. \quad (\text{C43})$$

For $W^{(4,0)}$, the $C^{(4)}$ matrix and its Smith Decomposition are

$$C^{(4)} = \begin{pmatrix} 1 & 2 \\ 1 & 2 \\ 1 & 0 \end{pmatrix} = \begin{pmatrix} 1 & 0 & 0 \\ 0 & 1 & 0 \\ 0 & 0 & 1 \end{pmatrix} \begin{pmatrix} 1 & 0 \\ 0 & 2 \end{pmatrix} \begin{pmatrix} 1 & 2 \\ 0 & 1 \end{pmatrix}, \quad (\text{C44})$$

The inversion of $L^{(4)}$ is

$$L^{(4)-1} = \begin{pmatrix} 1 & 0 & 0 \\ 0 & 1 & 0 \\ 0 & 0 & 1 \end{pmatrix}. \quad (\text{C45})$$

Substituting $L^{(4)-1}$ and $\Lambda^{(4)}$ into Eqs. (C30) and (C31) we obtain

$$y_3 = 0, \quad \text{and} \quad \delta^{(4)}(y) = y_2 \neq 0 \pmod{2}. \quad (\text{C46})$$

Now we consider the remaining part: the points in $\mathbb{Z}^r \cap W^{(i,d)} - \overline{W}^{(i,d)}$ for $d > 0$. In general, a point $x \in \mathbb{Z}^r \cap W^{(i,d)}$ decomposes into two parts $x' + x''$: the first part is generated from $\{C_1^{(i)}, C_2^{(i)}, \dots\}$ such that $(Ax')_i = 0$, and the second part is generated by the other columns of $R_{1:r,:}$ and $(Ax'')_i = d$. We denote the columns of $R_{1:r,:}$ that satisfy $(Ax)_i > 0$ as $\{D_1^{(i)}, D_2^{(i)}, \dots\}$, and the matrix consisting of these columns as $D^{(i)} = (D_1^{(i)}, D_2^{(i)}, \dots)$. (This decomposition is in general not unique due to the possible linear dependencies between columns of $R_{1:r,:}$. For example, if there is $C_1^{(i)} = D_1^{(i)} - D_2^{(i)}$, then $x = D_1^{(i)}$ has two at least different decompositions: $x' = 0, x'' = D_1^{(i)}$ or $x' = C_1^{(i)}, x'' = D_2^{(i)}$.) Then we can rewrite $\overline{W}^{(i,d)}$ as

$$\overline{W}^{(i,d)} = \left\{ x = x' + x'' \mid x' \in \overline{W}^{(i,0)}, x'' \in \overline{V}^{(i,d)} \right\}, \quad (\text{C47})$$

where

$$\overline{V}^{(i,d)} = \left\{ v \mid v = p_1 D_1^{(i)} + p_2 D_2^{(i)} + \dots, p_{1,2,\dots} \in \mathbb{N} \text{ and } (Av)_i = d \right\}. \quad (\text{C48})$$

Since all the columns in $D^{(i)}$ satisfy $(AD_j^{(i)}) > 0$ and the combination coefficients, p_j 's, are nonnegative integers and $(Av)_i = d$ is finite, $\overline{V}^{(i,d)}$ is always finite. Particularly, $\overline{V}^{(i,0)} = \{0\}$. By this construction, $\overline{W}^{(i,d)}$ can be thought as a sum of shifted $\overline{W}^{(i,0)}$'s shifted by vectors in $\overline{V}^{(i,d)}$, *i.e.*,

$$\overline{W}^{(i,d)} = \bigoplus_{v \in \overline{V}^{(i,d)}} v + W^{(i,0)}, \quad (\text{C49})$$

where $v + W^{(i,0)} = \{v + y \mid y \in \overline{W}^{(i,0)}\}$. The sum in Eq. (C49) is finite because $\overline{V}^{(i,d)}$ is a finite set. A point x belongs to $v + \overline{W}^{(i,0)}$ only if $x - v$ belongs to $\overline{W}^{(i,0)}$. For $x - v$ to belong to $\overline{W}^{(i,0)}$, first it should belong to the polyhedral cone $W^{(i,0)}$, i.e., $A(x - v) \geq 0$, and second it should have vanishing Z_n -type indices such that it is a trivial point in $\mathbb{Z}^r \cap W^{(i,0)}$. Thus for a point $x \in W^{(i,d)}$ we have

$$x \in v + \overline{W}^{(i,0)} \Leftrightarrow A(x - v) \geq 0, \text{ and } \delta^{(i)}(x - v) = 0, \quad (\text{C50})$$

where $\delta^{(i)}(x)$ is defined in Eq. (C31), and $\delta^{(i)}(x - v) = 0$ means $\delta_j^{(i)}(x - v) = 0$ for all j . As the Z_n -type fragile indices are additive (Eq. (C31)), this condition can be equivalently written as

$$x \in v + \overline{W}^{(i,0)} \Leftrightarrow A(x - v) \geq 0, \text{ and } \delta^{(i)}(x) = \delta^{(i)}(v). \quad (\text{C51})$$

For a point $x \in \mathbb{Z}^r \cap W^{(i,d)}$ to be outside $\overline{W}^{(i,d)}$, which is a sum of some shifted $\overline{W}^{(i,0)}$ (Eq. (C49)), x needs to be outside of all of the shifted $\overline{W}^{(i,0)}$'s. In other words, for a point x outside $\overline{W}^{(i,d)}$, the condition in Eq. (C51) is violated for any $W^{(i,0)}$. Mathematically, the condition for $x \notin \overline{W}^{(i,d)}$ is

$$x \notin \overline{W}^{(i,d)} \Leftrightarrow \forall v \in \overline{V}^{(i,d)} \text{ either } \exists j \text{ s.t. } (A(x - v))_j < 0 \text{ or } \delta^{(i)}(x) \neq \delta^{(i)}(v). \quad (\text{C52})$$

For simplicity, here we consider a sufficient condition (which will be shown also necessary later) for $x \in W^{(i,d)}$ to not belong to $x \notin \overline{W}^{(i,d)}$

$$x \notin \overline{W}^{(i,d)} \Leftarrow \forall v \in \overline{V}^{(i,d)} \delta^{(i)}(x) \neq \delta^{(i)}(v). \quad (\text{C53})$$

This condition is obtained by abandoning the $\exists j \text{ s.t. } (A(x - v))_j < 0$ condition in Eq. (C52). A point with the indices $(\delta^{(i)})$ which cannot be realized by any $v \in \overline{V}^{(i,d)}$ fulfills Eq. (C53). Thus we rewrite it as

$$\delta^{(i)}(x) \notin \left\{ \delta^{(i)}(v) \mid v \in \overline{V}^{(i,d)} \right\} \quad (\text{C54})$$

In principle, the criterion in Eq. (C54) will miss some cases, where $\delta^{(i)}(x)$ equals to $\delta^{(i)}(v)$ for some v in $\overline{V}^{(i,d)}$, but x does not satisfy $A(x - v) \geq 0$. However, as will be discussed in Appendix C3, such cases never appear in practical calculation with TRS and SOC. Therefore, we will treat Eq. (C54) as the fragile criterion in $W^{(i,d)}$ for $d > 0$.

Example. We take SG 150 as an example to show how the algorithm described above works. As discussed from Eq. (C37) to Eq. (C46), points in $\mathbb{Z}^r \cap X - \overline{X}$ are included in (at least) one of the three subpolyhedra $W^{(1,0)}$, $W^{(4,0)}$, and $W^{(4,1)}$. The fragile criteria in $W^{(1,0)}$ and $W^{(4,0)}$ are shown in Eqs. (C43) and (C46), respectively. Now we are going to work out the fragile criterion in $W^{(4,1)}$. First, due to the A matrix in Eq. (C1) and the $W^{(i,d)}$ definition in Eq. (C25), we obtain

$$W^{(4,1)} = \left\{ y \in \mathbb{R}^3 \mid y_3 = 1, y_1 \geq y_2, y_1 \geq 1, y_2 \geq \frac{1}{2} \right\}. \quad (\text{C55})$$

Second, we need to determine the set $\overline{V}^{(4,1)}$ and $\overline{W}^{(4,1)}$. Among the four columns in $R_{1:r,:}$ (Eq. (C20)), only the first $(1, 1, 1)^T$ and the fourth $(2, 1, 2)^T$ satisfy $(Ax)_4 > 0$. To be specific, the first gives $(Ax)_4 = 1$ and the fourth gives $(Ax)_4 = 2$. Then due to Eq. (C48), we obtain

$$V^{(4,1)} = \{(1, 1, 1)^T\}, \quad (\text{C56})$$

and due to Eqs. (C40) and (C49), we obtain

$$\overline{W}^{(4,1)} = \{(1, 1, 1)^T + p_1(1, 0, 0)^T + p_2(2, 2, 0)^T \mid p_1, p_2 \in \mathbb{N}\}. \quad (\text{C57})$$

In Fig. 9c we plot the $W^{(4,1)}$ and $\overline{W}^{(4,1)}$. From Fig. 9c we can see that the points with odd y_2 can always be reached by adding $(1, 0, 0)^T$ and $(2, 2, 0)^T$ to $(1, 1, 1)^T$, while the points even y_2 cannot. Thus we conclude that the criterion to diagnose the points in $\mathbb{Z}^3 \cap W^{(4,1)} - \overline{W}^{(4,1)}$ is $y_3 = 1$ and $y_2 = 0 \pmod{2}$, which is identical with Eq. (A14). Now we apply the algorithm described in the last paragraph to re-derive Eq. (A14). As we already have $V^{(4,1)}$, to get Eq. (C54) we only need to calculate the \mathbb{Z}_2 indices of the points in $V^{(4,1)}$. Due to Eq. (C56) and $\delta^{(4)}(y)$ shown in Eq. (C46), we obtain $\delta^{(4)}(v) = (v_2 \pmod{2}) = 1$. Then Eq. (C54) gives the criterion $\delta^{(4)}(y) = (y_2 \pmod{2}) \notin \{1\}$, which can be equivalently written as

$$y_3 = 1, \quad y_2 = 0 \pmod{2}. \quad (\text{C58})$$

3. Two observations about the results

In this subsection we discuss two observations about the results obtained from applying our algorithm for every SGs. These observations have been used to support some conclusions in Appendix C2. As discussed in Appendix C2b, the type-II nontrivial points, *i.e.*, $\mathbb{Z}^r \cap X - \bar{X}$, are close to the boundary of X and hence belong to some lower dimensional subpolyhedron of X (Eq. (C24)). In each of the subpolyhedron $W^{(i,d)}$ (Eq. (C25)), the trivial points are denoted as $\bar{W}^{(i,d)}$ (Eq. (C27)). First we focus on the $d = 0$ case. $\bar{W}^{(i,0)}$ is generated from the columns of $R_{1:r,:}$ that are exactly on the i -th boundary of X ($d = (Ac)_i = 0$). We denote these columns as $\{C_1^{(i)}, C_2^{(i)}, \dots\}$. In general, there are two kinds of nontrivial points in $\mathbb{Z}^r \cap W^{(i,0)}$: (i) the points cannot be written as any integer combination of $\{C_1^{(i)}, C_2^{(i)}, \dots\}$, (ii) the points can be written an integer combination $\{C_1^{(i)}, C_2^{(i)}, \dots\}$, but at least one of the coefficients is necessarily negative. However, we found by exhaustive computation that case-(ii) does not exists in practical calculation with TRS and SOC. Now we prove this statement based on an observation about the $\{C_1^{(i)}, C_2^{(i)}, \dots\}$. Let us assume there is a point x belonging to case-(ii). On one hand, as said above, x can be written as an integer combination $\{C_1^{(i)}, C_2^{(i)}, \dots\}$, but at least one of the coefficients is negative. On the other hand, as x belongs to $W^{(i,0)}$, x can be written as a linear combination of the columns of $\{C_1^{(i)}, C_2^{(i)}, \dots\}$ where the coefficients are positive and rational. x can in principle have two different decompositions because $\{C_1^{(i)}, C_2^{(i)}, \dots\}$ are not linearly independent. Now let us see whether the linear dependencies can change positive and rational coefficients into integers coefficients where at least one is negative. We enumerate all the linear dependencies of $\{C_1^{(i)}, C_2^{(i)}, \dots\}$ in all SGs, and we find there are only two kinds of dependencies: (A) $c_1 + c_2 = c_3 + c_4$ and (B) $\frac{1}{2}c_1 + \frac{1}{2}c_2 = c_3$, where $c_{1,2,3,4}$ represent different vectors in $\{C_1^{(i)}, C_2^{(i)}, \dots\}$. And, we find that for each $W^{(i,0)}$, different linear dependence equations involve completely different sets of vectors, *i.e.*, no $C_j^{(i)}$ is contained in two or more linear dependence equations. For example, in SG 188 ($P\bar{6}c2$), for a particular $\bar{W}^{(i,0)}$, there are two linear dependencies: $\frac{1}{2}C_1^{(i)} + \frac{1}{2}C_2^{(i)} = C_3^{(i)}$ and $\frac{1}{2}C_4^{(i)} + \frac{1}{2}C_5^{(i)} = C_6^{(i)}$. Thus we only need to deal with the linear dependencies separately. Obviously, $c_1 + c_2 = c_3 + c_4$ can only change an integer coefficient to another integer coefficient. Then we consider the linear dependence $\frac{1}{2}c_1 + \frac{1}{2}c_2 = c_3$, which in principle could change rational coefficients to integer coefficients. Now we prove this is not the case. Let x be a fragile phase spanned by three columns having dependence $\frac{1}{2}c_1 + \frac{1}{2}c_2 = c_3$. We notice that only the coefficients of c_1 and c_2 are fractions ($\frac{1}{2}$), and thus we consider three cases

$$x = \frac{1}{2}c_1 + p_1c_1 + p_2c_2 + p_3c_3, \quad (\text{C59})$$

$$x = \frac{1}{2}c_2 + p_1c_1 + p_2c_2 + p_3c_3, \quad (\text{C60})$$

and

$$x = \frac{1}{2}c_1 + \frac{1}{2}c_2 + p_1c_1 + p_2c_2 + p_3c_3 \quad (\text{C61})$$

where $p_{1,2,3} \in \mathbb{N}$. Due to the $\frac{1}{2}c_1 + \frac{1}{2}c_2 = c_3$, the first case can be equivalently written as

$$x = p_1c_1 + (p_2 - \frac{1}{2})c_2 + (p_3 - 1)c_3 = (p_1 - \frac{1}{2})c_1 + (p_2 - 1)c_2 + (p_3 - 2)c_3 = \dots, \quad (\text{C62})$$

all of which are not integer combinations. Similarly the second case cannot be written as an integer combination. The third case is a trivial point as it can be written as

$$x = p_1c_1 + p_2c_2 + (p_3 + 1)c_3. \quad (\text{C63})$$

Therefore, we conclude that the linear dependencies cannot change positive and rational coefficients into integers coefficients where at least one is negative. In other words, the points in $\mathbb{Z}^r \cap W^{(i,0)} - \bar{W}^{(i,0)}$ can never be written as an integer combination $\{C_1^{(i)}, C_2^{(i)}, \dots\}$ with at least one negative coefficient.

Now we consider the $d > 0$ case. In last section we derive a sufficient condition (Eq. (C54)) for a point in $\mathbb{Z}^r \cap W^{(i,d)}$ to be nontrivial ($\notin \bar{W}^{(i,d)}$). Here we show that this condition is necessary. As discussed in Appendix C2, Δy sets the upper bound of d . We find that in most SGs the maximal d determined by Δy is 0, and only for nine exceptions, *i.e.*, SGs 150 ($P321$), 157 ($P31m$), 185 ($P6_3cm$), 143 ($P3$), 149 ($P312$), 156 ($P3m1$), 158 ($P3c1$), 165 ($P\bar{3}c1$), 188 ($P\bar{6}c2$),

the maximal d is 1. No higher value is found. Hence we only need to check the $d = 1$ sub-polyhedra in the nine SGs. Due to the proof in Appendix C 4, SGs 157 and 185 are equivalent with SG 150, and SGs 149, 156, 158 are equivalent with SG 143. Here “equivalent” means that there is a one-to-one mapping between the fragile criteria in equivalent SGs [73]. Thus in fact we only need to check the four inequivalent SGs 150, 143, 165, and 188. In Appendices A 1 and A 3 we have derived all the fragile criteria in SG 150 and 143 by hand, which are all included in the polyhedron method based criteria, as shown in Table S2 of [74]. Therefore the only cases left to be checked are SGs 165 and 188. Because of the high-rank - ranks of SG 165 and SG 188 are 6 and 7, respectively - we did not derive all the criteria by hand. Instead, we apply numerical checks: we enumerate all the fragile phases up to a number of bands and then check whether they can be diagnosed by Eq. (C54). We use a very large of number of bands - six times the largest number of bands of band structures represented by the Hilbert bases of \bar{Y} - and find no fragile phase is missed by Eq. (C54). Here the symmetry data vector generators are the B vectors corresponding to the Hilbert bases of \bar{Y} .

4. Equivalent SGs

In this subsection we denote the \bar{Y} (\bar{X}) monoid for a given SG G as \bar{Y}_G (\bar{X}_G). The definition for two SGs to be equivalent is given as

Definition 1 For two given SGs G and H , if there exists an isomorphism between \bar{Y}_G and \bar{Y}_H , i.e., a linear one-to-one mapping $f : \bar{Y}_H \rightarrow \bar{Y}_G$ (Theorem 8), such that f is also an isomorphism between \bar{X}_H and \bar{X}_G , then we say G and H are equivalent SGs.

If G and H are equivalent, then there is a one-to-one mapping between the fragile phases in $\bar{Y}_G - \bar{X}_G$ and $\bar{Y}_H - \bar{X}_H$. Now we derive the equivalence condition. First we rewrite \bar{Y}_G and \bar{Y}_H as $\mathbb{Z}^r \cap Y_G$ and $\mathbb{Z}^r \cap Y_H$, respectively, where $Y_G = \{Ray \cdot p | p \in \mathbb{R}_+^n\} \subset \mathbb{R}^r$ and $Y_H = \{Ray' \cdot p | p \in \mathbb{R}_+^n\} \subset \mathbb{R}^r$ are two polyhedral cones. Here we assume both Ray and Ray' are $r \times n$ matrices, and $\text{rank}(Ray) = \text{rank}(Ray') = r$. (If Ray and Ray' have different shapes or ranks, G and H cannot be equivalent.) If \bar{Y}_G and \bar{Y}_H are isomorphic, we can represent the isomorphism map f by an $r \times r$ unimodular matrix F , the inverse of which is also an integer matrix, such that each column of $F \cdot Ray'$ gives a different column of Ray , and every column of Ray is given by some column of $F \cdot Ray'$. In other words, the columns of $F \cdot Ray'$ are given by an rearrangement of the columns of Ray . Mathematically, there exists an $n \times n$ permutation matrix S such that $Ray \cdot S = F \cdot Ray'$. Given a point $y' = Ray' \cdot p' \in \bar{Y}_H$, F maps it to $y = Fy' = Ray \cdot (Sp') \in \bar{Y}_G$; given a point $y = Ray \cdot p \in \bar{Y}_G$, F^{-1} maps it to $y' = S^{-1}y = Ray' \cdot (S^{-1})p \in \bar{Y}_H$. If there does not exist such F and S , \bar{Y}_G and \bar{Y}_H cannot be not isomorphic. Let us assume we have found the matrices F and S . Then we need to check whether F maps \bar{X}_H to \bar{X}_G . The condition for \bar{X}_G to \bar{X}_H to be isomorphic under F is that the Hilbert bases of \bar{X}_G and \bar{X}_H transform to each other under F .

In practice, given two SGs with Ray and Ray' two $r \times n$ matrices, we enumerate all the $n \times n$ permutation matrices, and for each permutation matrix S we try to solve the matrix equation $Ray \cdot S = F \cdot Ray'$. To solve this matrix equation, we write the Smith Decomposition of Ray' as $Ray' = L \begin{pmatrix} \Lambda & 0_{r \times (n-r)} \end{pmatrix} R$, where Λ is an r by r diagonal integer matrix. (One should not confuse this with the Smith Decomposition of the EBR matrix.) All the r diagonal elements in Λ are nonzero because the rank of Ray is r , which is true because the polyhedral cone Y_H spanned by Ray' has the dimension r . We can define the right inverse of Ray' as $\overline{Ray'} = R^{-1} \begin{pmatrix} \Lambda^{-1} \\ 0_{(n-r) \times r} \end{pmatrix} L^{-1}$ such that $Ray' \cdot \overline{Ray'} = \mathbb{1}_{r \times r}$.

Then a necessary condition of $Ray \cdot S = F \cdot Ray'$ is that

$$Ray \cdot S = F \cdot Ray' \quad \Rightarrow \quad F = Ray \cdot S \cdot \overline{Ray'} = Ray \cdot S \cdot R^{-1} \begin{pmatrix} \Lambda^{-1} \\ 0_{(n-r) \times r} \end{pmatrix} L^{-1}. \quad (\text{C64})$$

When $Ray \cdot S \cdot \overline{Ray'} \cdot Ray' = Ray \cdot S$, the right side of Eq. (C64) becomes sufficient

$$Ray \cdot S \cdot \overline{Ray'} \cdot Ray' = Ray \cdot S \quad \text{and} \quad F = Ray \cdot S \cdot \overline{Ray'} \quad \Rightarrow \quad Ray \cdot S = F \cdot Ray'. \quad (\text{C65})$$

However, this is not true in general since we usually have $\overline{Ray'} \cdot Ray' \neq \mathbb{1}_{n \times n}$. Therefore, the equation $Ray \cdot S = F \cdot Ray'$ has either no solution (when $Ray \cdot S \cdot \overline{Ray'} \cdot Ray' \neq Ray \cdot S$) or a unique solution (when $Ray \cdot S \cdot \overline{Ray'} \cdot Ray' = Ray \cdot S$). On the other hand, even if F in Eq. (C64) is a solution of $Ray \cdot S = F \cdot Ray'$, we still need to check whether F is an isomorphism between \bar{X}_H and \bar{X}_G . We change to different permutation matrix S until $Ray \cdot S \cdot \overline{Ray'} \cdot Ray' = Ray \cdot S$ and F in Eq. (C64) become an isomorphism between $\text{Hil}(\bar{X}_H)$ and $\text{Hil}(\bar{X}_G)$. As there are $n!$ distinct permutation matrices, this brute force algorithm takes a factorially long time as the n increases. We have to stop at some finite step. Therefore, for a given pair of SGs, with finite steps, we cannot guarantee to successfully find the possible equivalent relation.

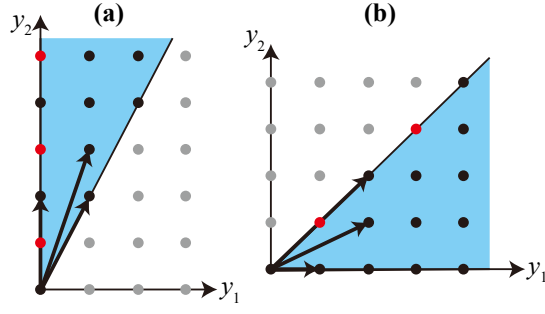


FIG. 10. Example of equivalent SGs. (a) SG 199. (b) SG 208. The polyhedral cone Y 's are represented by the shaded area, the generators of \bar{X} are represented by the bold black arrows, the points in $\mathbb{Z}^2 \cap Y$ are represented by black dots, and the points in $\mathbb{Z}^2 \cap Y - \bar{X}$ are represented by red dots. The transformation $F = \begin{pmatrix} 1 & -1 \\ 2 & -1 \end{pmatrix}$ transforms Y and \bar{X} in SG 208 to the Y and \bar{X} in SG 199.

Example. We take the equivalent SGs 199 and 208 as examples to show the algorithm. As shown in Fig. 10, the Ray matrices of Y_{199} and Y_{208} are

$$Ray = \begin{pmatrix} 0 & 1 \\ 1 & 2 \end{pmatrix}, \quad Ray' = \begin{pmatrix} 1 & 1 \\ 0 & 1 \end{pmatrix}, \quad (\text{C66})$$

respectively. On the other hand, the generators of \bar{X}_{199} and \bar{X}_{208} are

$$b_1 = (0, 2)^T, \quad b_2 = (1, 2)^T, \quad b_3 = (1, 3)^T, \quad (\text{C67})$$

and

$$b'_1 = (2, 2)^T, \quad b'_2 = (1, 0)^T, \quad b'_3 = (2, 1)^T, \quad (\text{C68})$$

respectively. We first choose the permutation matrix as $\begin{pmatrix} 1 & 0 \\ 0 & 1 \end{pmatrix}$, and, due to Eq. (C64), obtain the trial solution

$$F = \begin{pmatrix} 0 & 1 \\ 1 & 1 \end{pmatrix}. \quad (\text{C69})$$

This solution maps Ray' to $Ray \cdot S$. But this F is not an isomorphism between \bar{X}_{199} and \bar{X}_{208} , for example, $Fb'_1 = (2, 4)^T$ is not a generator of \bar{X}_{199} . Secondly, we choose the permutation matrix as $\begin{pmatrix} 0 & 1 \\ 1 & 0 \end{pmatrix}$ and obtain the trial solution

$$F = \begin{pmatrix} 1 & -1 \\ 2 & -1 \end{pmatrix}. \quad (\text{C70})$$

This solution maps Ray' to $Ray \cdot S$, and is an isomorphism between \bar{X}_{199} and \bar{X}_{208} . To be specific, there are $Fb'_1 = b_1$, $Fb'_2 = b_2$, $Fb'_3 = b_3$. Therefore, SG 199 and 208 are equivalent.

In the following are the equivalences found by the brute force algorithm (each line is a class of equivalent SGs)

- (1) 1, 3, 4, 5, 6, 7, 8, 9, 16, 17, 18, 19, 20, 21, 22, 23, 24, 25, 26, 27, 28, 29, 30, 31, 32, 33, 34, 35, 36, 37, 38, 39, 40, 41, 42, 43, 44, 45, 46, 76, 77, 78, 80, 91, 92, 93, 94, 95, 96, 98, 101, 102, , 105, 106, 109, 110, 144, 145, 151, 152, 153, 154, 169, 170, 171, 172, 178, 179, 180, 181.
- (2) 79, 97, 104, 107, 146, 155, 160, 161, 195, 196, 197, 198, 212, 213.
- (3) 90, 100, 108.
- (4) 199, 208, 214, 210.
- (5) 48, 50, 59, 68.
- (6) 52, 54, 56, 57, 60, 62, 73, 112, 113, 116, 117, 118, 120
- (7) 61, 75, 89, 99, 103, 114, 122.

- (8) 133, 142
- (9) 150, 157, 185.
- (10) 159, 173, 182, 186.
- (11) 209, 211.
- (12) 63, 72.
- (13) 135, 138.
- (14) 143, 149, 156, 158.
- (15) 168, 177, 183, 184.
- (16) 218, 219
- (17) 11, 13, 49, 51, 67.
- (18) 14, 53, 55, 58, 81, 82, 111, 115, 119.
- (19) 15, 66
- (20) 86, 134
- (21) 85, 125, 129.
- (22) 12, 65
- (23) 2, 10, 47
- (24) 162, 164.

Notice that the SGs equivalent to SG 1 are all the rank-1 SGs. Thus all the rank-1 SGs do not have EFPs. This will be explained in more detail in Ref. [73].

Appendix D: Twisted bilayer graphene

In this section, we apply our scheme to the twisted bilayer graphene (TBG). The single-valley Hamiltonian of TBG has the magnetic SG $P6'2'2$ [55]. The irreps of $P6'2'2$ are given in Table IV. We define the symmetry-data-vector as

$$B = (m(\Gamma_1), m(\Gamma_2), m(\Gamma_3), m(K_1), m(K_2K_3), m(M_1), m(M_2))^T. \quad (D1)$$

The EBRs of $P6'2'2$ can be found in Table 1 in the supplementary material of [55]. From the EBRs we construct the EBR matrix as

$$EBR = \begin{pmatrix} 1 & 0 & 0 & 2 & 0 & 0 \\ 0 & 1 & 0 & 0 & 2 & 0 \\ 0 & 0 & 1 & 0 & 0 & 2 \\ 1 & 1 & 0 & 0 & 0 & 2 \\ 0 & 0 & 1 & 1 & 1 & 1 \\ 1 & 0 & 1 & 2 & 0 & 2 \\ 0 & 1 & 1 & 0 & 2 & 2 \end{pmatrix}. \quad (D2)$$

Following the method introduced in Appendix A, we can parameterize the symmetry-data-vector as

$$B = (y_1 - y_4, y_2 - y_4, y_4, y_1 + y_2 - 2y_3, y_3, y_1, y_2)^T, \quad (D3)$$

where $y_{1,2,3,4}$ are

$$y_1 = m(\Gamma_1) + m(\Gamma_3), \quad y_2 = m(\Gamma_2) + m(\Gamma_3), \quad y_3 = m(K_2K_3), \quad y_4 = m(\Gamma_3). \quad (D4)$$

Following the machinery of the polyhedron method introduced in Appendix C we obtain two criteria

$$2y_3 - y_4 < 0, \quad (D5)$$

$$y_1 + y_2 - 2y_3 = 0, \quad y_2 - y_4 = 1 \pmod{2}. \quad (D6)$$

Following the algorithm in Appendix B2, we obtain two EFP roots

$$b_1 = (1, 1, 0, 1)^T, \quad b_2 = (1, 1, 1, 0)^T. \quad (D7)$$

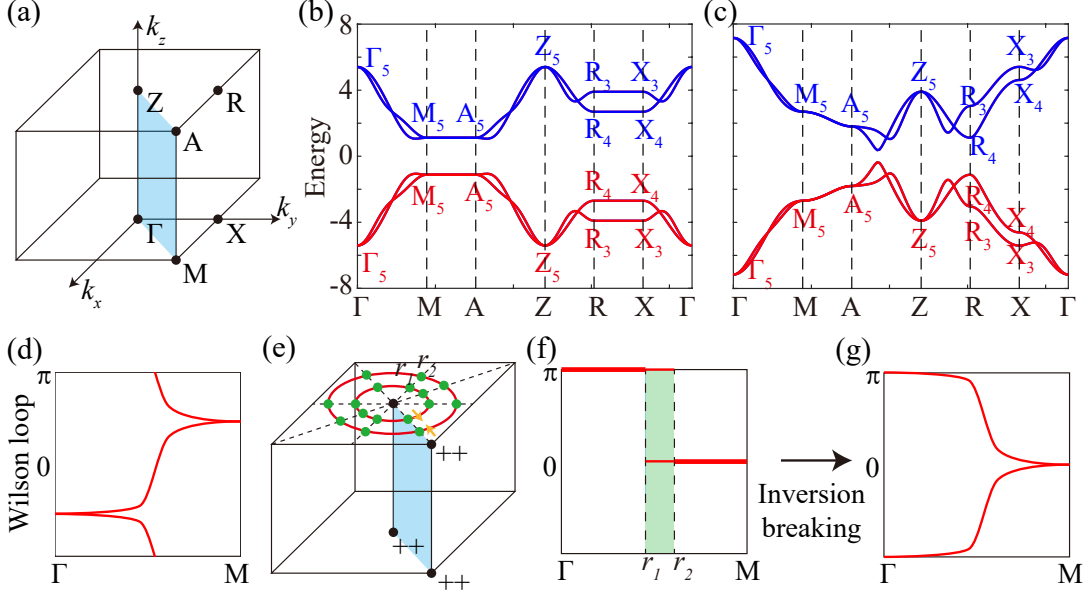


FIG. 11. Fu's topological crystalline insulator [24] and the generalized symmetry eigenvalue criterion. (a) Brillouin zone of the SG $P4$. (b) Band structure and the irreps in the trivial phase of Fu's model ($t' = 0$). (c) Band structure and the irreps in the topological phase of Fu's model ($t' = 2$). The irreps in (b,c) are same as the EBR induced from $p_{x,y}$ orbitals at the $1a$ position. (d) An illustration of the nontrivial Wilson loop spectrum. The Wilson loop operator $W(k_x, k_y)$ is calculated along the k_z direction. The spectrum is plotted along the line $(k_x, k_y) = \Gamma \rightarrow M$. The crossing at Γ and M are protected by C_4 and T . (e) For SG $P4/mmm$, which is a supergroup of $P4$, a \mathbb{Z}_2 invariant can be defined based on the inversion eigenvalues (Eq. (E2)). This \mathbb{Z}_2 invariant implies a nodal ring semimetal. The red circles represent the two nodal rings. The four dashed lines represent the four C_2 rotation axes. (f) The discontinuous Wilson loop spectrum of the nodal ring semimetal. (g) If the symmetry is slightly broken such that $P4/mmm$ reduces to $P422$ and no gap closing happens at Γ, M, Z, A , the Wilson loop will have a winding protected by C_4 and T .

Appendix E: Fu's topological crystalline insulator state and a generalized symmetry eigenvalue criterion

1. Symmetry eigenvalues of Fu's state

Here we explain why Fu's model cannot be diagnosed through usual symmetry eigenvalue analysis. Fu's model is

$$H = \tau_z \sigma_0 (\cos k_x + \cos k_y + \cos k_x \cos k_y) + \tau_z \sigma_z (\cos k_x - \cos k_y) + \tau_z \sigma_x \sin k_x \sin k_y + \tau_x \sigma_0 \left(\frac{5}{2} + \cos k_x + \cos k_y \right) + t' (\tau_x \sigma_0 \cos k_z + \tau_y \sigma_0 \sin k_z). \quad (\text{E1})$$

This model has TRS $T = K$, and C_4 -rotation symmetry $C_4 = i\sigma_y$, and an mirror symmetry $M_{1\bar{1}0} = \sigma_x$. The corresponding space group is $P4mm$. The model is a trivial insulator for $t' = 0$. As t' is increased, a phase transition happens at $t' = 3/2$, and then the state becomes topological. As shown in Fig. 11b,c, the trivial phase and the topological phase have the same irreps. These irreps are same as the EBR induced from $p_{x,y}$ orbitals at the $1a$ position. (See the [Irreducible representations of the Double Point Groups](#) and [Band representations of the Double Space Groups](#) on BCS [40] for the definitions of the irreps and EBRs.) Thus this state cannot be diagnosed through symmetry eigenvalues.

2. Topological invariant protected by C_4 and T

We define the topological invariant based on the Wilson loop. The Wilson loop matrix $W(k_x, k_y)$ is given as $W(k_x, k_y) = \lim_{N \rightarrow \infty} \prod_{i=0}^{N-1} U_{k_x, k_y, \frac{2\pi}{N}i}^\dagger U_{k_x, k_y, \frac{2\pi}{N}(i+1)}$. Here $U_{\mathbf{k}}$ is the matrix $(u_{1\mathbf{k}}, u_{2\mathbf{k}}, \dots)$ with $u_{n\mathbf{k}}$ the periodic part the n th occupied Bloch wavefunction at the wavevector \mathbf{k} . Now we show that the spectrum of $W(\mathbf{k}_0)$ for $\mathbf{k}_0 = (0, 0)$, (π, π) must be doubly degenerate. We denote the C_4 representation matrix at $(\mathbf{k}_0, 0)$ as $D_{\mathbf{k}_0}$. Since $C_4^2 = -1$ (because the model consists of $p_{x,y}$ orbitals), $D_{\mathbf{k}_0}$ has only two eigenvalues, i and $-i$, which transform

to each other under the action of TRS. As $W(\mathbf{k}_0)$ commutes with $D_{\mathbf{k}_0}$, $W(\mathbf{k}_0)$ is block diagonal in the bases of eigenvectors of $D_{\mathbf{k}_0}$. We denote the blocks in the i and $-i$ sectors as $W_i(\mathbf{k}_0)$ and $W_{-i}(\mathbf{k}_0)$, respectively. Since $W_i(\mathbf{k}_0)$ and $W_{-i}(\mathbf{k}_0)$ are related by TRS, they must have the identical eigenvalues. Therefore, each eigenvalue of $W(\mathbf{k}_0)$ is doubly degenerate. Now we consider the spectra of $W(\mathbf{k}_\perp)$ for a continuous path from $\mathbf{k}_\perp = \Gamma$ to $\mathbf{k}_\perp = M$. There are two possible types of connectivity: for the trivial phase, a doublet at $\mathbf{k}_\perp = \Gamma$ splits into two branches in the intermediate process and then the two branches connect to the same doublet at $\mathbf{k}_\perp = M$; for the topological phase, a doublet at $\mathbf{k} = \Gamma$ splits into two branches in the intermediate process and the two branches connect to two adjacent doublets at $\mathbf{k} = M$, as shown Fig. 11d.

3. Generalized symmetry eigenvalue criterion

In order to obtain the generalized symmetry eigenvalue criterion for the fragile topology protected by C_4 and TRS, we consider two additional symmetries, inversion (P) and C_{2x} rotation. (Eq. (E1) does not have these symmetries.) With the additional symmetries, the SG is enhanced to $P4/mmm$. We can think the subsystem in the line $(0, 0, k_z)$ as a 1D system with TRS, C_4 , and P symmetries. Since $C_4^2 = -1$, the 1D system decomposes into a $C_4 = i$ sector and a $C_4 = -i$ sector. The Berry's phase θ_1 in the $C_4 = i$ sector can be calculated from the inversion eigenvalues as $e^{i\pi\theta_1} = \prod_n \xi_{n,\Gamma}^{(i)} \xi_{n,Z}^{(i)}$, where $\xi_{n\mathbf{k}}^{(i)}$ is the inversion eigenvalue of the n th occupied state in the $C_4 = i$ sector at \mathbf{k} . Similarly, the Berry's phase θ_2 in the $C_4 = i$ sector in the line (π, π, k_z) can be calculated as $e^{i\pi\theta_2} = \prod_n \xi_{n,M}^{(i)} \xi_{n,A}^{(i)}$. Due to the TRS, the Berry's phases in the $C_4 = -i$ sectors are same as $\theta_{1,2}$. Then we define the \mathbb{Z}_2 invariant δ as the difference of θ_1 and θ_2

$$e^{i\pi\delta} = \prod_n \xi_{n,\Gamma}^{(i)} \xi_{n,Z}^{(i)} \xi_{n,M}^{(i)} \xi_{n,A}^{(i)}. \quad (\text{E2})$$

For $\delta = 1$, either Γ and M or Z and A will have opposite products of inversion eigenvalues in each C_4 sector. Since $M_z = C_2P$ and $C_2 = C_4^2 = -1$, opposite inversion eigenvalues imply opposite M_z eigenvalues. Therefore, the $\delta = 1$ phase has nodal rings protected by M_z . To be specific, we consider the parities shown in Fig. 11e, where the two nodal rings are denoted as r_1 and r_2 . The M_z eigenvalues ($m_1^{k_z=0} m_2^{k_z=0}$, $m_1^{k_z=\pi} m_2^{k_z=\pi}$) inside r_1 , between r_1 and r_2 , and outside r_2 are $(--, ++)$, $(--, +-)$, and $(--, --)$, respectively. According to the correspondence between inversion eigenvalues and Berry's phases [53], the Wilson loop matrices in the three regions have the spectra (π, π) , $(0, \pi)$, and $(0, 0)$, respectively, as shown in Fig. 11f.

Now we consider to break the inversion symmetry such that the SG reduces to $P422$. Since the mirror symmetry is absent, the nodal rings in Fig. 11e will be gapped. However, 16 exceptional gapless points in the four C_2 (C_{2x} , C_{2y} , C_{2xy} , $C_{2x\bar{y}}$) rotation axes will remain. These gapless crossing points are locally protected by the C_2T symmetries and are pinned in the four C_2 axes. There are two ways to gap out these gapless points. The first way is to annihilate two crossings in the same C_2 axes pairwise, which will not close the gap at the high symmetry points. This way is indicated by the yellow arrows in Fig. 11e. The second way is to annihilate the eight crossings from the same ring at the Z point or the A point. The second way will close the gap at the high symmetry points. Now we prove that the first way gives the topologically nontrivial phase. As we annihilate the two gapless points, the discontinuous region in the Wilson loop (green region in Fig. 11f) will be removed and the Wilson loop spectrum will become continuous. Due to the $C_{2x\bar{y}}T$ symmetry, the Wilson loop must be "particle-hole" symmetric [55]. Therefore, the Wilson loop must have the connectivity shown in Fig. 11g, which has a nontrivial winding protected by C_4 and T .

In the end, by a k-p model, we show that the two crossings in the same C_2 axes do annihilate each other. We consider a band inversion of two doublets at the Z point. Each of the two doublets has the C_4 eigenvalues $\pm i$, and the two doublets have opposite inversions. Thus the symmetries can be represented as $C_4 = i\tau_0\sigma_z$, $P = \tau_z\sigma_0$, $C_{2x} = \tau_0\sigma_x$, $T = K$. Then the Hamiltonian for the mirror protected nodal ring semimetal is

$$H = (M - q_x^2 - q_y^2)\tau_z\sigma_0 + q_z\tau_y\sigma_z, \quad (\text{E3})$$

where $\mathbf{q} = \mathbf{k} - (0, 0, \pi)$. In this Hamiltonian, the two nodal rings are degenerate. One can add perturbation terms to split them. But in order to show that the gapless points can be gapped symmetrically, this Hamiltonian is good enough. The term $m\tau_x\sigma_0$, which breaks P but preserves C_4 and C_{2x} , will fully gap the nodal rings.

Appendix F: Related mathematical theorems

In this section, we summarize the mathematical theorems used in the paper. The theorems are given without proof. Interested readers might look at Ref. [85] for Theorem 2, Ref. [86] for Theorems 3 and 4, Refs. [79, 87, 88] for Theorems 5 to 7.

Theorem 2 (Smith Decomposition.) *If A is an $n \times m$ integer matrix, then there is an $n \times n$ unimodular matrix L and an $m \times m$ unimodular matrix R such that $A = L\Lambda R$, where $\Lambda_{ij} = \delta_{ij}\lambda_i$ is an $n \times m$ integer matrix. λ_i is positive integer for $1 \leq i \leq \text{rank}(A)$ and zero for $i > \text{rank}(A)$. Λ is referred to as the Smith Normal Form of A .*

Theorem 3 (Minkowski-Weyl theorem for polyhedra.) *For $P \subseteq \mathbb{R}^d$, the following two statements are equivalent:*

1. (H-representation) *P is a polyhedron, i.e., there exist $A \in \mathbb{R}^{m \times d}$, $C \in \mathbb{R}^{m' \times d}$, $b \in \mathbb{R}^m$, and $f \in \mathbb{R}^{m'}$ for some m, m' , such that $P = \{x \in \mathbb{R}^d \mid Ax \geq b, Cx = f\}$.*
2. (V-representation) *P is finitely generated, i.e., there exist $V \in \mathbb{R}^{d \times n}$, $Ray \in \mathbb{R}^{d \times n'}$, and $Line \in \mathbb{R}^{d \times n''}$, for some n, n', n'' , such that $P = \{Vu + Ray \cdot p + Line \cdot q \mid u \in \mathbb{R}_+^n, u_1 + \dots + u_n = 1, p \in \mathbb{R}_+^{n'}, q \in \mathbb{R}^{n''}\}$.*

The dimension of the polyhedron P , which is given as $d - \text{rank}(C)$, is denoted as $\dim(P)$. The algorithm to get V-representation from H-representation or vice versa is available in many mathematical packages. In this work, we use the *SageMath* package [75]. A special kind of polyhedron is polyhedral cone, where $b = 0$, $f = 0$, and $V = 0$. For polyhedral cone, Theorem 3 becomes

Theorem 4 (Minkowski-Weyl theorem for polyhedral cones.) *For $P \subseteq \mathbb{R}^d$, the following two statements are equivalent:*

1. (H-representation) *P is a polyhedral cone, i.e., there exist $A \in \mathbb{R}^{m \times d}$ and $C \in \mathbb{R}^{m' \times d}$ for some m, m' , such that $P = \{x \in \mathbb{R}^d \mid Ax \geq 0, Cx = 0\}$.*
2. (V-representation) *P is a finitely generated cone, i.e., there exist $Ray \in \mathbb{R}^{d \times n}$, and $Line \in \mathbb{R}^{d \times n'}$, for some n, n' , such that $P = \{Ray \cdot p + Line \cdot q \mid p \in \mathbb{R}_+^n, q \in \mathbb{R}^{n'}\}$.*

A polyhedral cone is called *pointed* if it does not contain lines, i.e., $Line = 0$. $Line = 0$ if $\begin{pmatrix} C \\ A \end{pmatrix}$ is a full-rank matrix. In the case $C = 0$, $Line = 0$ if the A is a full-rank matrix.

Definition 5 *An affine monoid, denoted as M , is a finitely generated sub-monoid of a lattice \mathbb{Z}^d , i.e., there exist $r_1, r_2, \dots, r_n \in \mathbb{Z}^d$ such that $M = \{r_1p_1 + r_2p_2 + \dots + r_np_n \mid p_1 \dots p_n \in \mathbb{N}\}$. M is called positive if $a, -a \in M \Rightarrow a = 0$.*

Theorem 6 (Van der Corput theorem.) *Let M be a positive affine monoid. The elements in M that cannot be written as a sum of other elements with positive coefficients are referred to as irreducible elements. Then (i) every element of M is a sum of irreducible elements with positive coefficients, (ii) M has only finitely many irreducible elements, (iii) the irreducible elements form the unique minimal system of generators $\text{Hil}(M) = \{b_1, b_2, \dots\}$ of M , the Hilbert bases.*

Algorithms to find the Hilbert bases include the Normaliz algorithm [79] and the Hemmecke algorithm [80], which are available in the *Normaliz* package and the *4ti2* package, respectively.

Theorem 7 (Gordan's Lemma.) *Let $P \subseteq \mathbb{R}^d$ be a polyhedral cone. Then $P \cap \mathbb{Z}^d$ is an affine monoid. And when P is pointed, $P \cap \mathbb{Z}^d$ is a positive affine monoid.*

Definition 8 (Monoid homomorphisms.) *A homomorphism between two affine monoids M and N is a function $f : M \rightarrow N$ such that (i) $f(x + y) = f(x) + f(y)$ for all x, y in M , and (ii) $f(0) = 0$. A bijective monoid homomorphism is called a monoid isomorphism.*